

Durham E-Theses

Measurement of helium accumulating in nuclear reactions and the establishment of an absolute neutron standard

Desmond Hall

How to cite:

Hall, Desmond (1958) Measurement of helium accumulating in nuclear reactions and the establishment of an absolute neutron standard. Doctoral thesis, Durham University.

Use policy

The full-text may be used and/or reproduced, and given to third parties in any format or medium, without prior permission or charge, for personal research or study, educational, or not-for-profit purposes provided that:

- a full bibliographic reference is made to the original source
- a <https://etheses.durham.ac.uk/id/eprint/8937/> is made to the metadata record in Durham E-Theses
- the full-text is not changed in any way

The full-text must not be sold in any format or medium without the formal permission of the copyright holders.

Please consult the [full Durham E-Theses policy](#) for further details.

" MEASUREMENT OF HELIUM ACCUMULATING
IN NUCLEAR REACTIONS AND THE ESTABLISHMENT
OF AN ABSOLUTE NEUTRON STANDARD".

-o-o-o-

THESIS

presented in candidature for the

degree of

DOCTOR OF PHILOSOPHY

of the

UNIVERSITY OF DURHAM

by

DESMOND HALL, B.Sc. (Dunelm), A.R.I.C.

-o-o-o-

The work described in this thesis was performed in the Londonderry Laboratory for Radio-Chemistry, University of Durham, during the period from August 1954 to January 1957, under the supervision of G.R. Martin, B.Sc., A.R.C.S., F.R.I.C., Reader in Radio-Chemistry.

This thesis contains the results of some original research by the author, and no part of the material offered has previously been submitted by the candidate for a degree in this or any other university. Where use has been made of the results and conclusions of other authors in relevant studies care has been taken to ensure that the source of information is always clearly indicated, unless it is of such general nature that indication is impracticable.

Desmond Hall.

AN ACKNOWLEDGEMENT.

The author wishes to avail himself of this opportunity to extend sincere appreciation and gratitude to,

Mr. G.R.Martin, Reader in Radiochemistry, University of Durham for his expert advice and guidance during the course of this research, and for his unstinted encouragement of the author during the many years of their acquaintance.

Dr. S.J.Thomson for many useful and stimulating discussions on all aspects of this research.

Dr. J.Wilkinson for advice on tritium measurements and cheerful companionship.

Mr. R.Richmond, of the Reactor Physics Group, Harwell, for the provision of the neutron irradiation facilities and measurements of neutron flux.

Mr. H.Fettis for assistance in the construction of apparatus.

The Council of the Durham Colleges for the appointment of a Research Assistantship during the tenure of which this research was performed.

SUMMARY.

The technique of micro-analysis of helium developed by Paneth and collaborators is here applied to the study of the interaction of neutrons and γ -rays with beryllium.

The study of neutron interaction with beryllium is concerned with the measurement of the cross-section of the reaction $\text{Be}^9(n,2n)\text{Be}^8 \rightarrow 2\text{He}^4$ for neutrons arising from the fission of U^{235} . A value of this cross-section is obtained by measurement of the helium produced on irradiation of beryllium in a known flux of fission neutrons, the value being 109 ± 4 millibarns. This result compares favourably with the predictions of the 'compound nucleus' theory of nuclear reactions.

In these measurements a correction is necessary to allow for helium produced in beryllium by the reaction $\text{Be}^9(n,\alpha)\text{He}^6(\beta^-)\text{Li}^6$. An attempt was made to measure the cross-section of this reaction by estimation of the Li^6 produced using the technique of radio-activation analysis, via the reaction $\text{Li}^6(n,\alpha)\text{H}^3$. Apparatus was constructed for the estimation of tritium so produced in beryllium, but interpretation was rendered difficult by the fact that the tritium production was greatly in excess of the amount which could reasonably be expected from the above

reactions, and the observation that the level of tritium activity in the irradiated samples falls off rapidly with time. An explanation of these observations is offered.

An important question in the technology of a beryllium moderated nuclear reactor is that of the net contribution of the $(n,2n)$ and (n,α) reactions to the neutron balance. It has been suggested that an examination of the helium distribution in a mass of beryllium irradiated with fission neutrons would provide this information. An exploratory experiment has been performed, and is discussed.

The study of the interaction of γ -rays with beryllium is of interest in the establishment of an absolute neutron standard, since the number of neutrons emitted by a beryllium photoneutron source is directly related to the number of helium atoms produced. The accumulation in the beryllium of sufficient helium to permit of accurate measurement requires the combination of a long irradiation time, and a large mass of beryllium. A technique was developed for the successful handling of such large masses of beryllium. The author regrets however that time did not permit the completion of these measurements.

CONTENTS.

Chapter I - INTRODUCTION.

Section 1	- The interaction of neutrons with beryllium.	1.
Section 2	- The use of beryllium in nuclear reactors.	8.
Section 3	- Measurement of inelastic cross-sections.	11.
Section 4	- The nucleus Be^8 .	14.
Section 5	- Application of the associated residual nucleus method.	17.
Section 6	- Measurement of the enhancement	19.

Chapter II - RESULTS AND DISCUSSION.

Section 1	- Helium accumulating in irradiated beryllium.	22.
Section 2	- Correction for helium produced by $\text{Be}^9(\gamma, n)\text{Be}^8(\alpha)\text{He}^4$.	29.
Section 3	- Correction for helium produced by $\text{Be}^9(n, \alpha)\text{He}^6(\beta^-)\text{Li}^6$.	33.
Section 4	- Correction for helium arising from impurities.	38.
Section 5	- The $\text{Be}^9(n, 2n)\text{Be}^8(\alpha)\text{He}^4$ cross-section.	41.
Section 6	- $\text{Be}^9(n, 2n)\text{Be}^8$ excitation function.	42.

Section 7	- Measurement of the enhancement	51.
Section 8	- Measurement of neutron flux.	58.

Chapter III - THE PRODUCTION OF TRITIUM IN BERYLLIUM.

Section 1	- The reaction $\text{Be}^9(n,\alpha)\text{He}^6$.	59.
Section 2	- Experimental and results.	62.
Section 3	- Discussion of tritium measurements.	70.
Section 4	- Conclusion.	82.

Chapter IV - ESTABLISHMENT OF AN ABSOLUTE
NEUTRON STANDARD.

Section 1	- Introduction.	84.
Section 2	- Outline of the method.	85.
Section 3	- Comparison of photoneutron sources.	89.
Section 4	- Measurement of helium.	90.

Chapter V - THE ESTIMATION OF HELIUM IN
BERYLLIUM.

Section 1	- Introduction.	98.
Section 2	- The production of helium-free oxygen.	101.
Section 3	- Extraction procedures for helium.	109.
Section 4	- The Circulating system.	124.
Section 5	- The fractionating column.	126.

Section 6	- The pirani gauge.	137.
Section 7	- The pipetting system.	140.
Section 8	- The fractionation calibration.	142.
Section 9	- Results of air analyses.	144.
Section 10	- Concluding remarks.	146.

Chapter VI. - THE ESTIMATION OF TRITIUM IN
BERYLLIUM.

Section 1	- Introduction.	150.
Section 2	- Preparation of pure dry hydrogen bromide.	152.
Section 3	- Purification of bromine.	154.
Section 4	- The extraction of tritium from beryllium.	156.
Section 5	- Measurement of tritium.	159.

BIBLIOGRAPHY.

CHAPTER I.

INTRODUCTION.

I. 1. The interaction of neutrons with beryllium.

This discussion is confined to the interactions of those neutrons having energies lying within the U^{235} fission neutron spectrum, and in particular to neutrons having energies of interest in the operation of a nuclear reactor. The spectrum of neutron energies emitted in fission extends at least up to 20 MeV, but the region of interest for reactors lies primarily below 10 MeV (1).

The interaction of neutrons with nuclei in general, results in the following types of reaction: (n,n) ; (n,n') ; $(n,2n)$; (n,γ) ; (n,p) ; $(n;p,n)$; (n,d) ; (n,H^3) ; (n,He^3) ; (n,α) ; fission and spallation. Fission of light elements, and spallation being reactions characteristic of very high energy neutrons, lie outside the scope of this discussion. The $Be^9(n,He^3)$ reaction if it takes place would lead to the production of the isotope He^7 . Ajzenberg and Lauritsen (8) list this isotope, and suggest that the mass difference $He^7 - Li^7$ is about 14.5 MeV corresponding to a threshold of 29 MeV for the $Be^9(n,He^3)$ reaction. No evidence is found for the

reaction $\text{Li}^7(n,p)$ for $-1.0 < Q < -7.0$, but using the He^7 mass value from the lower limit would give a Q-value for $\text{Be}^9(n,\text{He}^3)$ of -11.08 MeV. Thus the minimum $\text{Be}^9(n,\text{He}^3)$ threshold energy would be 12.3 MeV.

Table I gives a list of other neutron reactions of beryllium with their associated Q_m values and threshold energies E_n , and it can be seen that the reactions (n,p) , $(n;p,n)$, (n,d) , and (n,H^3) are only possible at energies greater than 10 MeV, and consequently are of little interest in nuclear reactors. A measurement of the (n,H^3) cross-section at 14 MeV neutron energy will however be discussed.

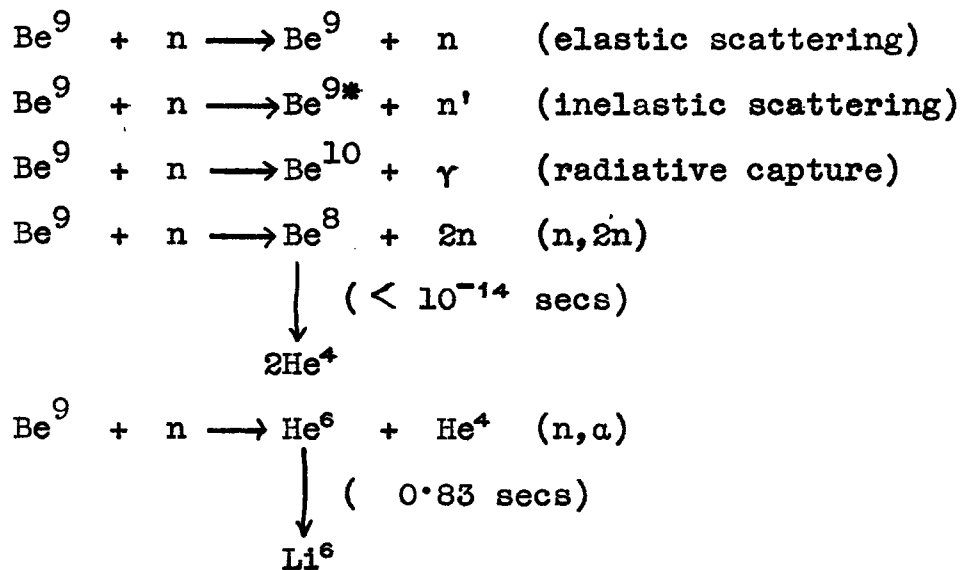
TABLE I.

Reaction	Q_m (MeV)	E_n (MeV)
(n,p)	- 13.27	14.74
$(n;p,n)$	- 16.87	18.74 σ
(n,H^3)	- 10.42	11.58
$(n,2n)$	- 1.666	1.85
(n,α)	- 0.585	0.65
(n,γ)	6.797	-
(n,d)	- 14.63	16.26

Table I has been constructed from currently available mass data (2), except in the case of the (n,α) reaction, where the mass has been computed from the more recent values of the β -disintegration energy of the $\text{He}^6(\beta^-)\text{Li}^6$ reaction (3). The mass of Li^9

involved in the determination of Q_m for the (n,p) reaction has been obtained from the reaction $\text{Be}^9(d,2p)\text{Li}^9$ (4). The value given for the (n,2n) reaction has been computed from the reaction $\text{Be}^9(n,2n)\text{Be}^8$ rather than the energetically more favourable $\text{Be}^9(n,2n)2\text{He}^4$, since the bulk of evidence indicates that the reaction goes through the intermediate Be^8 nucleus.

Thus the reactions of interest for beryllium with neutrons having energy below 10 MeV incident neutron energy are as follows;



The total cross-section σ_T will be made up of the sum of the partial cross-sections of these reactions, and measurements of σ_T have been made over the range of energies from thermal to 100 MeV (5).

Several attempts have been made to study the de-excitation of the residual Be^9 nucleus by γ -emission after an inelastic scattering event. Grace, Beghian,

Preston, and Halban (6), using neutrons of 2.5 MeV incident energy, were unable to detect γ -radiation, and concluded that the combined inelastic scattering and radiative capture cross-section was less than 14 millibarns. Day has pointed out however, that neutrons of this incident energy would be unable to reach the first excited level of Be^9 , and thus inelastic scattering is not possible. He has accordingly attempted to observe the γ -radiation using neutrons of sufficient energy to attain this level, but has been unable to find further evidence for this reaction to which he assigns an upper limit of 0.3 millibarns at the resonance energy (7). This result is not surprising since in the region of levels where particle emission is possible the relative probability of γ -emission is low, and in the case of beryllium there are no known levels stable to particle emission (8).

γ -rays from the radiative capture reaction have been observed by Bartholomew and Kinsey (9), of energy 6.8 and 3.41 MeV upon irradiation of beryllium with neutrons. The first of these is the transition to the ground state, and these correspond to the neutron binding energy of Be^{10} . A cross-section of 8.5 millibarns is reported by Ross and Storey (10). Thus it appears that the inelastic scattering and radiative capture reactions make only a small contribution to

the total cross-section.

The (n,α) reaction was first observed by Bjerger (11) who assigned to the reaction a cross-section of approximately 1 barn. In a study of the fast neutron resonances of beryllium Allen, Burcham, and Wilkinson (12) measured the cross-section of this reaction as a function of neutron energy over the range 1.85 to 4 MeV. The cross-section values observed were considerably less than that of Bjerger, and show a broad resonance corresponding closely in position with the resonance in the total cross-section at 2.73 MeV, with a peak value of 50 millibarns. A more recent determination by Stelson and Campbell (13) confirms the resonance, but gives a peak cross-section of 100 millibarns. The value of the threshold energy observed in both series of measurements is in agreement with that computed from mass data (Table I). Battat and Ribe (14) report a value of 10 millibarns for 14 MeV neutrons.

The $(n,2n)$ reaction in beryllium was first observed by Rusinov (15), who noted the increased activity induced in a silver target irradiated with fast neutrons when the source was surrounded with beryllium. Rusinov estimated the cross-section to be 100 millibarns. Several workers have attempted to measure this cross-section using a variety of methods, and the results of these measurements are shown in Table II. The

measurements quoted range in value from 40 millibarns to 4.1 barns. In all these cases the measurement has been made by observing the apparent yield of the neutron source with and without a surround of beryllium metal. Since the $(n,2n)$ cross-section is expected to be small, the measurements are open to the obvious criticism that the result involves the difference of two large quantities in which small observational errors would introduce quite large errors into the cross-section value. The large photon flux associated with most natural neutron sources, a large proportion of which exceed the photoneutron threshold of beryllium, will make necessary and undesirably large correction to the observed neutrons from the source surrounded with beryllium. The use of natural sources for this type of measurement is of doubtful utility since the result represents an average value over a considerable range of energies (0.5 to 12 MeV) for which the spectrum is imperfectly known, and indeed will vary among sources of the same kind since it is dependent on the relative geometry of the source materials. The spread in the published results testifies to the difficulty of this type of measurement. Fowler, Hanna, and Owen report the first measurement of this cross-section at a specific energy obtaining values ranging from 270 to 390 millibarns for 3.7 MeV

TABLE II.

Author	Primary source	Method of measurement	$\sigma(n,2n)$ mbarns	Reference
Rusinov	Rn- α -Be	A	100	(15)
Ollano	Rn- α -Be	B	3000	(16)
Houtermans	Rn- α -Be	B	4100	(17)
"	Po- α -Be	C	3100	(17)
"	Ra- α -Be	B	3100	(17)
Funfer	Ra- α -Be	B	300	(18)
and Bothe	Ra- α -Be	B	100	(18)
Teucher	Ra- α -Be	D	320	(19)
"	Ra- α -Be	E	470	(19)
Bernstein	Ra- α -Be	F	100	(20)
"	Ra- α -Be	F	40	(20)
Martin	Po- α -B	G	150	(21)
"	Po- α -Be	G	430	(21)
"	Po- α -Be	G	210	(21)
Agnew	Po- α -Be	H*	240 \pm 70	(22)
"	Ra- α -Be	H*	200 \pm 40	(22)
"	Mock fission**	H*	-160 \pm 130	(22)

A- silver activity
 B- foils in diffusing media
 C- gold foil
 D- uranium fission chamber
 E- thorium fission chamber
 F- indium foil in paraffin
 G- sphere multiplication
 H- " " "

** NaBF₄ + Na₂BeF₄ (mole ratio 96:4) impregnated with Po. The mixture gives neutrons with an energy distribution resembling that of a fission source (23).

* The difference between the (n,2n) cross-section and the adsorption cross-section is the quantity measured.

neutrons (24).

I.2. The use of beryllium in nuclear reactors.

Beryllium is being considered as a moderating material in nuclear reactors, either in the elemental state or as beryllium oxide (beryllia): As a reactor material it combines good mechanical and thermal stability with a relatively inert chemical nature, although in the case of beryllia an inert atmosphere or vacuum may be necessary owing to its volatility in the presence of water vapour (25). Its use as a moderating material makes possible the achievement of higher working temperatures which do not appear to be possible with commoner moderators (26). The 'slowing-down power' (27) is comparable with that of light and heavy water, and superior to that of graphite. The material is also much less likely to suffer from Wigner effects.

Calculations on the behaviour of a beryllium moderated reactor have been presented by Hurwitz and Ehrlich (28), who find some disagreement between theory and experiment. These errors are considered to arise from inadequate scattering cross-section data, the effect of self-shielding, and the neglect in their calculations of the (n,α) and $(n,2n)$ reactions in beryllium. They have estimated the effect of the (n,α) absorption of neutrons in reducing reactivity to be of the order of 3%, but have been unable to estimate the increase in

activity due to enhancement of the neutron flux by the (n,2n) reaction owing to lack of cross-section data.

From the list of neutron reactions of beryllium below 10 MeV neutron energy it can be seen that elastic and inelastic scattering do not involve loss of neutrons, the radiative capture and (n, α) reactions involve loss of neutrons, whilst the (n,2n) reaction represents a net gain of neutrons. In the earlier discussion it was pointed out that the radiative capture cross-section is small, and hence can be neglected to a first approximation. The threshold energies of the (n, α) and (n,2n) reactions are 0.65 and 1.85 MeV respectively, and it is clear that if the neutrons have initial energies greater than 0.65 MeV there may be a net gain or loss of neutrons depending upon the relative magnitudes of the (n, α) and (n,2n) cross-sections. The number of neutrons reaching thermal energies (N_{th}) can be expressed by

$$N_{th} = N_0 (1 + \delta)$$

where N_0 is the number of source neutrons, and δ is the enhancement factor whose value will depend upon the relative magnitudes of the (n, α) and (n,2n) cross-sections.

Since loss by radiative capture is to be ignored, the number of source neutrons of energy less than 0.65 MeV reaching thermal energies will be equal to the number of source neutrons, and δ will be zero. In the region

0.65 to 1.85 MeV, the region between the (n, α) and (n,2n) thresholds, there will be a net absorption of neutrons due to the (n, α) reaction, and N_{th} will be less than N_0 , in which case δ is negative. For source neutrons with energy greater than 1.85 MeV the (n,2n) reaction will increase their number, and hence will tend to make positive the value of δ . The value of the resultant δ for a fission neutron spectrum will depend upon the relative values of the (n, α) and (n,2n) cross-sections.

Sanders and Littler (29), using various assumed average values of the (n,2n) cross-section, and the (n, α) cross-section data of Allen, Burcham, and Wilkinson, have calculated δ taking into account the effect of multiple collisions in altering the neutron energy. Their results are given in Table III. Sanders and Littler point out that because of the approximation involved in using averaged cross-sections their results can only be considered as rough illustrations of the effect to be expected. It is clear however that the enhancement might be of considerable importance if the average (n,2n) cross-section lies outside the range 0.05 to 0.1 barns. In view of the high cost of beryllium considerable economies might be expected in the design and construction of a beryllium moderated reactor if the value of δ is positive. A recent Russian publication (30), on the operation of an experimental beryllium moderated reactor gives the result that

the calculated critical mass of U^{235} is greater than that required in practical operation, indicating that δ is indeed positive.

TABLE III.

σ (n,2n) barns	0	0.05	0.10	0.02	0.30
δ	-0.07	-0.02	0	+0.07	+0.11

Thus it appears that an accurate measurement of the (n,2n) cross-section using a fission neutron source would be desirable, and the present investigation was undertaken to provide this.

I.3. Measurement of Inelastic Cross-sections.

The methods available for the measurement of fast neutron cross-sections have been reviewed by Barschall (31). For inelastic collision cross-sections, i.e., the cross-section for all processes excluding elastic scattering, there are four main methods. These methods can be applied to the measurement of (n,2n) cross-sections, and are, the sphere transmission method, the detection of cascade γ -rays associated with an inelastic neutron event, the detection of the inelastic neutrons, and the associated residual nucleus method.

The sphere transmission method measures the total inelastic cross-section. When an isotropic neutron source is surrounded with a spherical shell of

absorbing material the measurement of the transmission through the shell using a threshold detector eliminates the effect of elastic scattering and gives the inelastic collision cross-section. When an energy insensitive detector such as a 'long counter' (32) is used the effects of inelastic scattering can be eliminated also. If the counter sensitivity is independent of energy and only scattering processes take place in the shell the transmission will be unity. When an absorption reaction occurs the transmission will be less than unity, but for (n,2n) reactions the transmission will be greater than unity. Thus if the absorption and radiative capture cross-sections are known the (n,2n) cross-section can be obtained.

The method requires the use of isotropic sources (33) and this limits its application to only a few types of source. The natural sources have been used by Teucher, Martin, and Agnew (See Table III), and although their results are of the same order of magnitude as obtained in this work the agreement is probably fortuitous in view of the different neutron spectra used. An almost isotropic source of 14 MeV neutrons is obtained from the $H^3(d,n)He^4$ reaction, and this has been used by Taylor (34) to measure the total inelastic collision cross-section of beryllium at this energy. Beyster and collaborators (35) using neutrons from the $H^3(p,n)He^3$

reaction have used the sphere transmission method to measure the inelastic collision cross-section of a large number of nuclei, obtaining for beryllium at 4.07 MeV the value of 0.62 ± 0.03 barns. An application of the method to the determination of δ has been suggested by Sanders and Littler (29), and will be discussed later.

The detection of cascade γ -rays from excited nuclei in coincidence with inelastic neutrons is a comparatively recent method (36) employing scintillation counters with NaI(Tl) crystals. The method is not applicable in the case of beryllium inelastic scattering ($n,2n$ process) since no γ -rays are emitted (7).

The direct observation of the inelastically scattered neutrons from $\text{Be}^9(n,2n)$ reaction has been used by Fowler, Owen, and Hanna (37) to estimate the cross-section at 3.7 MeV using neutrons from the $\text{D}(d,n)$ reaction. The inelastically scattered neutrons were detected using stilbene scintillators.

The most productive method is that of the 'associated residual nucleus'. Where neutron absorption leads to a radioactive residual nucleus the measurement of the radioactivity produced on irradiation in a known neutron flux enables the cross-section to be obtained. Thus Fowler and Slye (38) have measured the ($n,2n$) cross-section for the reaction $\text{Cu}^{63}(n,2n)\text{Cu}^{62}$, by observing the β^+ activity of Cu^{62} produced on irradiation with

fast neutrons. Paul and Clarke (39) have measured the $(n,2n)$ cross-section of 34 elements having β active products. A compilation of $(n,2n)$ reactions by Segre (40) shows the great number of nuclei to which this method is applicable.

In the case of the $\text{Be}^9(n,2n)$ reaction the immediate residual nucleus Be^8 breaks down into two α -particles, at least in the energy range of interest. The measurement of the helium associated with the disintegration, already used to prove that such breakdown occurs (41) can be used to measure the $(n,2n)$ cross-section. This method is the one used in this work, and will be discussed in more detail in a later section, together with the application of the associated residual nucleus method to the $\text{Be}^9(n,\alpha)$ and $\text{Be}^9(n,\text{H}^3)$ reactions.

I 4. The nucleus Be^8 .

Before discussing the application of the associated residual nucleus method to the $\text{Be}^9(n,2n)\text{Be}^8$ reaction it is necessary to consider the nucleus Be^8 . The reaction may leave the Be^8 nucleus in one of several excited states, or its ground state, and it is essential to the success of the method that all states capable of being reached in the bombardment decay by α -emission before analysis of the beryllium for helium.

Early work on this nucleus is full of contradiction.

Atkinson and Houtermans (42) from theoretical considerations postulated the instability of Be^8 . Rayleigh (43) in considering that the helium content of beryllium minerals was derived from this unstable nuclide suggested that it must therefore have existed in geological time subsequent to the formation of the minerals, and on this basis Watson and Parker (44) sought and reported lines due to Be^8 in the arc spectrum of beryllium hydride. In the same year (1931) Olssen (45) failed to observe lines due to Be^8 in the same spectrum. Mass spectroscopic observations of Neir (46) and Bleakney and collaborators (47) set an upper limit of one part of Be^8 to 10^5 parts of Be^9 . Cockroft and Lewis (48) looked for Be^8 recoils in the postulated reaction



but were unable to observe them, and they suggested that their results could be explained in terms of the simultaneous production of two α -particles. No positive evidence for a stable Be^8 could be obtained. Dee and Gilbert (49) proposed that Be^8 was formed as an intermediate product in this reaction in a 2.8 MeV excited state.

The first conclusive proof that Be^8 disintegrated into two α -particles was obtained by Glueckauf and Paneth,

(41), who examined beryllium after irradiation with γ -rays for the presence of helium. Positive evidence of the formation of helium was found, the only possible source being from the break-up of Be^8 , and they concluded that the decay time was less than 1 second. Kirchner and Neuert (50) examining the reaction $\text{B}^{11}(\text{p},\alpha)\text{Be}^8$ found that frequently 2 α -particles entered the detecting apparatus simultaneously with a small angle between the directions of flight which is just what would be expected if the Be^8 formed broke up into two α -particles, and from the angles of flight estimated the instability of the nucleus as lying between 100 and 200 keV corresponding to a lifetime between 10^{-16} and 10^{-19} seconds (51).

Wheeler (1941) (52) reviewed the experimental evidence available at that time, and concluded that the excited states disintegrated into two α -particles, but that the evidence with regard to the ground state was inconclusive. In the following years the evidence for the instability of the ground state accumulated (53). The currently accepted view (8) is that the ground state is unstable by 96 keV, and that all levels up to about 19 MeV excitation are unstable to α -emission, and above this other modes of decay are possible. An excitation of Be^8 of this order corresponds to an incident neutron energy for Be^9 greater than 20 MeV, and this is above the range of energies of interest in this work. The

of beryllium together with flux monitoring devices were therefore irradiated inside a hollow uranium slug of the reactor.

The fission neutron spectrum currently accepted is that quoted by Leachman (54), and is expressed in the semi-empirical equation.

$$N(E) \propto \exp(-E/0.965) \cdot \sinh \sqrt{2.29E} \cdot dE.$$

The normalising factor obtained by graphical integration of this function is 0.455, the units being in MeV. The expression used throughout this work is therefore

$$N(E) = 0.455 \exp(-E/0.965) \cdot \sinh \sqrt{2.29E} \cdot dE.$$

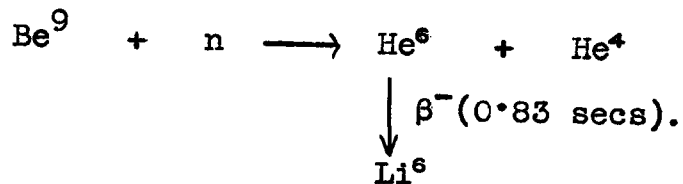
where $N(E)$ is the number of neutrons of energy between E and $E + dE$. The cross-section obtained in this work is therefore an average value over a known spectrum.

The helium is measured essentially by the method developed by Paneth and collaborators (55).

Under the conditions of irradiation inside a 'pile' the beryllium samples will be exposed to a large γ -ray flux, and helium could be produced by the $\text{Be}^9(\gamma, n)$ reaction (41). Calculations of the helium production from this source are given later and indicate that this effect is negligible.

A more serious source of error is the helium accumulating from the (n, α) reaction. As mentioned earlier, two excitation functions are available for this

reaction and by integration of these over a fission spectrum the amount of helium arising from this reaction can be calculated. The amount represents some 10% of the total helium.



It will be noted that one product of the (n, α) reaction is the nucleus Li^6 . The cross-section for the $\text{Li}^6(n,\alpha)\text{H}^3$ reaction for slow neutrons is approximately 1000 barns, and this high cross-section makes possible a radioactivation analysis (56) of the beryllium for Li^6 , by determination of the tritium produced. The tritium production is too small to measure by gas volumetric methods, but can be detected by virtue of its β^- activity. The measurement of the Li^6 produced in the (n, α) reaction makes possible a measurement of the reaction cross-section averaged over a fission spectrum, and thus helium arising from this source can be experimentally determined. In connection with this determination it was necessary to measure the (n,t) cross-section of beryllium for 14 MeV neutrons, and this measurement will be described later.

The experimental determination of helium and tritium in beryllium will be discussed in a separate section.

I. 6. Measurement of the enhancement δ .

Sanders and Littler (29), have suggested two methods

whereby the enhancement δ of a fission neutron source surrounded with beryllium could be measured experimentally.

The first method is essentially that used by previous workers (18, 22), namely the sphere multiplication method, differing only in the use of a fission neutron spectrum and a beryllium surround of dimensions greater than a few scattering lengths. The scattering length of beryllium is approximately 3.3 cms., and they suggest using a 10 cm. radius sphere. As a source of fission neutrons a few grams of plutonium immersed in a thermal neutron beam would be used, and a long counter or integrating tank detector (57) would be used to measure the neutron yield. The authors suggest that the comparison of source strength could probably be done to $\pm 2\%$ accuracy. In addition to the difficulties of this method discussed earlier, the method suffers from the disadvantage that the 2% error is in the quantity $(1 + \delta)$ and not in δ itself. Since δ is expected to be small, a large uncertainty in δ will result, e.g., $\pm 50\%$ if $\delta = 0.04$.

The second method uses a measurement of the helium content of the irradiated beryllium to obtain δ . The (n, α) process yields one helium atom, and the (n,2n) process yields two. Combined with a 'Monte-Carlo' calculation (58) of the helium produced by the (n, α) process alone using the known excitation function of the

reaction, the number of $(n,2n)$ processes per fission neutron can be determined, and δ can be calculated. A beryllium surrounded plutonium sample was suggested as in the experiment above. The determination described in another section of this work was a test experiment to study the feasibility of the method, and was performed using a smaller sphere than that suggested.

The advantage of this latter method is that even if the results were only good to an accuracy of 20%, this is 20% in the quantity δ itself which for smaller values of δ is much better than that obtained from the source comparison method discussed above.

Barrett (113) has recently described a method for the determination of the effective neutron multiplication due to beryllium. In this method beryllium samples irradiated in a reactor core are subsequently analysed for Li^6 , He^4 , and H^3 . A sample of fuel situated near the beryllium sample is then analysed for a particular fission product concentration, and from this the ratio of the number of $n,2n$ processes to the number of fissions can be obtained. These measurements, together with other information obtained from multi-group calculations or foil activation measurements in a critical assembly, can be used to determine the over-all reactivity change brought about by the production and absorption of neutrons in beryllium.

CHAPTER II.

RESULTS AND DISCUSSION.

II.1. Helium accumulating in irradiated beryllium.

The results of four separate irradiations of pieces of beryllium in a hollow slug of the BEPO pile at Harwell are given in Table IV. The cross-section for helium production σ_{He} given in the last column has been calculated from the equation

$$\sigma_{\text{He}} = \frac{N_{\text{He}}}{\bar{\Phi} \cdot N_{\text{Be}} \cdot t.}$$

where N_{He} is the number of atoms of helium produced, $\bar{\Phi}$ is the fast neutron flux, N_{Be} the number of atoms of beryllium irradiated, and t the time of irradiation in seconds.

For irradiation III the measured flux values were inconsistent with those deduced from the pile power level, and it was later found that the counting system used was at fault. The value computed from the pile power level gives a value of σ_{He} consistent with the other determinations but the result will be rejected in the final analysis because of the uncertainty existing in the flux measurements.

Table IV. Helium produced in Beryllium irradiated with Fission neutrons

Irrad- iation No.	Sample No.	Mass of Beryllium gms.	Volume of Helium at S.T.P. ccs. x 10 ⁶	Atoms He Atoms Be x 10 ⁸	Flux N/cm ² /sec x 10 ⁻¹¹	Irrad- iation time secs. x 10 ⁻⁵	σ_{He} mbarns
I	1	0.5830	40.33	2.78	2.131	5.04	259
	2	0.3108	8.50	1.10	2.022	2.142	254
II	3	0.2388	6.554	1.10	2.022	2.142	254
	7	0.0814	3.161	1.56	2.798	2.226	250
IV	8	0.0593	2.280	1.55	2.798	2.226	249
	9	0.0673	2.64	1.58	2.798	2.226	254
	10	0.0590	2.264	1.55	2.798	2.226	249
III*	4	0.3180	9.57	1.21	2.022	2.421	247
	5	0.3198	9.75	1.22	2.022	2.421	249
	6	0.2976	9.51	1.28	2.022	2.421	261

Average $\bar{\sigma}_{He}$ for irradiations I, II, IV, = 253 ± 4 millibarns.

* Flux deduced from pile power level

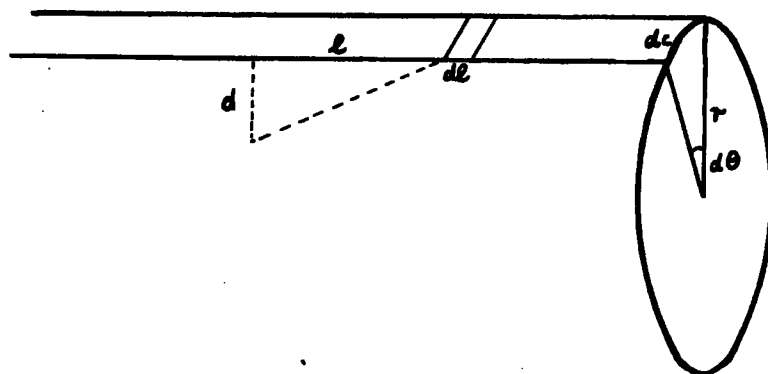
The results of σ_{He} obtained from irradiations I, II, and IV show a standard deviation of approximately $\pm 0.7\%$. It will be noted that there is an apparent correlation between the mass of beryllium and the effective cross-section deduced. This effect may be illusory, in that only three irradiations were involved, but it may be a genuine effect resulting from one of the following causes.

- (a) larger pieces of beryllium received an effectively greater flux on account of closer proximity to the walls of the hollow slug.
- (b) There is some surface loss of helium from the smaller pieces, which will not be so serious in the larger ones.
- (c) Enhancement of the flux, arising from the $(n, 2n)$ reaction, will be greater in the larger pieces.

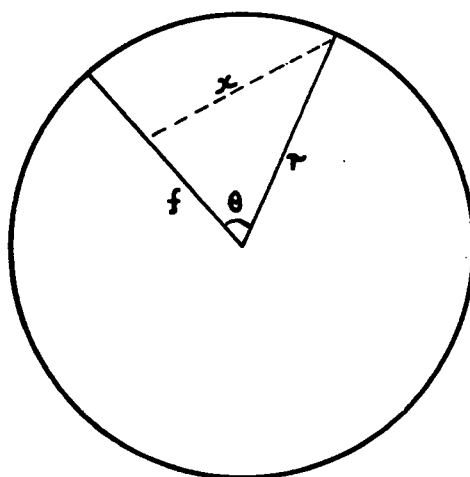
In the case of (a) the inhomogeneity of the flux distribution inside the hollow slug can be shown in the following way;

Assume an infinitely long thin cylindrical shell of radius r emitting n neutrons/cm²seconds, and a strip of width $dc (= r \cdot d\theta)$ taken along the length of the shell (see figure Ia). At a point distant d from this shell the neutron flux passing through this point due to an element dl of the strip will be

FIGURE 1.



(a)



(b)

$$\frac{n \cdot dc \cdot dl}{4\pi(d^2 + l^2)}$$

Integrating from $-\infty$ to $+\infty$ with respect to dl gives the flux through the point due to the whole strip.

$$\begin{aligned} \frac{n \cdot dc}{4\pi} \int_{-\infty}^{+\infty} \frac{dl}{d^2 + l^2} &= \frac{n \cdot dc}{4\pi d} \cdot \left(\tan^{-1} \frac{l}{d} \right)_{-\infty}^{+\infty} \\ &= \frac{n \cdot dc}{4d} \end{aligned}$$

This is for an infinite strip, which is probably a good enough approximation. Now consider the effect of all such strips (figure Ib).

$$x^2 = r^2 + f^2 - 2f \cdot r \cdot \cos \theta$$

where x is the distance from the strip dc , and f the distance from the centre. The total flux at the point will be given by

$$\begin{aligned} 2 \int_0^{\pi} \frac{n \cdot dc}{4x} &= 2 \int_0^{\pi} \frac{n \cdot r \cdot d\theta}{4\sqrt{(r^2 + f^2 - 2r \cdot f \cdot \cos\theta)}} \\ &= \frac{n \cdot r}{2} \int_0^{\pi} \frac{d\theta}{\sqrt{(r^2 + f^2 - 2r \cdot f \cdot \cos\theta)}} \end{aligned}$$

By means of the substitution $\cos\theta = 2\cos^2\theta/2 - 1$ this can be reduced to an elliptic integral of the first kind, the standard form of which is

$$K = F(k, \phi) = \int_0^{\phi} \frac{d\phi}{\sqrt{(1 - k^2 \sin^2\theta)}}$$

thus the integral becomes

$$\int_0^{\pi} \frac{d\theta}{\sqrt{(r^2 + f^2 + 2r.f - 4r.f.\cos^2\theta/2)}}$$

$$= \frac{I}{r + f} \int_0^{\pi/2} \frac{2 d(\theta/2)}{\sqrt{(I - \frac{4r.f.\cos^2\theta/2}{(r + f)^2})}}$$

put $\theta/2 = \pi/2 - \phi$; $\cos\theta/2 \rightarrow \sin\phi$, and $d(\theta/2) \rightarrow -d\phi$

Then the flux F at f is

$$F(f) = \frac{2}{(r + f)} \int_0^{\pi/2} \frac{d\phi}{\sqrt{(I - \frac{4r.f}{(r + f)^2} \sin^2\phi)}}$$

$$\text{Thus } k^2 = \frac{4r.f}{(r + f)^2} = \frac{4f/r}{(I + f/r)^2}$$

The fractional increase in flux as we move out from the central axis of the cylinder is given by

$$\frac{F(f) - F(0)}{F(0)} = \frac{F(f)}{F(0)} - I$$

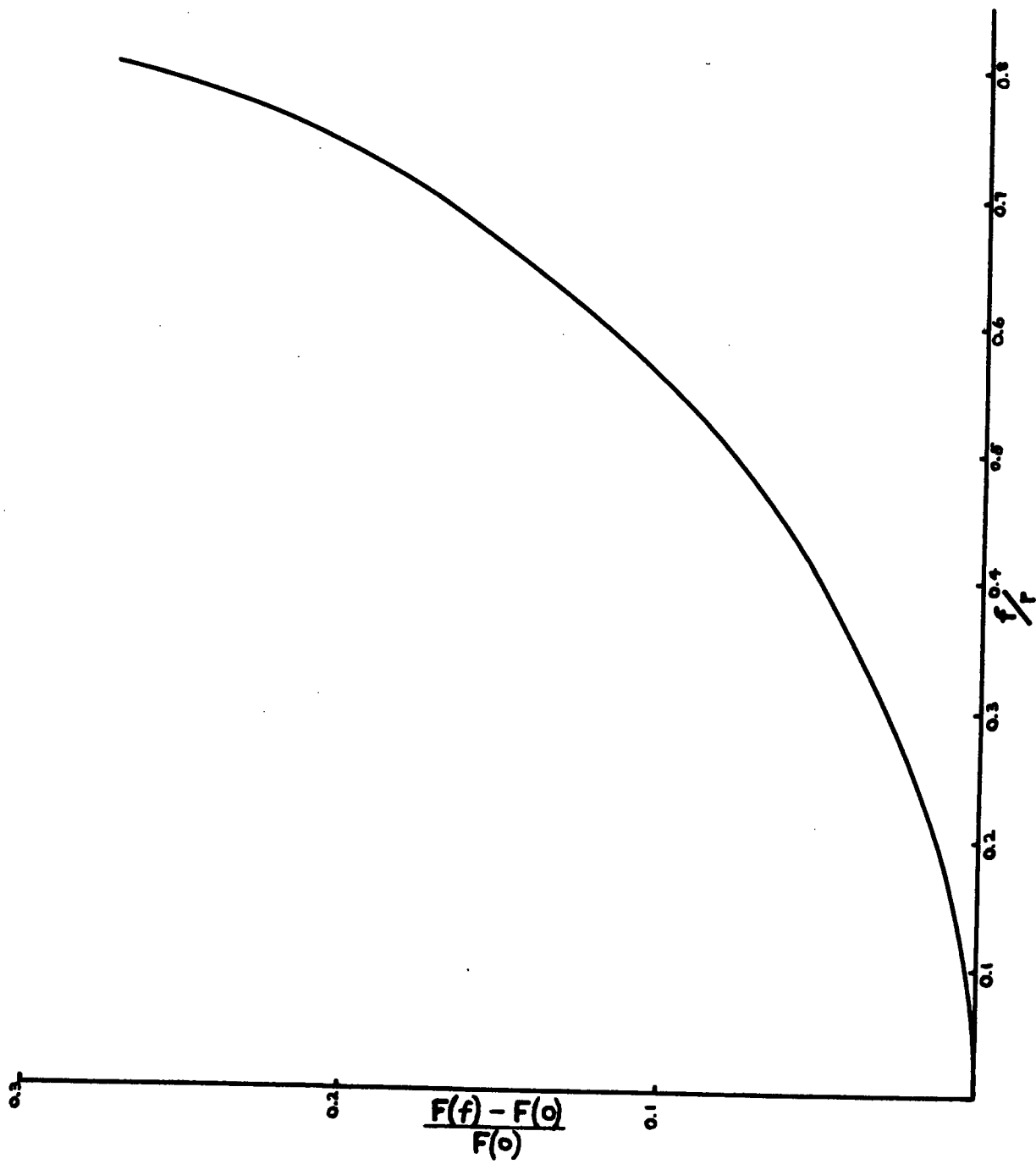
and

$$\frac{F(f)}{F(0)} = \frac{2}{\pi(I + f/r)} \int_0^{\pi/2} \frac{d\phi}{\sqrt{(I - \frac{4r.f}{(r + f)^2} \sin^2\phi)}}$$

Figure 2 shows the fractional increase in flux as a function of f/r. The integral solutions were obtained from the tables of elliptic integrals (59).

FIGURE 2.

Flux distribution inside a hollow uranium slug.



From figure 2 it can be seen that larger pieces of beryllium are exposed to higher flux values, and the order of magnitude of the effect is well able to account for the observed mass correlation. However it must be remembered that the flux monitors are of finite size giving an average flux over the volume occupied, and therefore will tend to minimise errors arising from this source.

In the case of (b) Gluckauf and Paneth (41) have reported that all metals are perfectly helium tight. No indication is given as to the source of this information, but their conclusion appears to be based on earlier work on the loss of helium from iron meteorites reported by Paneth (60). Reasbeck (61) reports an attempt to study the loss of helium from stone meteorites, in which a specimen of meteorite was sealed in an evacuated vessel for a suitable period of time, and then the flask was examined for helium. The result was compared against an empty identical flask, but little conclusive evidence was gained. Although no experimental evidence is available on the diffusion of helium in beryllium the effect has been assumed negligible throughout this work. The following experiment is proposed to check the validity of this assumption.

A cylindrical piece of beryllium metal is first irradiated in a fission flux of neutrons in order to

accumulate helium. The diffusion could be observed in two ways:

- (1) The beryllium specimen is heated for a fixed length of time at a high temperature under conditions of high vacuum. The heating is discontinued, and layers of beryllium are removed at known radii and are analysed for helium. From the shape of the radial distribution of helium, the initial distribution being assumed homogeneous or measured on a similar specimen, the diffusion coefficient can be obtained. Repetition of the experiment at several different temperatures will enable the activation energy of the diffusion to be obtained, and from this the diffusion coefficient at room temperature.
- (2) The experiment is similar except that the specimen is removed from time to time and small pieces cut from the cylinder, and analysed. From the time dependence of the diffusion the diffusion coefficients at several temperatures can be measured and hence the activation energy obtained as before.

Equations for the diffusion in each case are given by Barrer (62). The diffusion study would also be of some interest in reactor technology according to Cottrell (63).

The increase in helium content due to (c) is certainly a possibility. However the scattering length of fast neutrons in beryllium is of the order of 3.3cms., and this is much greater than the dimensions of the beryllium specimens used in these experiments, and hence the effect is likely to be extremely small.

The apparent mass correlation is not a serious effect however, the error being less than the absolute errors in flux values.

II. 2. Correction for helium produced by $\text{Be}^9(\gamma,n)\text{Be}^8(\alpha)\text{He}^4$.

Associated with the neutrons from the uranium fission is a fairly intense γ -radiation, and helium will be produced in the beryllium as a result of the interaction of these γ -rays. From a knowledge of the intensity and spectrum of the γ -rays from fission, together with the photo-disintegration excitation function of the Be^9 , a correction for the helium arising from this source can be obtained.

The photo-disintegration cross-section of Be^9 as a function of photon energy has been observed by several workers from the threshold of 1.666 MeV to 24 MeV. A theoretical function calculated by Guth and Mullin (64) is in good agreement with the results of several workers and provides a convenient summary of the data over the required range. The full range of the excitation function is indeed covered by Nathans and Halpern (65), but

because of the limitations of their method at low energy they were unable to give the fine structure in this region, which has been observed by several workers (64). Since the intensity of the fission γ -rays is highest in this region, the low energy spectrum is of the most importance, and in this region the calculations of Guth and Mullin reproduce the spectrum very well.

Guth and Mullin use the valence neutron model of Be^9 in which the final neutron in the nucleus is regarded as moving in the force field of the Be^8 nucleus. The low binding energy of the final neutron in Be^9 suggests that this neutron spends the greatest part of its time on the fringe of the nuclear forces, and the model is therefore not unreasonable. The photons produce photo-electric and photo-magnetic transitions in the system. At the comparatively low energies involved only electric and magnetic dipole transitions are effective, and of these the magnetic dipole contribution can be neglected for our purpose. Assuming a P ground state for Be^9 the selection rules permit $P \longrightarrow S$ and $P \longrightarrow D$ transitions for electric dipoles, the total cross-section being the sum of these effects.

$$\sigma_T = \sigma_{P \longrightarrow S} + \sigma_{P \longrightarrow D}$$

Guth and Mullin give excitation functions for $\sigma_{P \longrightarrow S}$ and $\sigma_{P \longrightarrow D}$, and these have been added to give the total

cross-section (figure 3).

Leachman (54) quotes the work of Gamble and Francis who observed the spectrum of γ -rays in coincidence with U^{235} fission by means of a NaI scintillation detector. The results, expressed as the number of photons/fission/100 keV energy interval (figure 4), show a yield probability decreasing with energy. The number of photons/fission (I) is then

$$I = k \int_0^{\infty} f(E) \cdot dE$$

The number of photons/fission with sufficient energy to produce photo-disintegration of beryllium is

$$I (E_{\gamma} > 1.666 \text{ MeV}) = k \int_{1.666}^{\infty} f(E) \cdot dE$$

Since the number of neutrons/fission (ν) is known (64), the photon flux can be related to the fission neutron flux. Thus the number of photons/fission neutron is (I/ν), and hence the flux of photons with $E > 1.666$ MeV is

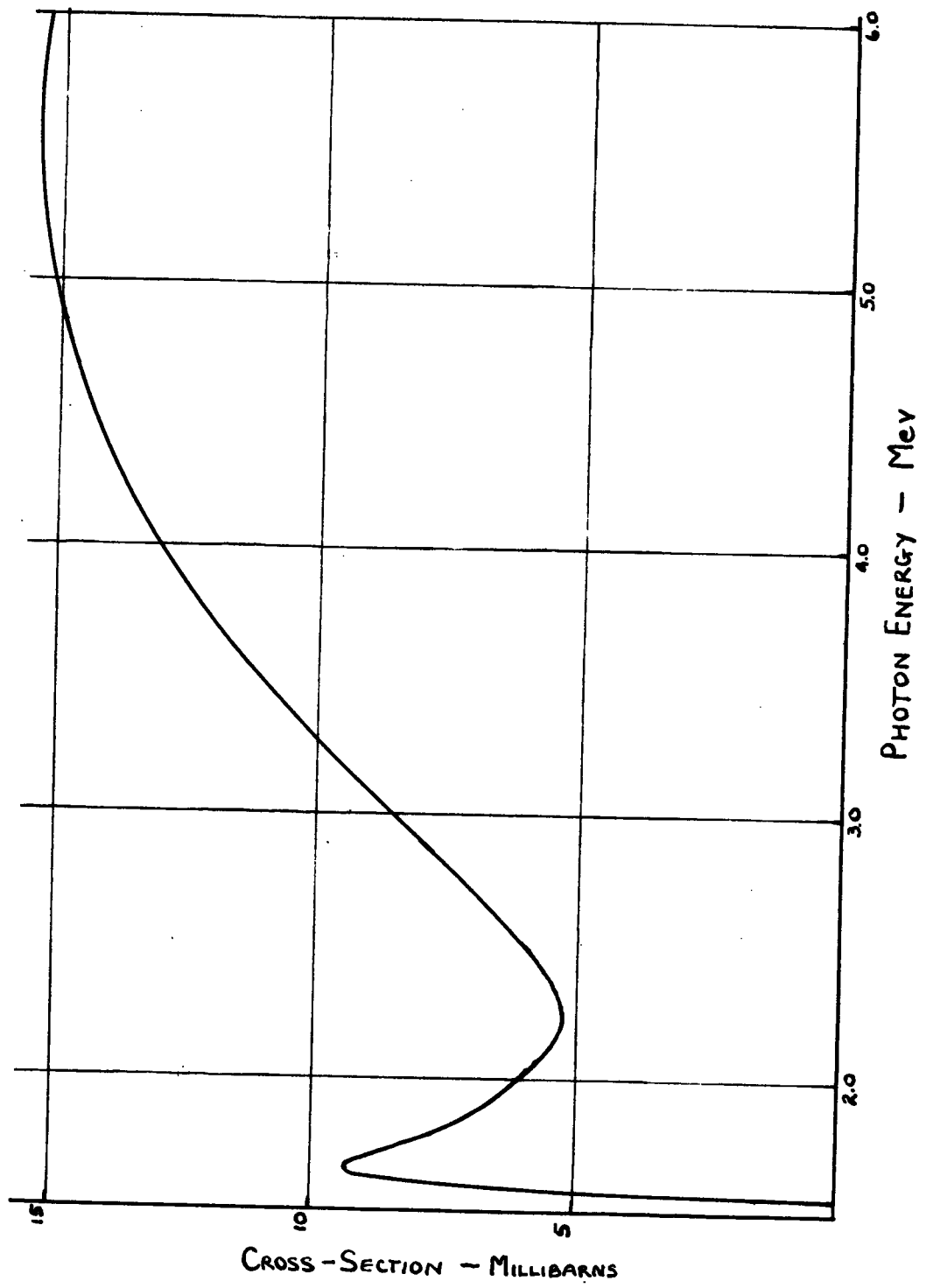
$$\bar{I}_{\gamma} = \frac{\bar{I}_n \cdot k}{\nu} \int_{1.666}^{\infty} f(E) \cdot dE$$

where \bar{I}_n is the fission neutron flux. The average cross-section for the photo-disintegration $\bar{\sigma}_{\gamma}$, is

FIGURE 3.

Be⁹ photodisintegration excitation function.

Guth and Mullin (64).



$$\bar{\sigma}_\gamma = \frac{\int_{1.666}^{\infty} \sigma(E) \cdot f(E) \cdot dE}{\int_{1.666}^{\infty} f(E) \cdot dE}$$

Hence the number of interactions/second is given by

$$\begin{aligned} \bar{I}_\gamma \cdot \bar{\sigma}_\gamma \cdot N_{\text{Be}} &= \frac{\bar{I}_n \cdot k \cdot N_{\text{Be}}}{\nu} \int_{1.666}^{\infty} f(E) \cdot dE \frac{\int_{1.666}^{\infty} \sigma(E) \cdot f(E) \cdot dE}{\int_{1.666}^{\infty} f(E) \cdot dE} \\ &= \frac{\bar{I}_n \cdot k \cdot N_{\text{Be}}}{\nu} \int_{1.666}^{\infty} \sigma(E) \cdot f(E) \cdot dE \end{aligned}$$

Since two helium atoms are produced for each interaction the number produced after irradiation for time t is

$$H = \frac{2\bar{I}_n \cdot k \cdot N_{\text{Be}} \cdot t}{\nu} \int_{E_t}^{\infty} \sigma(E) \cdot f(E) \cdot dE$$

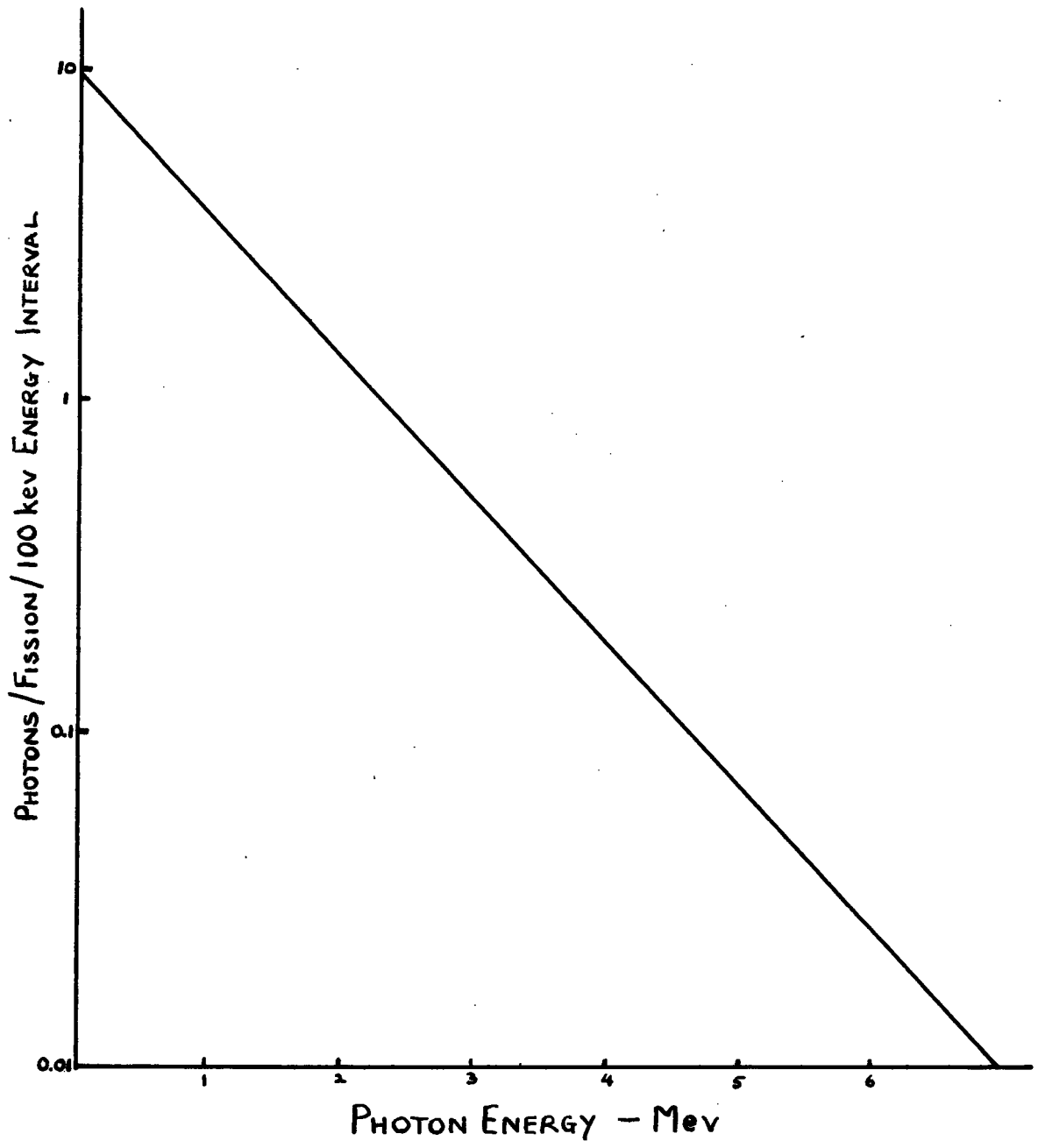
Using a typical set of experimental data the magnitude of the photo-disintegration correction can be computed. A suitable basis for comparison with the overall helium production from the irradiation is the number of helium atoms/atom of beryllium/fission neutron/secons. This can be obtained from the last equation

$$= \frac{2k}{\nu} \int_{E_t}^{\infty} \sigma(E) \cdot f(E) \cdot dE$$

FIGURE 4.

Intensity and spectrum of γ -rays from U^{235} fission.

Leachman (54).



Using $D = 2.5$ this gives the number of helium atoms/atom of beryllium/fission neutron/second, i.e. the cross-section for helium production from the (γ, n) reaction, as 1.8 millibarns. This must be deducted from the observed helium cross-section.

II. 3. Correction for Helium Produced by $\text{Be}^9(n, \alpha)\text{He}^6(\beta^-)\text{Li}^6$.

In order to calculate the helium arising from this source a knowledge of the (n, α) excitation function, together with the intensity and spectrum of the incident neutrons, is required. Sanders and Littler (29) in their enhancement calculations have assumed a step function form of the excitation function based on the results of Allen, Burcham, and Wilkinson (12). Thus from 0.6 to 1.85 MeV neutron energy the cross-section is assumed to be 15 millibarns, and above 1.85 MeV a cross-section of 50 millibarns is assumed.

The measurements of Allen, Burcham, and Wilkinson cover a range from 1.83 to 4 MeV incident neutron energy (figure 5), and were made using neutrons from the $\text{D}(d, n)\text{He}^3$ reaction. A beryllium walled Geiger counter was irradiated with these neutrons, and the $\text{He}^6 \beta^-$ activity produced was observed. The cross-section was deduced from the absolute flux of neutrons through the counter, and the efficiency of the counter for He^6 detection. Since the full energy range of the fission neutron spectrum is not covered by these measurements an extrapolation is necessary.

The method of extrapolation is given below.

At the low energy end of the spectrum only elastic scattering and the (n, α) reaction are possible, and in this region the extrapolation is made by assuming that the relative rates of the two competing reactions are governed by a simple barrier penetration relationship. The relative probability of neutron and α -particle emission from the compound nucleus Be^{10} will be determined by the lifetime of this nucleus for the respective processes. The cross-sections $\sigma_{n,n}$, and $\sigma_{n,\alpha}$ will be in the inverse ratio of the lifetime $T_{n,n}$, and $T_{n,\alpha}$, i.e.,

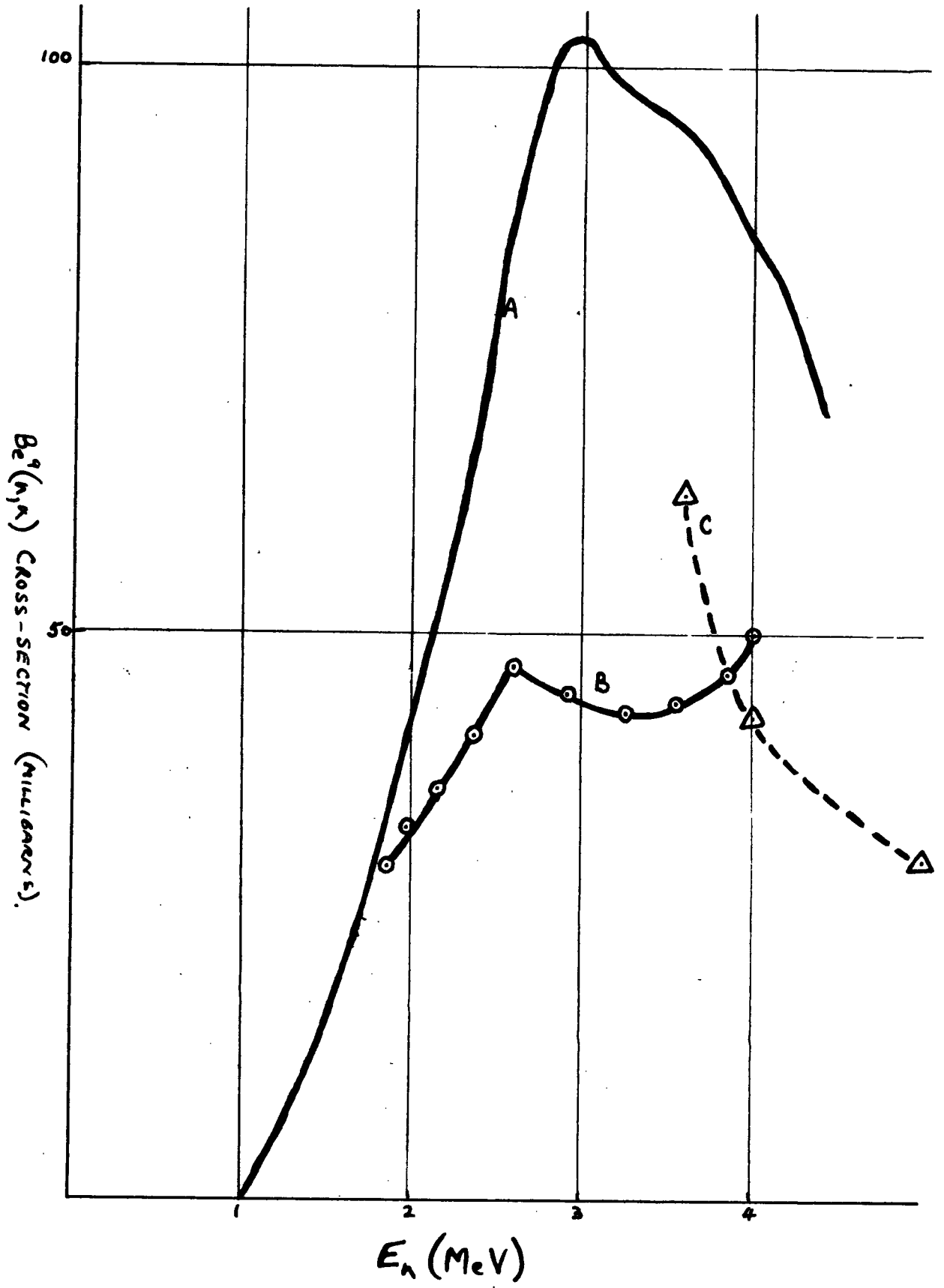
$$\frac{\sigma_{n,\alpha}}{\sigma_{n,n}} = \frac{T_{n,n}}{T_{n,\alpha}}$$

Assuming that the total cross-section of Be^9 at 1.83 MeV (the first energy used to measure the cross-section by Allen et al.) is made up of capture scattering and (n, α) reactions, and that the α -emission lifetime of Be^{10} are not substantially different from those of Be^8 , the cross-section ratio can be obtained at this energy from the measured values, and $T_{n,\alpha}$ from the data given by Bethe (67). Thus $T_{n,n}$ can be found at this energy, and can safely be considered constant over the small range of extrapolation since there is no potential barrier opposing the process. For other energy values $\sigma_{n,n}$ can be found from the total cross-section, and $T_{n,\alpha}$ values for various

FIGURE 5.

Be⁹(n, α)He⁶ Excitation Function.

- (a) Stelson and Campbell (13).
- (b) Allen, Burcham and Wilkinson (12).
- (c) Suttar, Morgan and Hudspeth (69).



excitation energies from Bethe (67). The results are given in Table V.

Table V - Extrapolated values of $\sigma_{n,\alpha}$.

Neutron Energy MeV	$\sigma_{n,\alpha}$ Millibarns
0.6	3.6×10^{-2}
0.8	2.1
1.0	3.0
1.5	15
1.83	29*

* Experimental value (12).

Above 4 MeV the cross-section is assumed constant at 45 millibarns, following Sanders and Littler (29). The extrapolation in this region is not very serious since the neutron intensity falls off rapidly above 4 MeV. The extrapolation is shown in figure 5.

In order to obtain the average value of the cross-section $\bar{\sigma}_{n,\alpha}$ for a fission spectrum, the excitation function $\sigma(E)$ must be integrated over the fission spectrum $f(E)$. The average cross-section is given by

$$\bar{\sigma}_{n,\alpha} = \frac{\int_0^{\infty} \sigma(E) \cdot f(E) \cdot dE}{\int_0^{\infty} f(E) \cdot dE}$$

$f(E)$ is plotted in figure 6, and $\sigma(E) \cdot f(E)$ in figure 7.

By graphical integration of figure 7 the average cross-section is obtained as

$$\bar{\sigma}_{n,\alpha} = \underline{23 \text{ millibarns.}}$$

Results obtained by Stelson and Campbell (13) for the (n, α) excitation function using neutrons from the $T(p,n)He^3$ and $Li^7(p,n)Be^7$ reactions are also shown in figure 5. The measurements are taken from the reaction threshold up to 4.4 MeV incident neutron energy. The (n, α) cross-section at 14 MeV is reported to be 10 millibarns (68), and the results of Stelson and Campbell have been extrapolated to this energy by drawing a smooth curve between the two sets of results. The neutron intensity is falling off so rapidly in this region that the assumption makes little difference to the average value of the cross-section. The average cross-section over a fission spectrum has been obtained as before by graphical integration. The result is

$$\bar{\sigma}_{n,\alpha} = \underline{33 \text{ millibarns.}}$$

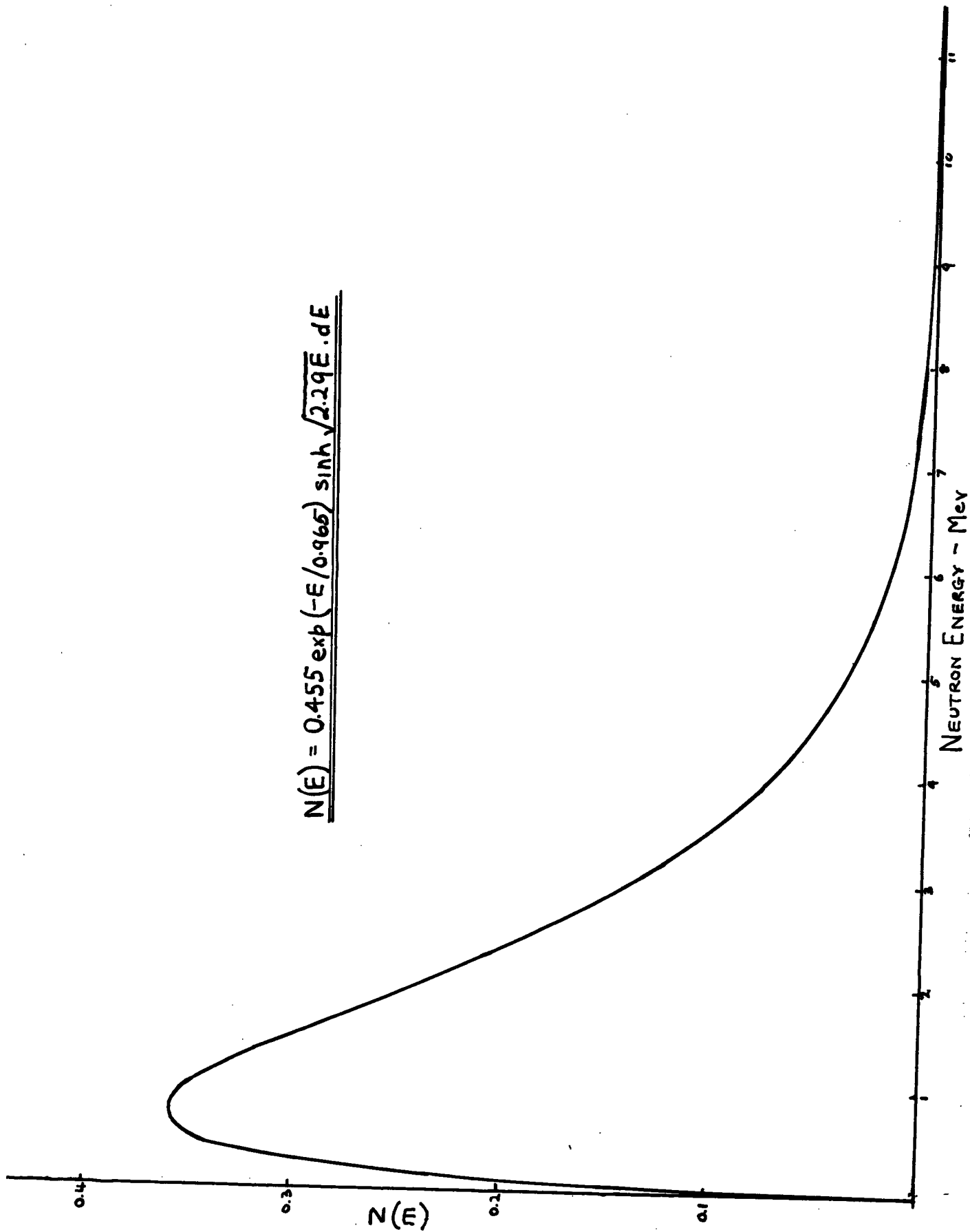
The value of $\bar{\sigma}_{n,\alpha}$ obtained from the two sets of measurements are in reasonable agreement considering the difficulty involved in such measurements. The result of Stelson and Campbell is probably the better of the two, since better neutron sources were used and the neutron flux measurements are likely to be better. A clean neutron spectrum is difficult to obtain with the D + D

FIGURE 6.

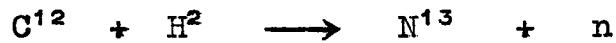
Spectrum of neutrons from U^{235} fission.

Leachman (54).

$$N(E) = 0.455 \exp(-E/0.965) \sinh \sqrt{2.29E} \cdot dE$$



reaction. The major contributing factor in distorting the spectrum is the build up of carbon deposit on the heavy ice target when the deuteron beam is on. The following reaction can occur in the target



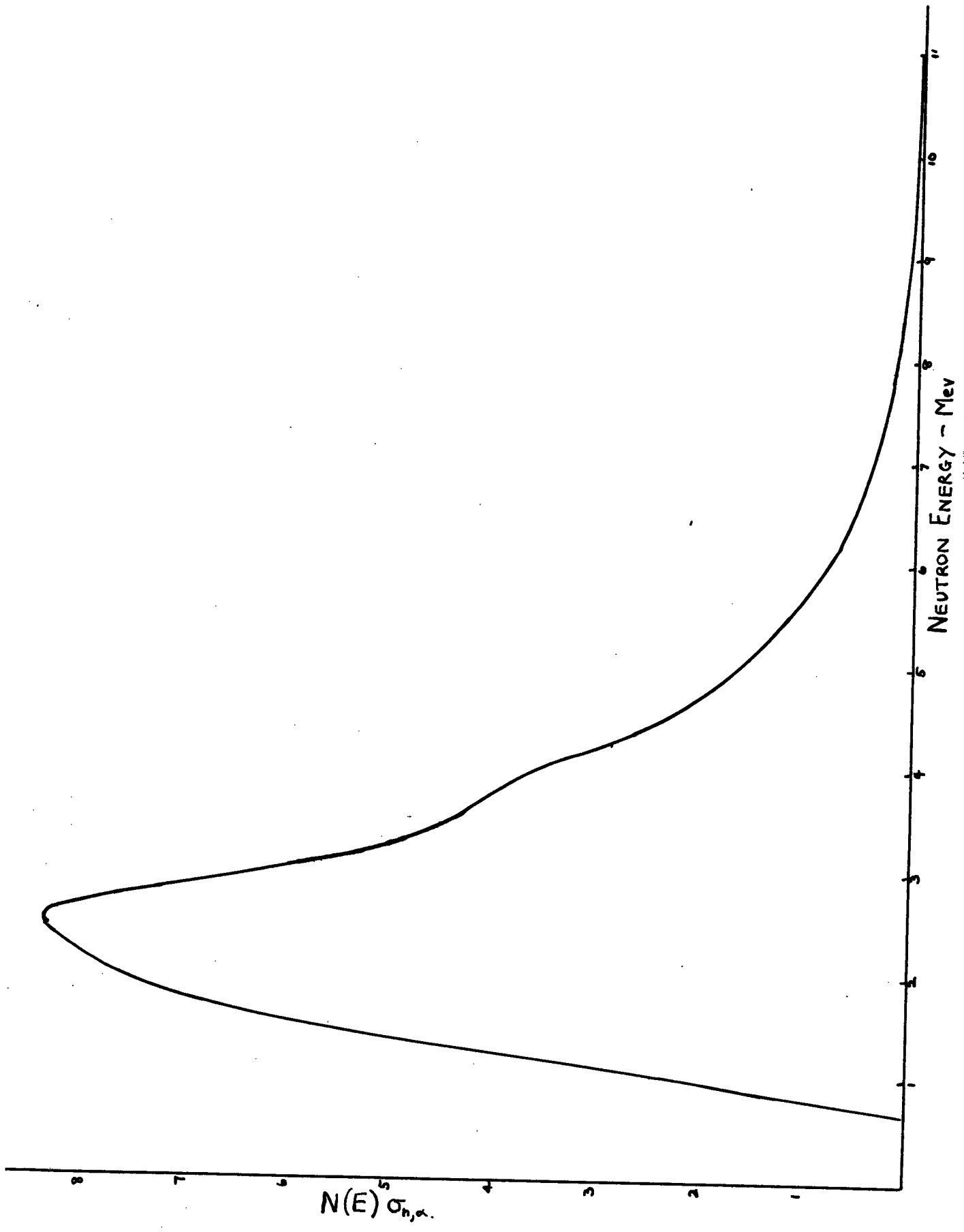
The neutrons from the $\text{C}^{12}(\text{d},\text{n})$ reaction have an energy of about 500 keV, and thus would be recorded in the absolute flux measurements but would not initiate an (n,α) process. The results would be correspondingly low. The $\text{T}(\text{p},\text{n})$ source used by Stelson and Campbell is to be preferred since it is a good continuously variable monoenergetic source. The $\text{Li}^7(\text{p},\text{n})\text{Be}^7$ is also a good source but the two neutron groups present are a disadvantage. Both of the latter sources are capable of high neutron intensities.

Also shown in figure 5 are three values of the (n,α) cross-section obtained by workers at the University of Texas (69), but no details are yet available as to the method of measurement. It is of interest to note however that the curve obtained by combining these results with the rising part of the Stelson and Campbell function can be fitted to a Breit-Wigner resonance curve, whereas the complete function of Stelson and Campbell cannot be fitted to such a curve.

In view of the discrepancy existing in these measurements it was considered that a direct measurement of

FIGURE 7.

$\sigma(n,\alpha)$ for fission spectrum neutrons.



the cross-section integrated over the spectrum of fission neutrons would be desirable. Such a determination, involving the determination of the Li^6 produced in the reaction, will be described later.

II. 4. Correction for helium arising from impurities.

In addition to the foregoing corrections it is necessary in these determinations to include two further possible sources of helium:

(a) The presence of occluded air in the metal.

(b) (n, α) reactions in impurities in the metal.

Since in all determinations it was the practice to perform blank determinations, and no helium was ever found, it is unnecessary to make a correction for helium from source (a). It is more difficult to make a correction for (b).

In order that (n, α) reactions in impurities should give rise to significant quantities of helium a high cross-section value is necessary, and this consideration will exclude fast neutron reactions. Irradiation with thermal neutrons followed by analysis for helium would appear therefore to be sufficient to evaluate the contribution from impurities. Such an irradiation was performed with the following results

Irradiation time = 604.5 hours.

Slow neutron flux = 2.78×10^{10} n/cm²/sec.

Helium/gm beryllium = 3.45×10^{-7} ccs. at S.T.P.

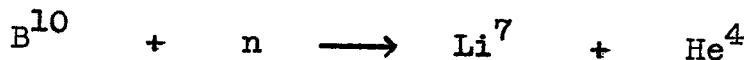
It is expected that this result will be in error by a factor dependent on the fast neutron contamination in the thermal column.

In order to apply such a correction to the helium found in the hollow slug irradiations it is necessary to know the slow neutron flux in these irradiations. Unfortunately the slow flux was not monitored during the hollow slug irradiations, and subsequently measurements yielded slow to fast neutron ratios varying between 1 and 2.5. When the higher of these values is used to compute the slow neutron flux in the hollow slug irradiations, the correction for helium accumulating from the thermal neutrons is approximately 2%. This value represents the upper limit of contamination from this source.

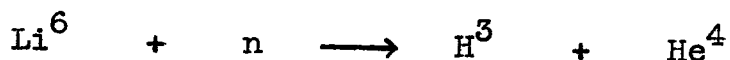
TABLE VI.

<u>Determination</u>	<u>Average analysis</u>	<u>Determination</u>	<u>Average analysis</u>
Total Be	99.1%	Si	600 ppm
Fe	1350 ppm	B	0.5 ppm
Al	300 ppm	BeO	0.80%
Mg	80 ppm	Be ₂ C	0.14%
Cr	100 ppm	Ag	3 ppm
Ni	200 ppm	Co	3 ppm
Cu	100 ppm	Cd	0.2 ppm
Mn	150 ppm	Pb	30 ppm

Table VI (70) gives an average analysis of commercial beryllium. Of the impurities listed only boron would give rise to appreciable helium on slow neutron irradiation by the reaction



The value given together with the isotopic abundance of B^{10} and the slow to fast neutron ratio can be used to evaluate the helium arising from this source. The reaction



should also be considered since it has a very high cross-section for thermal neutrons, and trace quantities of this isotope in beryllium would give rise to significant quantities of helium. A measurement of this isotope was made, and is described later, by estimation of the tritium yield on slow neutron irradiation. Allowance for these two sources of helium gives a correction factor of about 0.5% to the total helium observed in the hollow slug irradiations. In view of the uncertainty introduced by the fast neutron contribution to the thermal column irradiations, this estimate is probably the more reliable, although it may be an overestimate due to use of the highest observed value of the slow to fast neutron ratio.

Since there is some uncertainty in evaluating a correction for helium arising from impurities, the corr-

ection will be ignored in the final result. This is clearly not a serious correction, and is probably a good deal less than the uncertainty existing in the absolute flux values.

II. 5. The $\text{Be}^9(n,2n)\text{Be}^8(\alpha)\text{He}^4$ cross-section.

The helium production cross-section averaged over a fission neutron spectrum, $\bar{\sigma}_{\text{He}}$, is the sum of the contributions from the (n,2n) and (n, α) reactions. Each (n,2n) process yields two helium atoms, and therefore the average helium production cross-section after correction for (γ ,n) produced helium is given by

$$\bar{\sigma}_{\text{He}} = 2\bar{\sigma}_{n,2n} + \bar{\sigma}_{n,\alpha}$$

Accepting the value of $\bar{\sigma}_{n,\alpha}$ obtained by integration of the excitation function of Stelson and Campbell as the contribution from this reaction, and the value deduced for $\bar{\sigma}_{\gamma,n}$, the correction for these contributions is $(33 + 1.8) = 34.8$ millibarns. From table IV the helium production cross-section is 253 ± 4 millibarns. Therefore

$$\bar{\sigma}_{n,2n} = \underline{\underline{109 \pm 4 \text{ millibarns}}}$$

This value is, of course, averaged over the whole of the fission neutron spectrum, whereas the reaction is impossible below the threshold energy of 1.85 MeV. From a graphical integration of the fission neutron spectrum (figure 6) the fraction of fission neutrons with energy

above 1.85 MeV is 0.435, and hence the average cross-section for that part of the fission neutron spectrum where the reaction is energetically possible is (120.6/0.435)

$$\bar{\sigma}_{n,2n}(E \geq 1.85 \text{ MeV}) = \underline{\underline{250.5 \pm 4 \text{ millibarns}}}$$

Interpolating from the results of Sanders and Littler (Table III) this corresponds to an enhancement for a beryllium moderated reactor of + 0.09.

II. 6. Be⁹(n,2n)Be⁸ excitation function.

Suitable sources of monoenergetic neutrons were not available during the course of this work to enable measurements of the excitation function to be made. It is therefore of some interest to compare the results with theoretical predictions.

Attempts to calculate the excitation function for the (n,2n) reaction have been made by Schlogl (71), and by Mamasakhlisov (72). Both authors employ the valence neutron model of Be⁹, which has been applied with some measure of success by Guth and Mullin (64) to the photo-disintegration excitation function of this nucleus. The model has also been used by Caldirola (73) to predict the electro-disintegration function. In this model the final neutron is regarded as moving in the force field of the Be⁸ nucleus, the field being described by a spherical potential well of radius equal to the radius of the

Be^9 nucleus. Using this model Schlogl has calculated the (γ, n) , (n, n) , and $(n, 2n)$ excitation functions, the first two being in reasonable agreement with experiment, but the $(n, 2n)$ cross-section is too low. The calculations are given for various assumed nuclear radii, showing a strong dependence on this. Even for the smallest radius assumed the peak cross-section is only 10 millibarns. The predicted shape (figure 8) is however that which would be expected for an endoergic reaction with subsequent neutron emission (74).

Mamasakhlisov gives his results in the following form

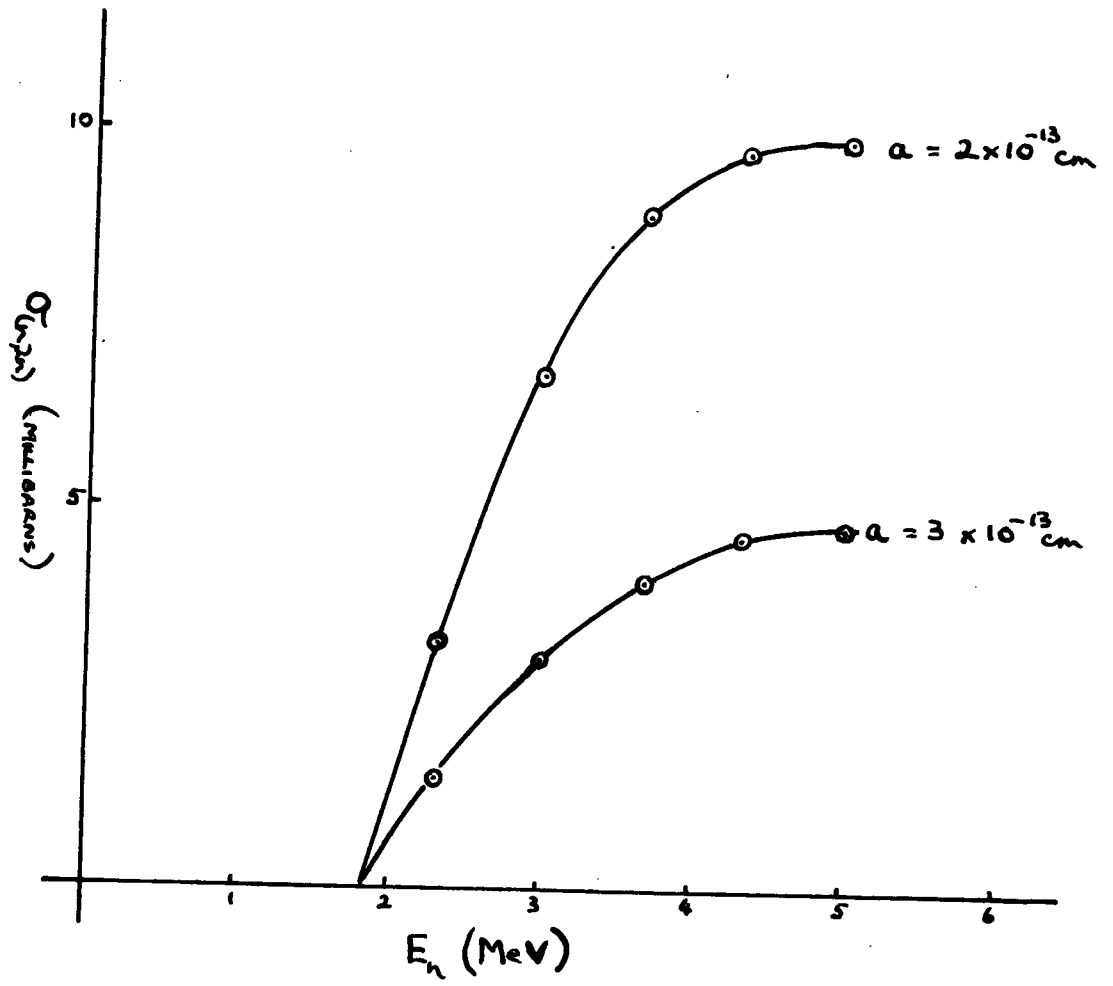
$$\sigma_{n, 2n} = 0.08 \times 10^{-24} \frac{(\gamma - 1)^2}{\sqrt{\gamma}} \text{ cm}^2$$

where $\gamma = E/e$, E being the incident neutron energy, and e the binding energy of the final neutron in the Be^9 nucleus. The shape of this function near the threshold has more the form to be expected for an endoergic reaction with charged particle emission (74), than for neutron emission. For high incident neutron energies the function increases as $\gamma^{3/2}$ and becomes infinite for very high energies, whereas for high incident neutron energies the cross-section would be expected to approach the geometrical cross-section πR^2 , where R is the nuclear radius. At 14 MeV the predicted cross-section of 1.5 barns is equal to the total cross-section, and the total inelastic cross-

FIGURE 8.

Be⁹(n,2n) excitation function.

Schlögl (71).



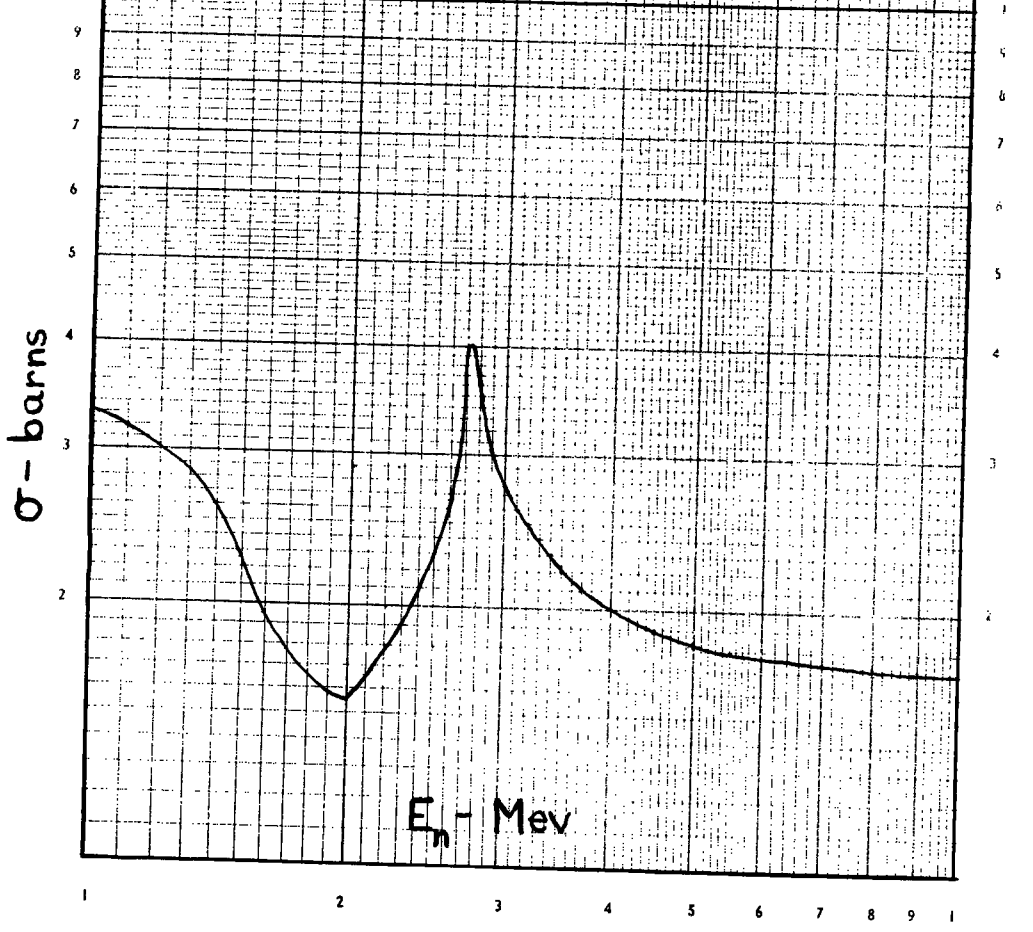
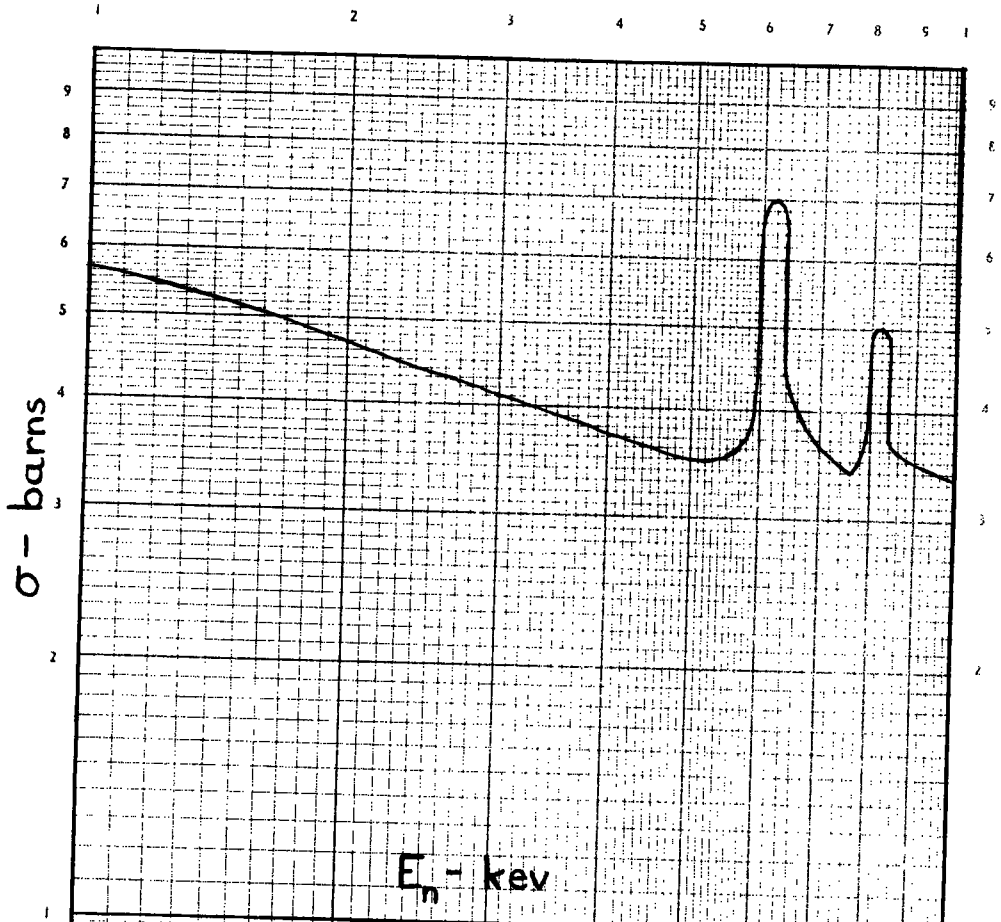
section at this energy is about 350 millibarns. Mamasakhliov claims good agreement with the results of Funfer and Bothe (18), namely 0.3 barns averaged over the Ra- α -Be spectrum. For this average he has taken the mean energy of the spectrum to be 6 MeV. When his spectrum is averaged over the spectrum quoted by Dacy, Paine, and Goodman (75) the result is 0.2 barns which is in reasonable agreement with some of the values quoted in Table II. Over a fission neutron spectrum the value of the average cross-section is 35 millibarns. The agreement obtained with the natural sources is probably due to the higher mean energy, and in this region the function of Mamasakhliov is rising steeply.

The model cannot be regarded as useful in the case of the (n,2n) reaction. The authors have assumed that a single potential well is sufficient to specify the system, whereas Guth and Mullin require different potential wells to treat different transitions. In addition the photo-disintegration is a very much weaker interaction, as evidenced by its smaller cross-section, and hence will involve weak perturbations of the nucleus.

There are two possible mechanisms for the (n,2n) reaction in beryllium. In the first the incident neutron is inelastically scattered leaving the Be^9 nucleus in an excited state which subsequently decays by emission of a neutron, i.e., $\text{Be}^9(n,n')\text{Be}^{9*}(n')\text{Be}^8$

FIGURE 9.

Total neutron cross-section of beryllium (5).



Evidence for this mechanism is given by Fowler, Owen, and Hanna (37) who have observed two neutron groups emerging from the interaction of Be^9 with 3.7 MeV neutrons. The second is a 'knock-on' process in which the incident neutron shares its energy with a bound neutron which is emitted, the nucleus being left with sufficient excitation to 'boil-off' a further neutron.

Fowler, Owen, and Hanna suggest that the excited state of Be^9 involved in this process is the 2.43 MeV level, this being the only accepted level in this energy range. Reference to the total cross-section curve of beryllium (figure 9) shows a broad resonance at an incident neutron energy of 2.75 MeV, this energy, when allowance is made for momentum transfer in the reaction, corresponds to about 2.4 MeV excitation. At this excitation the Be^9 nucleus is unstable to neutron emission by 0.76 MeV, and thus a broad resonance for neutron emission would be expected, making the proposed mechanism highly probable. However the results of several experimenters suggest that the width of this level for neutron emission is extremely narrow. Thus in a study of the reaction $\text{B}^{11}(\text{d}, \alpha)\text{Be}^{9*}$ Van Patter and collaborators (76) conclude that the neutron width of the 2.43 MeV state of Be^9 is 5 keV, and neutron emission is improbable. Dissanaiké and Newton (77) found that whilst this level decayed by neutron emission the level width was small, and they attribute this to the possibility of a large

spin change in the decay. Other workers report a narrow width, the most recent report being that of Gossett et al., (78) who conclude that the state has no observable natural width, and assign an upper limit of 1 keV for the natural width of the state. The conclusion is that a high spin change occurs in neutron emission from this excited level, and thus such transitions are strongly inhibited. This also receives some support from the absence of a resonance in the photo-disintegration excitation function at this energy (64). Thus the mechanism proposed by Fowler et al., whilst still possible, becomes less probable.

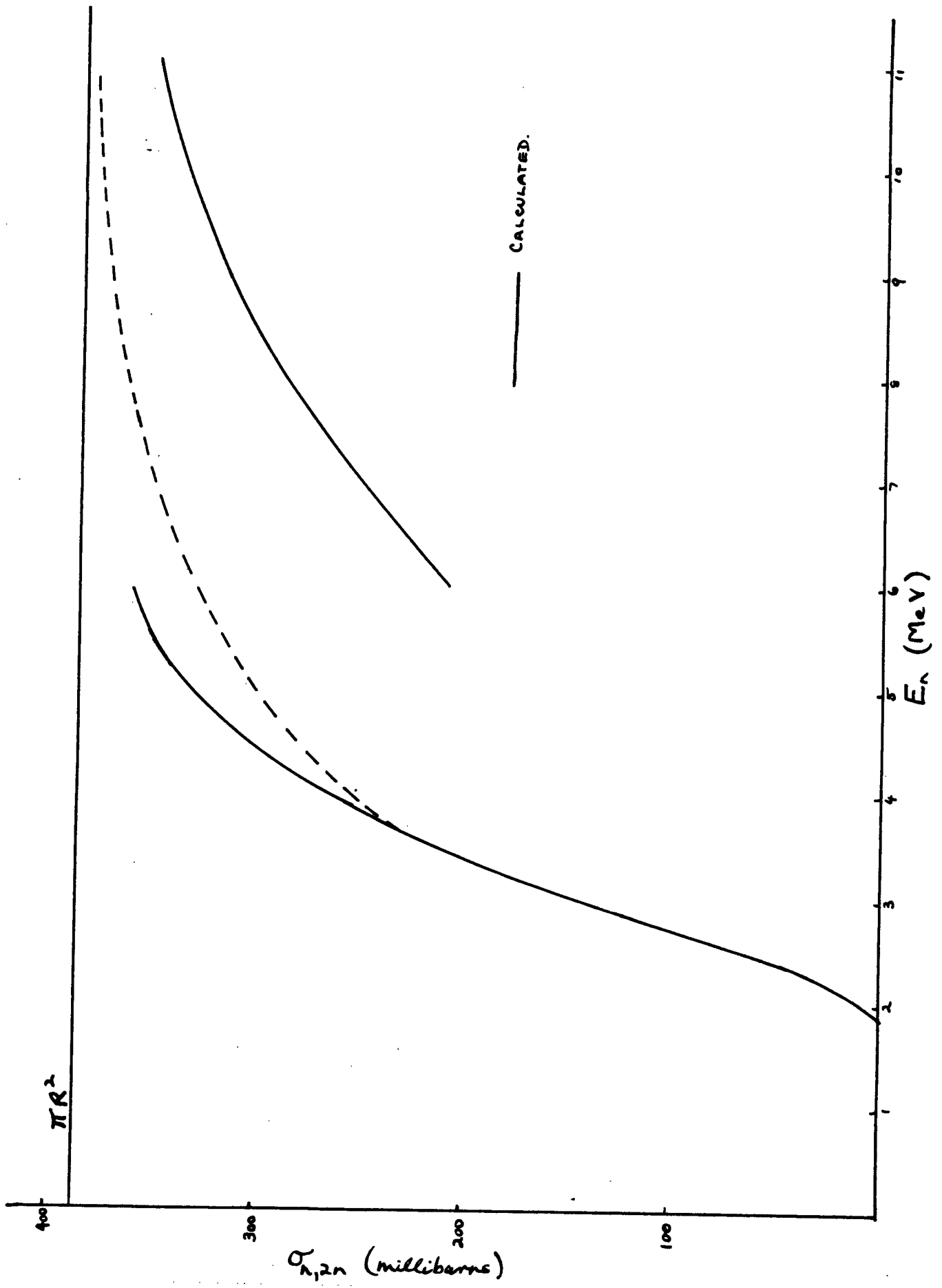
The second method corresponds to the 'evaporation model' of the compound nucleus (79). On this model the $(n,2n)$ cross-section is given by

$$\sigma(n,2n) = \underline{\underline{\sigma_c \left[1 - \left(1 + \frac{e}{\theta} \right) \exp\left(-\frac{e}{\theta}\right) \right]}}$$

where σ_c is the cross-section for the formation of the compound nucleus, θ the 'nuclear temperature', and e is the difference between the incident neutron energy and the threshold energy. This formula is only strictly applicable to nuclei of medium and high mass number where the concept of the nuclear temperature can be applied owing to the density of energy levels in such nuclei. In view of the development of methods for studying the energy distribution of emitted particles in reactions, data which enables the nuclear temperatures to be com-

FIGURE 10.

Be⁹(n,2n) excitation function (I).



puted (79), and the application of such methods by Gugelot (80) to the measurement of nuclear temperatures, it becomes of some interest to examine the predictions of this model.

Paul and Clarke (37) have used the above formula to examine the results of their measurements of 34 (n,2n) reactions, the experimental results showing good agreement with theory in most cases. Cohen (81) has also applied the theory to a number of elements, including a number of the lighter ones. Gugelot has assigned nuclear temperatures to the nucleus Be^9 , and since the parameters in the formula for the 'nuclear temperature' are slowly varying functions of the mass number it seems reasonable to use these values for the nucleus Be^9 .

It is necessary to know the cross-section for compound nucleus formation σ_c . Paul and Clarke (39) have used values of σ_c quoted by Phillips (82), and Cohen has argued that since the neutron faces no Coulomb barrier the cross-section for compound nucleus formation is simply the geometrical cross-section πR^2 . Figure 10 shows the excitation function computed for Be^9 using the geometrical cross-section, and the nuclear temperatures of Gugelot. The nuclear temperatures are

$$\theta = 2.3 \pm 0.3 \text{ MeV} \quad \text{for } e > 4 \text{ MeV}$$

$$\theta = 0.9 \pm 0.1 \text{ MeV} \quad \text{for } 1 < e < 4 \text{ MeV}$$

and in the function presented the break which would

occur at 4 MeV by strict adherence to these temperatures has been smoothed out. The radius used is that given by Cook and Bonner, 3.51×10^{-13} cms., and corresponds to a geometrical cross-section of 386.5 millibarns (83). The cross-section integrated over a fission spectrum is

$$\sigma_{n,2n} = \underline{64.75 \text{ millibarns}}$$

the result being lower than the experimental value. This low result probably arises from the use of the geometrical cross-section, which cannot be expected to apply at such low energies. σ_c can however be computed from the compound nucleus theory.

The treatment used is that of the continuum theory given by Blatt and Weisskopf (79), and is here restricted to S wave neutrons ($l = 0$). For this condition the capture cross-section is given by

$$\sigma_{c,0} = \pi\kappa^2 \frac{4kK}{(k+K)^2} \quad (\text{neutrons, } l=0)$$

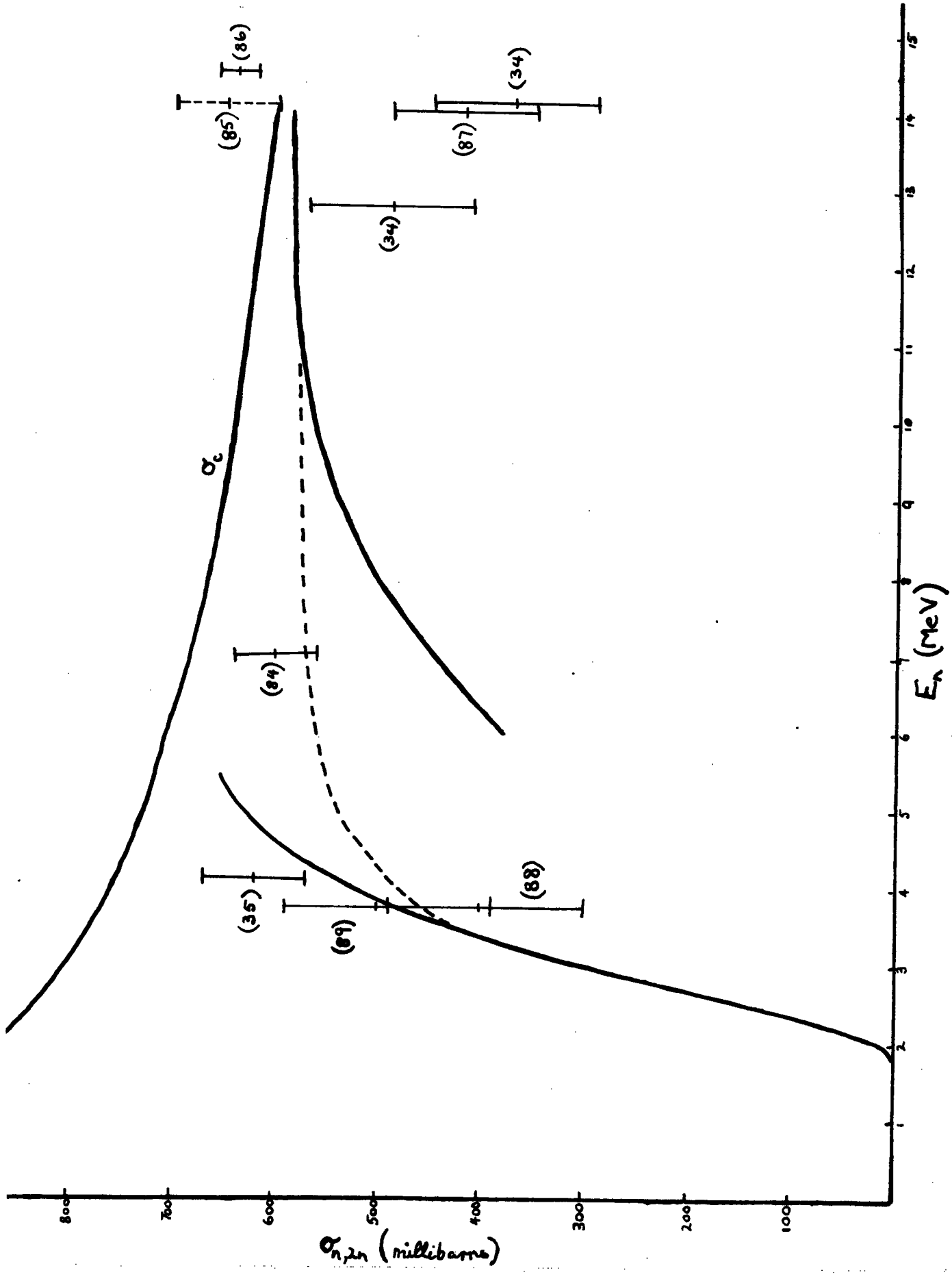
where k is the wave number of the incident particle outside the nucleus, K the wave number after penetration of the nuclear surface, and $\kappa = \lambda/2\pi$, λ being the neutron wavelength. It is shown (79) that K is given by

$$K = \sqrt{K_0^2 + k^2}$$

where $K_0 = 1 \times 10^{13} \text{ cm}^{-1}$, for incident nucleons. Values of $\sigma_c/\pi R^2$ as a function of $x=kR$ for various $X_0 = K_0 R$, are given by Blatt and Weisskopf (79), and from these the curve σ_c against incident neutron energy E (figure 11)

FIGURE 11.

Be⁹(n,2n) excitation function (II).



has been obtained. Using these values and the nuclear temperatures of Gugelot the excitation function of figure 11 has been computed. The integration of this excitation function over the spectrum of fission neutrons gives an average cross-section of

$$\bar{\sigma}_{n,2n} = \underline{117 \text{ millibarns}}$$

This is in better agreement with the experimental value of 109 ± 4 millibarns.

Table VII: Total inelastic collision cross-section.

Neutron Energy (MeV)	$\sigma_{\text{inel.}}$ (barns)	Reference
4.0	0.62 ± 0.05	(35)
7.0	0.60 ± 0.04	(84)
12.7	0.49 ± 0.08	(34)
14.1	0.37 ± 0.08	(34)
14.1	0.65^*	(85)
14.5	0.64 ± 0.02	(86)
14.0	0.42 ± 0.07	(87)

* A reported preliminary value - $(\sigma_t/\sigma_1) - 1 = 2.25$
 Values of σ_t obtained from 'Neutron Cross-section Data', Brookhaven National Laboratory, B.N.L. 325, U.S.A.E.C. Document.

Table VII gives a number of determinations of the total inelastic cross-section measured by the sphere transmission technique. The points at 4 and 7 MeV are in good agreement with the derived curve (figure 11) when allowance is made for the contribution of the (n, α)

reaction. At higher energies the spread in the experimental results is much broader but the results are of the same order as the derived curve. Reference to the work of Taylor, Lonsjo, and Bonner (34) indicates that for many nuclei studied, the total inelastic excitation functions flatten out at higher excitation energies, and hence the shape of the computed (n,2n) excitation function for beryllium appears to be justified. Fowler, Owen, and Hanna (88) give the cross-section at 3.7 MeV as 400 ± 100 millibarns. Huber and Wagner (89) have measured the differential cross-section at this energy at 90° to the incident neutron beam obtaining $\sigma_{\text{diff}}(90^\circ) = 39 \pm 8$ mb/stearadian. If spherical symmetry of emission is assumed, and the results of Fowler (90) would seem to indicate that this is approximately so, then the cross-section is calculated as 490 ± 100 millibarns. All these determinations are shown in figure 11 with their associated errors.

The agreement between the experimental and calculated values of the integrated cross-section is remarkable in the case of a light element such as beryllium. The treatment has been restricted to the interaction of S-wave neutrons ($l = 0$), but it is certain that at the high energies involved some P-wave interaction must occur. This latter would have the effect of increasing the value of the calculated cross-section. It would seem probable that the neglect of this contribution is compensated

by ignoring the contribution of 'capture elastic scattering' to the capture cross-section.

Table VIII: Calculated values of $\sigma_{n,2n}$

Incident neutron energy E_n	Nuclear Temperature T	Excitation energy $E_n - E_t$	Capture cross- section σ_c	$n,2n$ cross- section $\sigma_{n,2n}$
2.0	0.9	0.15	869	13.4
2.5	0.9	0.65	832	135.4
3.0	0.9	1.15	799	293
3.5	0.9	1.65	775	354
4.0	0.9	2.15	760	524
4.5	0.9	2.65	745	587
5.0	0.9	3.15	730	631
6.0	2.3	4.15	707	380
7.0	2.3	5.15	684	448
8.0	2.3	6.15	668	498
9.0	2.3	7.15	657	537
10.0	2.3	8.15	645	560
11.0	2.3	9.15	634	575
12.0	2.3	10.15	622	581
13.0	2.3	11.15	611	583
14.0	2.3	12.15	603	584

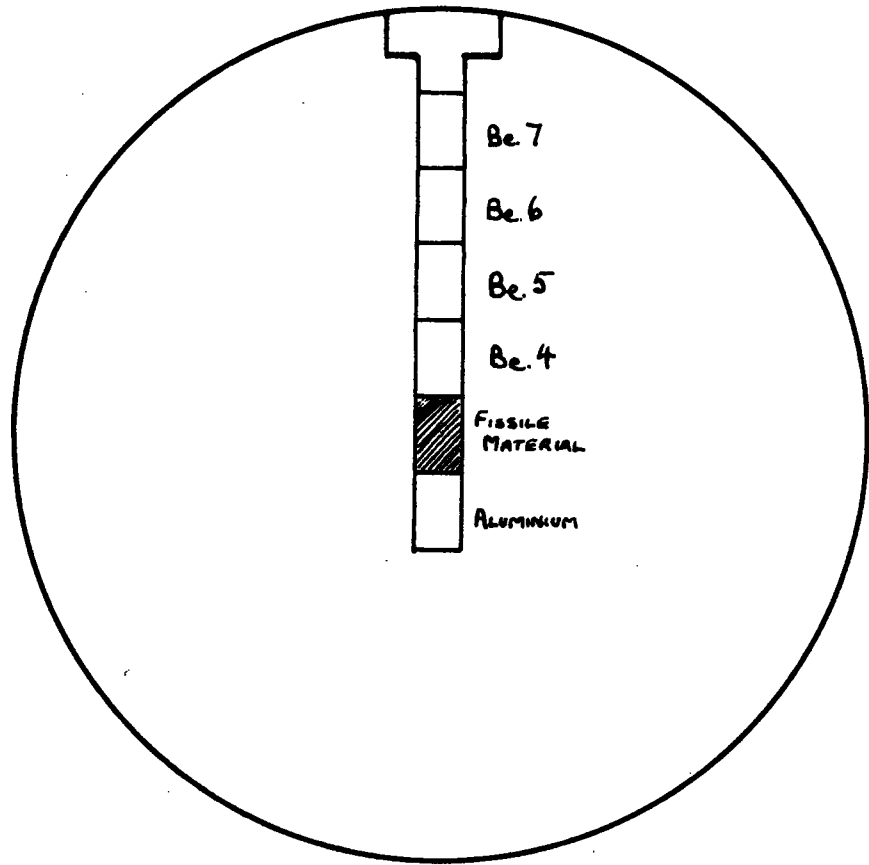
II. 7. Measurement of the enhancement δ

This experiment was performed at the request of the Reactor Physics Group at Harwell, who were to be responsible for the calculation of the enhancement δ from the experimental results. At the time of writing the calculations were not available, but the experimental arrangement and results are given.

The experimental arrangement is that suggested by Sanders and Littler (29) and is illustrated in figure 12. An 11 cm. beryllium sphere having an 0.5 cm diameter hole drilled along a radius, the hole extending 1.5 cms. beyond the centre of the sphere, was packed with cylindrical slugs of length 1 cm. and diameter 0.5 cms. The

FIGURE 12.

Beryllium sphere experiment.



first slug was of aluminium for use as a neutron monitor. The second was of fissile material situated such that its centre coincided with the centre of the beryllium sphere, and this was followed by four beryllium slugs. Thin cobalt foils were placed between the slugs to monitor the slow neutron flux. The whole sphere was then immersed in a slow neutron flux provided by one of the experimental holes in the thermal column of BEPO, these neutrons being converted to a fission flux by interaction with the fissile material.

After a suitable irradiation period the beryllium slugs were removed and analysed for helium. A further irradiation was performed without the fissile material at the centre in order to check the system for the effects of 'background'. The results of these measurements are given in Table IX.

As can be seen from the table of results the slow neutron effect is quite large and since there is no interaction which can give rise to helium directly from beryllium with neutrons of this energy the following effects are suggested:

- (a) Contamination of the slow neutron flux by fast neutrons.
- (b) The presence of boron and lithium impurity in the beryllium metal would give rise to helium

TABLE IX. Helium measurements on beryllium sphere.

Sample position	Radial distance r cms.	Mass gms.	He found cc. x 10 ⁷ at S.T.P.	He/gm. Be cc. x 10 ⁷ at S.T.P.	He/gm. Be $\frac{He}{gm. Be} \times r^2$
<u>Irradiation time: 193.5 hrs. Slow neutron flux: 2.5 x 10¹⁰ n/cm²/sec.</u>					
1	1	0.5825	8.28	14.2	11.9
2	2	0.5865	2.58	4.40	8.2
3	3	0.5503	1.545	2.81	4.14
4	4	0.5851	1.75	2.99	0.64
<u>Blank irradiation with no fissile material</u>					
<u>Irradiation time: 153.5 hrs. Slow neutron flux: 2.68 x 10¹⁰ n/cm²/sec.</u>					
3	3	-	1.013	-	-
4	4	0.5815	1.083	1.86	-

** The figure 1.86 x 10⁻⁷ cc./gm. Be has been taken as the contribution of the 'slow neutrons', and after correction for different irradiation time and flux this implies a contribution of 2.35 x 10⁻⁷ cc./gm. Be in the fission flux irradiation. This quantity has been deducted from the observed helium.

on slow neutron irradiation.

Since in order to obtain the high thermal neutron exposures required to accumulate sufficient helium for measurement, the sphere was placed as near the reactor system as possible, some exposure to fast neutrons was unavoidable. Using the value given in Table IV (page 23) for the helium production cross-section averaged over a fission spectrum, the fission neutron flux required to accumulate the quantity of helium observed for the slow neutron irradiation can be calculated. This flux is 4.5×10^8 neutrons/cm² seconds, and corresponds to 1.8% of the slow neutron flux. This value has little meaning however since the fission neutron spectrum would be considerably degraded by the time these neutrons reach the thermal column, and it is only useful in illustrating the order of magnitude of fast neutron contamination required.

The contamination due to impurities can be estimated. Thus the value for boron (5 ppm) given in Table VI (page 39), together with the thermal neutron cross-section of natural boron (754 barns) and the flux values used in this determination indicate that the helium accumulating from this source is about 1.16×10^{-7} ccs./gram of beryllium. This represents some 60% of the observed helium. Using the value observed for the earlier slow neutron irradiation

(page 38) the contamination from this source is estimated at 0.85×10^{-7} ccs./gram of beryllium, and represents about 45% of the observed helium. These figures indicate an appreciable fast neutron effect.

It will be observed that only the outermost positions of the slugs were checked for the slow neutron effect (Table IX), since it was not expected that this would be appreciable. The value obtained for the slow neutron effect has therefore been deducted from the values observed with the converter present, and these 'corrected' values are given in Column 6, Table IX. In view of the fast neutron contribution in the thermal irradiation this practice is questionable, since some decrease in the fast contribution would be expected on penetration of the sphere. However it is not possible to estimate the extent of this decrease.

The aluminium monitor indicated a fission flux of 3.28×10^9 neutrons/cm²/second, and this should be approximately the same for beryllium sample 1. Using the value of the helium production cross-section obtained from the hollow slug irradiations (Table IV) the helium accumulating in beryllium sample 1 can be calculated, the value obtained being 12.9×10^{-7} ccs./gram of beryllium. This is to be compared with the 'corrected' observed value of 11.9×10^{-7} ccs./gram of beryllium. The agreement between these values is

reasonable when the uncertainties in these measurements are considered. Somewhat better agreement is obtained if one disregards the fast neutron contribution in the thermal irradiation, and uses the value calculated from the earlier slow neutron measurement (page 38) to correct for the slow neutron effect.

Unfortunately it is not possible to estimate the fission flux through the other beryllium samples with the present experimental arrangement. The non-uniform distribution of points of origin of the fission neutrons makes it virtually impossible to calculate solid angles for these samples.

It had been hoped that the mode of fall-off of helium concentration would enable the enhancement δ for an infinite moderating system to be calculated. An examination of the present results (114) suggests that a worthwhile precision cannot be obtained with the present experimental arrangement, and this experiment was therefore abandoned. In the design of a future experiment on these lines the following points deserve attention,

- (a) The variation of slow neutron flux along the radius of the sphere.
- (b) The relative contributions of slow neutron reactions (e.g. on boron impurity, the lithium contribution being negligible - Chapter III).

and of reactions induced in the beryllium itself by the fast neutron 'tail' still present with the 'slow' neutrons.

- (c) Arrangement of the fissile material in such a manner that points of origin of the fission neutrons is uniform, or at least makes possible a calculation of effective solid angles of the beryllium slugs.
- (d) A reduction in the size of the beryllium slugs. The present method of helium analysis is capable of sufficient sensitivity to perform the analysis on samples of beryllium five to ten times smaller than those used in this experiment, without much sacrifice in accuracy. Such samples would enable many more points to be obtained on the helium concentration curve.

The enhancement δ for an infinite beryllium moderator could be calculated were an excitation function for the $n,2n$ reaction available. This could be most easily obtained by the helium method using suitable mono-energetic neutron sources. Alternatively, the excitation function deduced in the preceding pages would appear to give sufficient agreement with experiment to justify its use for this purpose. Together with the known n,α excitation function, this data could be submitted to a 'Monte-Carlo' calculation (58) in

order to obtain δ .

II. 8. Measurement of neutron fluxes (114).

The threshold reactions used to monitor the fission flux during these irradiations were the $\text{Al}^{27}(\text{n},\alpha)\text{Na}^{24}$ and $\text{Mg}^{24}(\text{n},\text{p})\text{Na}^{24}$. In a separate series of measurements the cross-section for these reactions were compared with those of the $\text{Al}^{27}(\text{n},\text{p})\text{Mg}^{27}$, and $\text{S}^{32}(\text{n},\text{p})\text{P}^{32}$ reactions. All these cross-sections have been measured in terms of the fission cross-section of U^{238} in a fission spectrum, this being taken as 0.304 barns (114). The accuracy of the fission flux measurements is 5%. Thermal fluxes were measured using Co^{59} detectors, the thermal cross-section being taken as 37.0 barns (5). The experimental error in the thermal fluxes is estimated at 2%.

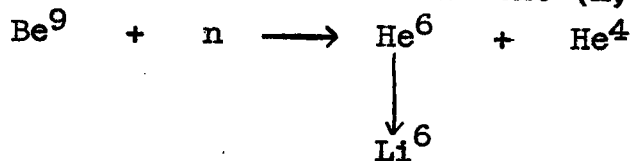
CHAPTER III.

The production of tritium in beryllium.

III. 1. The reaction $\text{Be}^9(n,\alpha)\text{He}^6$.

An essential requirement in the determination of the $\text{Be}^9(n,2n)\text{Be}^8$ cross-section by the helium method is an accurate knowledge of the helium produced by the $\text{Be}^9(n,\alpha)\text{He}^6$ reaction. As was pointed out earlier there is some uncertainty in the published values for the cross-section of the latter reaction, and this uncertainty is the major source of error in the value deduced for the $(n,2n)$ cross-section. In addition the published cross-section values for the (n,α) reaction cover a limited, but nevertheless important, range of the fission neutron spectrum. It was therefore considered that an independent measurement of this cross-section should, if possible, be made covering the whole range of the fission neutron spectrum.

A suitable method of measurement is suggested when one considers in more detail the (n,α) reaction.



One of the immediate products of the reaction, He^6 , is β -active with a half-life of 0.83 seconds, and results in the production of the stable isotope Li^6 . The half-life of He^6 is much too short to hope to measure its β -activity after extraction from the beryllium, but the Li^6 produced undergoes reaction with thermal neutrons to produce tritium with a half-life of 12.5 years which can be extracted and measured.



It is apparent therefore that a measurement of the tritium produced on irradiation in a known neutron flux (thermal) will enable the amount of Li^6 formed to be determined, and this will give the $\text{Be}^9(n,\alpha)\text{He}^6$ cross-section. A method for the analysis of trace quantities of tritium in beryllium was developed, and is described in Chapter VI.

Under the conditions of irradiation of beryllium in a hollow uranium slug in a nuclear reactor, the sample is subjected to the simultaneous action of a direct fission flux, and a thermal flux. The above reaction sequence resulting in the production of tritium will therefore occur.

Let N_0 = Total number of Li^6 atoms produced.

N_{Be} = Number of beryllium atoms irradiated.

N_{Li} = Number of Li^6 atoms present.

N_{T} = Number of H^3 atoms produced

ϕ_f = Fission neutron flux.

ϕ_s = Slow neutron flux.

t = Time of irradiation.

σ_α = $\text{Be}^9(n,\alpha)\text{He}^6$ cross-section.

σ_T = $\text{Li}^6(n,\alpha)\text{H}^3$ cross-section.

Rate of production of Li^6

= Rate of production by $\text{Be}^9(n,\alpha)$ - Rate of $\text{Li}^6(n,\alpha)$

i.e.

$$\frac{d}{dt}(N_{\text{Li}}) = N_{\text{Be}} \cdot \phi_f \cdot \sigma_\alpha - N_{\text{Li}} \cdot \phi_s \cdot \sigma_T$$

This may be written as

$$\frac{d}{dt}(N_{\text{Li}}) + \phi_s \cdot \sigma_T \cdot (N_{\text{Li}}) - N_{\text{Be}} \cdot \phi_f \cdot \sigma_\alpha = 0$$

The solution of this equation being

$$N_{\text{Li}} = \frac{\phi_f \cdot \sigma_\alpha \cdot N_{\text{Be}}}{\phi_s \cdot \sigma_T} \left\{ 1 - \exp(-\phi_s \cdot \sigma_T \cdot t) \right\}$$

The total number of lithium atoms produced (N_0) is given by

$$N_0 = N_{\text{Be}} \cdot \sigma_\alpha \cdot \phi_f \cdot t$$

and hence the number of tritium atoms is

$$\begin{aligned} N_T &= N_0 - N_{\text{Li}} \\ &= \phi_f \cdot \sigma_\alpha \cdot N_{\text{Be}} \left\{ t - \frac{1}{\phi_s \cdot \sigma_T} + \frac{\exp(-\phi_s \cdot \sigma_T \cdot t)}{\phi_s \cdot \sigma_T} \right\} \\ &= \phi_f \cdot \sigma_\alpha \cdot N_{\text{Be}} \left\{ \frac{\phi_s \cdot \sigma_T \cdot t^2}{2} - \frac{\phi_s^2 \cdot \sigma_T^2 \cdot t^3}{6} + \dots \right\} \end{aligned}$$

Neglecting powers of t higher than t^2 , and also the decay

of tritium, this gives

$$\underline{N_T = \frac{1}{2} N_{Be} \cdot \sigma_T \cdot \sigma_\alpha \cdot \phi_s \cdot \phi_f \cdot t^2}$$

Thus a measurement of the total number of tritium atoms produced with known thermal and fission neutron exposures enables the $Be^9(n,\alpha)He^6$ cross-section to be determined.

The quantities of tritium obtained proved to be much higher than expected, and this at first suggested that the direct production of tritium by the fast neutron reaction $Be^9(n,H^3)Li^7$ might occur with an appreciable cross-section within the spectrum of fission neutrons. A measurement of this cross-section for neutrons of 14 MeV incident energy was attempted, and is described later.

III. 2. Experimental and results:

Samples of beryllium were irradiated inside one of the hollow slugs of uranium in the BEPO pile at Harwell. The fission neutron flux was monitored using the $Ni^{58}(n,p)$ reaction, the cross-section of this reaction being subsequently measured in terms of the U^{238} fission cross-section. The flux values are therefore consistent with the earlier determinations of $\bar{\phi}_{He}$ for fission neutrons. The thermal fluxes were measured using the reaction $Co^{59}(n,\gamma)Co^{60}$, for which the thermal neutron cross-section was taken as 37.0 barns. The

beryllium samples were removed after a known time and analysed for tritium. The analytical method is described in Chapter VI.

Altogether three irradiations were performed, and for the first two of these small pieces of cast beryllium of 50 to 100 milligrams weight were used. In order to ensure that the samples analysed were subject to the same neutron exposures, the third irradiation was performed using a cylindrical specimen of beryllium from which small pieces were cut for the tritium analysis. The material in this case was fabricated by a powder metallurgical process. The results of these determinations are given in Table X.

In addition to these irradiations the beryllium was checked for Li^6 impurity by irradiations in the thermal column of the pile. The material used for these determinations was the same as that used in the hollow slug irradiations. The results of these measurements gave the following Li^6 contents:

Cast beryllium :- $1.5 \pm 0.5 \times 10^{-9}$ grams $\text{Li}^6/\text{gm. Be}$

Sintered beryllium :- 4.9×10^{-9} grams $\text{Li}^6/\text{gm. Be}$

In Table X the column given as Tritium 'background' gives the correction to be applied for tritium produced from Li^6 impurity, allowance being made for the thermal flux in the hollow slug irradiations.

Table X. Tritium produced in neutron-irradiated beryllium.

Irradiation number		I	II	III
Fission neutron flux (neutrons/cm ² seconds x 10 ⁻¹¹)	ϕ_f	4.76	2.41	2.57
Fission neutron exposure (neutrons/cm ² x 10 ⁻¹⁷)	$\phi_{f \cdot t}$	10.5	2.49	2.27
Slow neutron flux (neutrons/cm ² seconds x 10 ⁻¹¹)	ϕ_s	4.67	6.07	5.15
Slow neutron exposure (neutrons/cm ² x 10 ⁻¹⁷)	$\phi_{s \cdot t}$	10.3	6.27	4.55
Tritium content (total) (atoms/gram beryllium x 10 ⁻¹¹)		34.9 ± 0.3	9.34	11.5 ± 0.2
Tritium 'background' (atoms/gram beryllium x 10 ⁻¹¹)		1.48	0.90	2.14
Corrected tritium (atoms/gram beryllium x 10 ⁻¹¹)	N _t	33.5 ± 0.3	8.44	9.36 ± 0.2
----- Irradiations within cadmium sheath -----				
Fission neutron flux (neutrons/cm ² seconds x 10 ⁻¹¹)	ϕ_f	-----	2.67	2.51
Fission neutron exposure (neutrons/cm ² x 10 ⁻¹⁷)	$\phi_{f \cdot t}$	-----	2.76	2.22
Tritium content (atoms/gram beryllium x 10 ⁻¹¹)		-----	7.0 ± 0.21	1.31 ± 0.02

The results of the first irradiation showed an unexpectedly high tritium content. Subsequent irradiations were therefore performed with some of the material sheathed in cadmium in an attempt to measure the fast neutron contribution to the total production of tritium. The results of these measurements are given in Table X.

The results given in Table X are expressed, where appropriate, as the arithmetic mean of the determinations. The determinations were always performed as soon as possible after removal from the pile, and in general were performed on successive days. Even with this short delay successive measurements of the radioactivity of the hydrogen fraction always showed a decrease with time, and this together with the high activity observed suggested that some short-lived products might be present. Consequently the tritium collected from one determination was observed in the gas counter over a period of time. No decrease in activity was observed over a 14 day period, at the end of which the counter became unstable and measurements could not be continued. During the period of observation the fluctuations in observed counts were no more than would be expected from statistical considerations.

After about six months the beryllium samples from irradiation III were examined again with the following result (91):

Normal irradiation :- 2.38×10^{11} atoms H^3 /gram Be.
Cadmium sheathed irradiation :- 2.83×10^9 atoms H^3 /gram Be.
Thermal irradiation :- 2.83×10^9 atoms H^3 /gram Be.

The tritium 'background' correction to be applied to this result from the normal irradiation, after allowance for decay over a six month period, is 2.12×10^{11} atoms H^3 /gram beryllium. Comparison with the results of Table X for the same irradiation indicates that a considerable loss in activity has occurred, and this loss is too great to account for by tritium decay.

In addition to the pile irradiations, an attempt was made to observe the $Be^9(n,H^3)Li^7$ reaction and to measure its cross-section for 14 MeV neutrons. This reaction has not previously been observed but should be energetically possible at neutron energies greater than 11.6 MeV, its calculated threshold energy. The reaction $H^3(d,n)He^4$ was used as a source of 14 MeV neutrons, the target consisting of tritium adsorbed on a zirconium foil. The neutron flux was monitored using the $Mg^{24}(n,p)Na^{24}$ reaction, and the time variations of the flux were observed throughout the irradiation by means of a boron trifluoride counter.

(a) Irradiation details:

The beryllium used in these irradiations was in the form of turnings sieved to 24 standard mesh. The

magnesium monitor was in the form of small plates about 2 millimeters square obtained as clippings from magnesium ribbon. Suitable quantities of beryllium and magnesium (about 100 milligrams) were mixed together and sealed into a polythene envelope 1 cm. square. This envelope was then strapped to the back of the tritium target, the envelope being separated from the zirconium foil by a layer of brass. The deuteron beam was then switched on, and the time variation of the neutron flux was observed using a boron trifluoride counter in a fixed geometry relative to the target, the total counts being recorded at regular intervals. At the end of the irradiation the polythene envelope was opened and the beryllium and magnesium were then separated from one another. This separation was readily accomplished using a pair of forceps. The beryllium was immediately examined for tritium content, and the magnesium was examined for Na^{24} activity in order to determine the neutron exposure.

The magnesium after weighing was placed in a standard volumetric flask, and a sufficient quantity of concentrated hydrochloric acid added to dissolve completely the metal. The solution was then made up to a standard volume with distilled water. Aliquots of this standard solution were then transferred to a liquid counter of known counting efficiency for Na^{24} , and the activity observed over about two half-lives (30 to 40 hours observation). The decay curve was used to obtain the activity

at the end of the irradiation, and a correction applied for decay during irradiation, allowance for the time variation of the neutron flux being made. The total activity A_0 produced during the irradiation was thus obtained, the total neutron exposure being given by the expression,

$$\phi \cdot t = \frac{A_0}{\lambda \cdot N \cdot \sigma}$$

where λ is the disintegration constant of Na^{24} , N the total number of atoms of magnesium irradiated, and σ is the cross-section of the reaction $\text{Mg}^{24}(n,p)\text{Na}^{24}$ for 14 MeV neutrons (39).

The liquid counter was calibrated for Na^{24} in the following manner. Na^{24} was prepared by pile irradiation of a sample of sodium carbonate, and a standard solution of this sample was prepared. Weighed aliquots of this standard solution were evaporated on to counting trays consisting of a thin film of plastic (V.Y.N.S.). The prepared trays were then counted over two half-lives in a 4π -counter, and from this the absolute activity of the prepared Na^{24} solution was obtained. The solution of Na^{24} was then diluted to provide a convenient counting level for the liquid counter, and aliquots of this solution were counted in the liquid counter. The efficiency of the particular counter used in this work was 13.34%.

(b) Results of 14MeV irradiations:

The results of the 14 MeV irradiations are given in Table XI.

Table XI. $\text{Be}^9(n, \text{H}^3)\text{Li}^7$ cross-section for 14 MeV neutrons.

Irradiation number	I	II
Irradiation time (hours)	1.0	6.0
Neutron exposure (neutron/cm ² × 10 ⁻¹¹)	5.6	11.25
Observed activity (counts/minute)	90 ± 1	74.3 ± 0.9
Background (counts/minute)	73 ± 0.9	48.2 ± 0.7
Tritium activity (counts/minute)	17 ± 1.3	26.1 ± 1.1
Counting factor	2.372	2.372
Mass of beryllium (grams)	0.0760	0.1514
Specific activity (counts/minute/gram)	530 ± 40	403 ± 17
Tritium content (atoms H ³ /gram Be. × 10 ⁻⁹)	5.0	3.82
Cross-section (millibarns)	134 ± 10	51 ± 2

The cross-section values deduced above show a wide discrepancy. This is to be expected considering the conditions under which this experiment was performed. The neutron source available was not capable of giving higher neutron exposures than those obtained, and

this resulted in a low tritium production. The low activity obtained as a result of these irradiations does not permit of high accuracy in counting, particularly in the presence of such a high background. The results can only be of use in indicating the order of magnitude of the effect.

III. 3. Discussion of tritium measurements.

Using the results of Table X, and the formula deduced in section III.1 the $\text{Be}^9(n,\alpha)$ cross-section can be calculated. The results of these calculations are given in Table XII, the cross-section being deduced first from the result without cadmium, and then from the same results after deduction of the tritium produced in cadmium.

Table XII: $\text{Be}^9(n,\alpha)\text{He}^6$ cross-section.

Irradiation number	I	II	III
Cross-section from total tritium. (millibarns)	97	170	284
Cross-section after correction for Cd effect. (millibarns)	-	43	243

From the integration of the excitation functions available (see II.3.) the cross-section of this reaction over a fission spectrum is known to lie in the region of 30 millibarns. Only one of the results obtained, that

from irradiation II after correction for the fast neutron contribution, lies in this region. There is however no apparent reason why this particular result should be chosen. Examination of the results given in Table X indicates that within a given irradiation the analyses for tritium are consistent, and it is therefore reasonable to suppose that the analytical technique is reliable.

The fall in activity after a period of six months in the sample from irradiation III, and the high observed tritium values are the two main problems which must be settled. These facts lead immediately to the suggestion that some short-lived isotope is produced by reaction with impurity in the beryllium during the neutron irradiations. Having regard to the analytical technique for the extraction of activity from the beryllium, an examination of the isotope tables indicates that the most probable isotope is argon 37, with a half-life of 35 days, which could arise from the reaction $\text{Ca}^{40}(\text{n},\alpha)\text{A}^{37}$. This reaction is exothermic and hence can occur with thermal neutrons. This possibility must be rejected however, since an observation of the extracted activity over a period of 14 days showed no decrease in activity. For the excess of activity observed in the tritium determinations a decay of about 25% would have been expected for A^{37} contamination. In addition, the $\text{Ca}^{40}(\text{n},\alpha)$

reaction would also have taken place in the thermal column irradiations, and high activities were not observed. One is forced to the conclusion that the high activity is indeed due to tritium, and that the fall in activity is due to some other process.

There are two further processes which might be used to account for the fall in tritium activity in the six month period:

(a) The excess tritium could be present as a surface contamination arising from the adsorption of externally produced tritium. Such tritium could arise from (n, H^3) reactions in surrounding material. The tritons could be directly captured by embedding in the beryllium surface, or could first be captured by water molecules present in the surrounding atmosphere, replacing the hydrogen atoms, and this followed by adsorption of the 'tritiated' water molecule on the beryllium surface. Exchange of this adsorbed 'tritiated' water with the water vapour of the atmosphere would provide a mechanism for the fall in activity.

(b) The excess of tritium could be present in the body of the material, and might diffuse out of the beryllium. No information is available on the diffusion of gases in beryllium. The earlier experiments on the helium production cross-section suggest that the diffusion of helium, if it occurs at all, must be slow since the helium analyses were consistent, and in most cases

the time between irradiations and analysis were quite different. However this argument may not be applicable to the diffusion of hydrogen or tritium since in this case the diffusion could be due to a chemical process as in the case of palladium. In the absence of information to the contrary it can be assumed that such diffusion is possible.

The pieces of beryllium were irradiated in aluminium cans. Li^6 impurity in the aluminium could give rise to tritons on neutron irradiation, and since the reaction is exothermic to the extent of about 4 MeV such tritons would have sufficient energy to escape from at least the surface layer of the aluminium can. These might embed in the beryllium surface, or collect within the can and be subsequently adsorbed on the beryllium surface. An examination of a typical can showed a tritium content of 5.52×10^{11} atoms of tritium/gram of aluminium, the analysis being conducted as for beryllium. The tritium might thus contaminate the beryllium by either of the mechanisms discussed. This possibility is rendered unlikely however, when one considers that such contamination would also occur in the irradiations with thermal neutrons, and no high activities were observed in these irradiations. It can be seen from the results of the thermal column irradiations that the correction to be applied is small comp-

ared with the tritium excess.

Tritium could also arise from the reaction $N^{14}(n,H^3)$ C^{12} by interaction of neutrons with nitrogen in the air surrounding the irradiated sample. This reaction has an energy threshold of 4.4 MeV, and the cross-section for fission spectrum neutrons having energies above the threshold is 11 ± 2 millibarns (92). Taking into account the fact that only 7.6% of fission neutrons have energy above 4.4 MeV, and that the volume of the irradiation cans was about 5 ccs., calculation indicates that for irradiation I (Table X) about 2×10^{11} atoms of tritium could accumulate in the can from this source. This represents somewhat over 5% of the total tritium observed. The $N^{14}(n,H^3)$ reaction is endothermic and consequently relatively few of the tritons formed would have sufficient energy to embed in the beryllium surface. Although exchange with water molecules is still a possible mechanism for surface adsorption, such adsorption would be governed by an equilibrium between adsorbed water and water vapour in the surround. An order of magnitude calculation assuming a 100 milligram spherical specimen of beryllium, and a vapour pressure of 1 cm. of water vapour in the surround indicates that a surface monolayer of water molecules contains only 10^{-9} parts of the total water. Under such conditions the bulk of tritium would remain in the surround. Thus

it appears improbable that this reaction makes a significant contribution to the tritium excess.

Of the possible reactions which could give rise to surface contamination the Li^6 and N^{14} reactions appear to be the most likely. The Li^6 cannot be a contributing factor because of the absence of high activity in the thermal neutron irradiations, and the N^{14} reaction whilst still a possibility would appear to give insufficient tritium to account for the observed tritium excess. Contamination of the beryllium surface by fission products from the uranium seems unlikely since the uranium slugs would be completely enclosed in a canning material. In addition the beryllium slugs were themselves enclosed in aluminium.

It would appear therefore that the diffusion of tritium from the body of the material is the most likely cause of the fall in activity observed. If this is indeed the case then the present method of observation would need to be considerably modified. The high observed tritium activities require to be accounted for.

The (n,α) cross-section obtained by integration of the published excitation functions is in the region of 30 millibarns, and this is lower than those in Table XII deduced from tritium measurements. These high results must be due to an excess of tritium, rather than to an underestimated cross-section in the excitation

functions, since the cross-section deduced from the results out of cadmium in irradiation III (Table X) is higher than the helium production cross-section (Table IV). Furthermore there is a considerable tritium production in the cadmium sheathed specimens which should not be present as a result of the $\text{Be}^9(n,\alpha)$ reaction. The excess of tritium must therefore have its origin in some epi-cadmium neutron reaction.

The tritium excess is too large to be accounted for by the neglect of the $\text{Li}^6(n,\alpha)$ cross-section for fast neutrons. The excitation function for this reaction is given by Ribe (93) for fast neutrons, and integration over the fission spectrum gives a cross-section of 405 millibarns. It is readily shown that the tritium produced from this is several orders of magnitude lower than that observed.

Having established that the tritium excess is due to an epi-cadmium neutron reaction it is considered improbable that the tritium would arise from neutron reactions with impurity in the beryllium. The known impurities in commercial beryllium have been given in Table VI, and Q-values of the isotopes of these impurities have been computed from mass values where these are available. These Q-values are given in Table XIII. It can be seen that with the exception of B^{10} all possible impurity reactions involve high threshold energies, and this fact

considered together with the low content of these impurities rules out the possibility of this type of interference.

Table XIII: Calculated Q-values for (n,H³) reactions in impurities in beryllium metal.

Isotope	Q-value (MeV)	Isotope	Q-value (MeV)	Isotope	Q-value (MeV)
Fe ⁵⁶	-11.55	Al ²⁷	-10.87	Mg ²⁴	-15.47
Mg ²⁵	-10.53	Mg ²⁶	-14.69	Cr ⁵²	-12.30
Cr ⁵⁰	-15.30	Ni ⁵⁸	-11.36	Cu ⁶³	- 8.06
Si ²⁸	-17.06	Si ²⁹	-11.56	Si ³⁰	-14.44
B ¹⁰	+ 0.23	B ¹¹	- 9.55	-	-

The B¹⁰(n,H³)Be⁸ reaction is exothermic and hence from energetic considerations should occur with thermal neutrons. The reaction of thermal neutrons with B¹⁰ is known to proceed via the (n,α) reaction with a cross-section of 4010 barns (5), and if the (n,H³) reaction were to proceed with a similar cross-section the reaction would make a significant contribution to the observed tritium excess. The reaction is not reported in the literature for thermal neutrons, and it would appear that the reaction is forbidden at these neutron energies. The reaction is reported at higher energies (94; 95), but apart from a measurement of the differential cross-section at 14 MeV (96) no cross-section values are reported. The cross-section for the reaction integrated

over a fission spectrum will be insufficient to account for the observed tritium excess, since a calculation based on the total cross-section (5) gives an insignificant quantity of tritium. The differential cross-section at 14 MeV is reported as 3 millibarns/steradian (96), and assuming isotropic emission as an approximation this gives a cross-section of 40 millibarns. Having regard to the low B^{10} content, this cross-section is insufficient to account for the tritium observed in the 14 MeV irradiations also.

From the results of the 14 MeV irradiations it would appear that the $Be^9(n,H^3)Li^7$ reaction occurs with an appreciable cross-section, although the results did not show good agreement. In view of a possible bulk diffusion of tritium in beryllium such a result is not surprising since the beryllium used for the irradiations was in the form of turnings sieved to 24 standard mesh, in which the bulk diffusion would be more rapid than in larger pieces. It will be noted that in the 14 MeV irradiations the sample giving the lower cross-section was irradiated for the longer period (6x) and diffusion out of the material during the irradiation would be greater than in the sample irradiated for a short period. The actual cross-section for the reaction at 14 MeV is possibly larger than that observed if diffusion of tritium in beryllium occurs. It is of some interest to consider

the cross-section values which would be required if this reaction is to account for the observed tritium excess.

Table XIV: Calculated values of $\text{Be}^9(n, \text{H}^3)$ cross-section.

Irradiation number	I	II	III
Normal irradiation			
Average over fission spectrum (millibarns)	0.033	0.041	0.055
Average for fission neutrons 11.6 MeV (millibarns)	97	117	157
Cadmium sheathed irradiations			
Average for epi-cadmium neutrons in fission (millibarns)	-	0.038	0.009
Average for epi-Cd neutrons 11.6 MeV in fission (Millibarns)	-	109	25

The $\text{Be}^9(n, \alpha)$ cross-section is assumed to be 33 millibarns integrated over a fission spectrum as in the earlier discussion of the $\text{Be}^9(n, 2n)$ cross-section. Using this value in the formula deduced earlier, the contribution of the $\text{Be}^9(n, \alpha)$ reaction to the total tritium can be calculated. Deducting this from the observed tritium, the remainder can be used to calculate the value of the cross-section of the $\text{Be}^9(n, \text{H}^3)$ reaction. Using the information that only 3.5×10^{-4} neutrons/fission neutron have energy sufficient to initiate the reaction, the average value of the cross-section above this energy which is required to account for the observed tritium can also

be calculated. Similar calculations can be made for the results observed in cadmium. The results of these calculations are given in Table XIV.

These calculations indicate that the values of the $\text{Be}^9(n, \text{H}^3)\text{Li}^7$ reaction cross-section required to account for the tritium excess are of a reasonable order of magnitude. Two explanations might be advanced for the lack of agreement of the values obtained.

(a) Variations in the intensity of the fast neutron tail of the fission spectrum in different irradiations. Such an effect would account for the results of the tritium measurements. A comparison of the fast to slow neutron ratios between different irradiations indicates that the samples were subject to somewhat different irradiation conditions:

Irradiation I	ϕ_f/ϕ_s	=	1.02
" II	"	=	0.40
" III	"	=	0.50

The thermal and fast neutron flux in a reactor core should be proportional being dependent only on the thermal absorption cross-section of the fissile material (97). It is not known whether these different irradiation conditions would affect the proportion of higher energy neutrons to which the beryllium samples were exposed.

It would be expected however that the energy spectrum of the neutrons from fission would be invariant. Since the distance of the beryllium sample from the fission source is small, significant energy degradation of the fast neutron tail seems unlikely.

(b) Diffusional loss of tritium from the irradiated samples. The evidence available suggests that diffusion does occur, and that it is a rapid process. This would account readily for the variations in the observed tritium production, and is the most acceptable explanation.

The tritium observed in the 14 MeV neutron irradiations of beryllium gives the cross-section listed in Table XI. (Page 69). If diffusional loss of tritium occurs then these cross-sections will be underestimated, particularly the value obtained for the six hour irradiation. It would appear reasonable therefore to accept that the higher cross-section is nearer to the true value, and as an approximation use the value of 150 millibarns as the $\text{Be}^9(n, \text{H}^3)$ cross-section at 14 MeV neutron energy. Graphical integration of the fission neutron energy spectrum (54) indicates that the fraction of neutrons in the energy interval 13.5 to 14.5 MeV is 5×10^{-5} . Using the data for irradiation III (Table X, page 64) calculation indicates that neutrons from

this energy interval would account for over 10% of the observed tritium. From 14 MeV to the threshold of 11.6 MeV the cross-section for the reaction will decrease with the energy of the neutron, but the number of neutrons available is increasing exponentially. Thus lower energy intervals could contribute similar quantities of tritium. Thus it would appear reasonable to attribute the high tritium yields to the reaction $\text{Be}^9(n, \text{H}^3)\text{Li}^7$.

III.4 Conclusion.

The method proposed for the measurement of the $\text{Be}^9(n, \alpha)\text{He}^6$ cross-section, whilst simple in principle, has been found wanting in practice. Two effects, both previously unreported, are suggested to account for the failure of the method. These effects are:

- (1) The diffusion of tritium from beryllium.
- (2) Tritium production from the direct reaction $\text{Be}^9(n, \text{H}^3)\text{Li}^7$.

Consideration of these factors suggests that the tritium analysis method in a slightly modified form might still be used to measure the $\text{Be}^9(n, \alpha)\text{He}^6$ cross-section over a fission neutron spectrum. The following method is suggested:

The samples of beryllium for irradiation could be enclosed in evacuated gold envelopes. Metallic gold would be free from impurity which could give

rise to tritium, and would effectively prevent access of recoil tritons. Evacuation of the envelopes would prevent possible contamination from the $N^{14}(n,H^3)C^{12}$ reaction, and gold having excellent cold welding properties could readily be sealed off after evacuation. Alternatively the beryllium samples could be sealed in a coating of evaporated gold. The analytical technique for tritium would require no modification since the beryllium sample and envelope could both be dissolved by the action of halogen, and hence all tritium produced on irradiation could be collected. A minor disadvantage would be the high Au^{198} activity produced, but this has a half-life of 2.7 days, and would have disappeared at the end of one month. The samples could be analysed for tritium at the end of this period. Observation of the tritium production with and without a shield of cadmium would be necessary in order to assess the contribution from the direct reaction $Be^9(n,H^3)Li^7$. The method could be subject to quite large errors, since the $Be^9(n,\alpha)He^6$ cross-section is obtained as a small difference between two large quantities.

It is regretted that time was not available during the course of this work to perform these measurements.

CHAPTER IV.

Establishment of an absolute neutron standard.

IV. 1. Introduction.

The problem of standardisation of neutron sources has been recently reviewed by Wattenberg (98), who concludes that at the time of writing absolute neutron measurements are only accurate to about 4 per cent for neutrons of almost all energies, whilst relative measurements can be made to an accuracy of a few tenths of a per cent. The uncertainty in absolute neutron measurement represents one of the most serious errors in the measurement of absolute values of neutron cross-sections. Since accurate absolute values of neutron cross-sections are becoming increasingly necessary in nuclear physics, it is considered desirable that the present accuracy of neutron measurements should be improved. One method of achieving this would be the establishment of an accurately calibrated neutron source.

In July 1954 a conference was convened at Harwell to discuss the present status of work on neutron

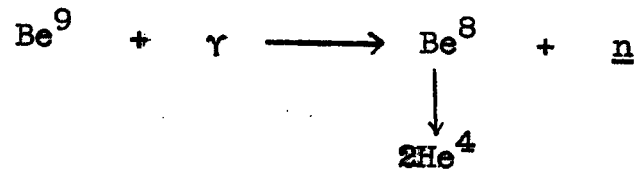
sources, and to consider various proposals for the establishment of an absolute neutron standard (99). At this conference proposals for the establishment of an absolute neutron standard were presented by E.B.M. Martin and G.R. Martin (100). In these proposals the programme outlined was divided into three component parts;

- (I) The production of a reproducible arbitrary standard source.
- (II) The development of a source whose yield is known absolutely.
- (III) The development of a technique for the accurate comparison of sources which will, in general, be of rather low intensity and/or have different neutron energy spectra.

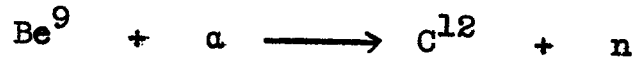
The work described in this thesis is concerned with part II of this programme.

IV. 2. Outline of the method.

The source chosen for the determination of the absolute yield in these determinations was the beryllium photoneutron source. The source consisted of a machined cylinder of beryllium of about six grammes weight containing at its geometrical centre a radium preparation (approximately 500 milligrams of radium) sealed in a platinum case. Neutrons are produced according to the nuclear reaction,



Contamination of the source with neutrons from the reaction,



is avoided by the sealing of the radium preparation inside a platinum case.

The method of calibration of the neutron source is based on the original proposal of Glueckauf and Paneth (41). It will be observed that in the beryllium photoneutron reaction the emission of a neutron results in the formation of the nucleus Be^8 which is unstable and breaks down into two α -particles, i.e., helium nuclei. The helium yield is directly related to the number of neutrons produced, and hence measurement of the helium gives the absolute neutron emission. The assumptions embodied in this method of calibration are few, and have been enumerated by E.B.M. Martin and G.R. Martin (100):

- (a) Each neutron produced is accompanied by two α -particles; i.e.,
 - (i) Be^8 disintegrates immediately on formation, or at least before measurement of the helium.

(ii) no other (γ, α) or (γ, n) reactions are possible with beryllium or with impurities contained in it.

(b) The resulting helium is retained within the metal until dissolution.

The disintegration of the nucleus Be^8 was discussed at some length in Section I. 4 (page 14) where it was concluded that all states of the nucleus are unstable with respect to breakdown into two α -particles. The maximum energy of the γ -rays from a radium preparation is 2.4 MeV (from radium C). Only two (γ, n) reactions are known with the threshold energies below this value, the reactions $\text{Be}^9(\gamma, n)\text{Be}^8$ and $\text{H}^2(\gamma, n)\text{H}^1$. Contamination of beryllium metal with deuterium is extremely unlikely, and hence the only photoneutron reaction which needs to be considered is that with beryllium. $\text{Be}^9(\gamma, \alpha)\text{He}^5(n)\text{He}^4$ - energetic threshold 2.229 MeV - is merely an alternative to $\text{Be}^9(\gamma, n)\text{Be}^8(\alpha)\text{He}^4$. Of the known impurities in commercial beryllium (page 39) the lowest (γ, α) energetic threshold is 4.45 MeV with B^{10} , and thus contamination from this source is improbable.

The loss of helium from the beryllium before dissolution is the only question concerning which no data is available. The energy available from the break-up of Be^8 is only 96 keV (8) and hence the α -particle recoil range is much less than the linear

dimensions of the beryllium capsule. Thus little loss is to be expected from this source. It has been stated that all metals are perfectly helium tight (41), but there appears to be no experimental evidence for this in the case of beryllium. Methods by which this diffusion might be studied have been suggested in Section II.1 (page 28). The results obtained in the study of the $\text{Be}^9(n,2n)$ reaction (Table IV, page 23) would appear to justify the assumption that at room temperature the diffusion, if it occurs at all, is slow.

Thus it would appear that the assumptions, on which the source calibration is based, are reasonable. The calibration method suffers from the disadvantage that the act of calibration destroys the source, but this disadvantage can be eliminated by comparison of the source with other beryllium photo-neutron sources. Relative measurements of neutron source strength can be made with an accuracy of a few tenths of a per cent, particularly if the neutron energy spectra are the same (98). After determination of the relative neutron emissions of such sources the absolute emission can be determined by measurement of the helium produced in one of them. Thus sources are made available whose absolute neutron emission is known.

The helium is analysed by the methods developed by Paneth (55), and his collaborators, with the addition of some techniques developed during the course of this work.

IV. 3. Comparison of photoneutron sources.

Six machined capsules fabricated from a helium-free specimen of cast beryllium were constructed for this experiment. The capsules were in the form of cylinders about six grammes in weight, having a cylindrical cavity at the centre in which the platinum covered radium sources were fitted. Cast beryllium was chosen as the constructional material since this had been shown to be free from helium by previous workers. Beryllium fabricated by powder metallurgical processes was found to be unsuitable, having a measurable helium content (101).

Three of the sources thus constructed were chosen for subsequent helium analysis. For the purpose of comparison the sources were placed alternately in a fixed position in a paraffin block in which was embedded a boron trifluoride counter for neutron detection. Observation of neutron counts for every combination of radium source and beryllium capsule were made, the observations being continued for a sufficient time to achieve the required statistical accuracy in the counting. In this way random errors in the counting were

reduced to about 0.15 per cent in the ratios between sources.

IV. 4. Measurement of Helium.

From the known approximate neutron emission of the photoneutron sources it was estimated that about 10^{-7} ccs. of helium would accumulate in the beryllium capsule for every six months of irradiation. During the course of the work described in this thesis the quantity of helium available for measurement varied from 10^{-7} ccs. to 6×10^{-7} ccs., this quantity being contained in about six grammes of beryllium. This represents quite a formidable problem in analysis.

A number of methods were considered for the extraction of the helium from the beryllium sample. Attack by halogens was rejected because of the difficulty involved in handling the material in a vacuum system containing mercury. An attempt was made to amalgamate beryllium with mercury, which if successful would have been an ideal method of extraction, but in pilot experiments beryllium resisted attack by mercury. The method finally accepted was that of dissolution in dilute sulphuric acid, or a nearly saturated solution of potassium cupric chloride. These methods have the disadvantage that large volumes of hydrogen are produced during the dissolution.

Dissolution in dilute sulphuric acid has the

advantage that the solution and dissolving vessel are readily freed from helium by flushing the solution with electrolytic gas derived from the electrolysis of the solvent. The rate of solution in dilute sulphuric acid is slow, and seemed to depend to some extent on the nature of the surface of the beryllium metal. In one determination on a half-gramme quantity of beryllium some ten hours was required for complete solution. This situation was improved by using a nearly saturated solution of potassium persulphate in dilute sulphuric acid, the rate of solution in this case being much more rapid. It is necessary in determinations of this kind to avoid saturated solutions, since the process of degassing the solution produces supersaturation with consequent crystallisation of the solute. It is possible that such crystals could carry down occluded helium. However whilst dilute sulphuric acid was always used for helium determinations on approximately half-gramme quantities of beryllium, it was not used for larger quantities because of the large volumes of hydrogen involved.

Potassium cupric chloride solutions were used for the dissolution of larger quantities of beryllium because of the lower hydrogen yield. Six gramme quantities of beryllium give with acid solution about

fifteen litres of hydrogen. This is reduced to six litres of hydrogen by the use of potassium cupric chloride. This solvent has been successfully used for the dissolution of iron meteorites for the determination of their helium content (102). The use of this solvent has some disadvantages. The solution cannot be de-gassed by electrolysis because of the production of chlorine, and consequently degassing is performed by prolonged flushing with helium free oxygen. This involves the transfer of large quantities of oxygen and water vapour through the pumping system. The process of solution in this solvent is erratic, the surface of the beryllium becoming coated with a layer of deposited copper which impedes solution until the layer is dissolved. This copper coating has other undesirable features. During the process of solution small quantities of beryllium are sometimes broken off the main mass, become coated with copper, and fall into the sediment of cuprous chloride at the bottom of the dissolving vessel. It is possible that such pieces might remain undissolved. The process of solution therefore requires to be watched carefully. This flaking was only observed with unmachined samples of cast beryllium which were very rough, and contained cracks. With machined samples the effect may not occur. A further

disadvantage is that comparatively large volumes of oxygen are required to sweep helium from the solution and dissolving vessel when dissolution of the beryllium is complete. The great reduction in the production of hydrogen obtained by the use of this solvent was considered to outweigh these disadvantages.

Having settled the choice of solvent, the problem of removing the hydrogen without loss of helium required to be solved. An attempt was made to remove the hydrogen, or at least a large proportion of it, by leaking it away through a heated palladium thimble. However with the size of thimble available the leakage rate was found to be too slow for this method to be practicable. The method finally used was that of burning with helium-free oxygen, a method used by previous workers (41,102). Detailed accounts of the method are given in Chapter V.

The methods used by previous workers for the preparation of helium-free oxygen are satisfactory where the quantities of hydrogen involved are small, but are tedious and difficult to apply with certainty for larger amounts. Since it was proposed to perform blank determinations on samples of beryllium before and after the determinations on the neutron standard capsules, a procedure requiring the burning of some 18 to 20 litres of hydrogen, quan-

quantities of helium-free oxygen of the order of 10 litres were required for each analysis. A method involving the distillation of liquid oxygen was developed to provide the oxygen, and was found to be satisfactory in practice.

Detailed accounts of the procedures adopted for the extraction of the helium from beryllium in a form suitable for measurement are to be found in Chapter V. The main difficulty in the work was that of obtaining satisfactory blank determinations on quantities of beryllium of the order of six grams. Since it was required to obtain an accuracy of one per cent or better on the neutron standard determinations, it was necessary that the blank determination should give somewhat less than 6×10^{-9} ccs. of helium at S.T.P., this quantity being that contained in 10^{-3} ccs. of air.

An early difficulty was that of determining whether the methods adopted were suitable for the final analysis. Thus the testing of the oxygen preparation methods required that the oxygen be burnt with helium-free hydrogen, which could only be satisfactorily obtained by the dissolution of a helium-free metal. The testing of the metal sample required the use of samples of helium-free oxygen. No independent method for the testing of either the oxygen or the metal was available. A procedure was adopted by which it was

hoped to resolve the difficulty. This consisted in dissolution of the same mass of metal in dilute sulphuric acid and also in potassium cupric chloride, different amounts of hydrogen being given in each case. Thus if the quantities of helium obtained were the same the impurity should then be contained in the metal, and if different the helium impurity would be in the oxygen. Ideally this procedure should give the required answer, but in practice never did, the reason being that these are not the only possible sources of helium contamination. The most satisfactory method is that of obtaining a blank determination.

A sample of helium-free metal was available in the laboratory, this being the sample of cast beryllium which Reasbeck had found to be free from helium, (see page 89), but there being only about 10 grams of this material remaining it was considered that this sample should remain as a reference standard until such time that the procedures adopted were found satisfactory.

A satisfactory blank determination was eventually achieved on a specimen of cast beryllium. The results of this analysis were:

Mass of beryllium :- 6.3 grams.

Helium fraction :- 6.5×10^{-9} ccs. at S.T.P.

Neon fraction :- 1.0×10^{-7} ccs. at S.T.P.

The amount observed for the helium fraction will be seen to be about one per cent of the helium expected on dissolution of the neutron standard capsules. The actual amount of helium in the sample measured must however be somewhat less than this for the following reason. In practice a blank measurement made on the fractionating column always gave a measurable quantity of helium, which was considered to arise from air contamination. This point is discussed in Chapter V, section 10, figures for typical blank analyses being given in Table XVII. In this table it can be seen that typical contamination from the column is about 2.5×10^{-9} ccs. of helium. Thus the observed helium should be corrected by this amount, the result being therefore 4.0×10^{-9} ccs. of helium per 6.3 grams of beryllium.

The neon fraction observed is high, but it is obvious that this is not due to air contamination, at least not completely, since the helium to neon ratio is very much less than that of air. This high neon value might be explained in two ways:

- (a) The neon may not have been completely removed from the oxygen in the distillation process.
- (b) The neon fraction may actually be due to a small quantity of hydrogen which has survived attempts to remove it in the earlier stages.

The measuring technique would not discriminate

between hydrogen and neon, and the quantity of hydrogen required to give the observed deflection would be very much less than that recorded as the neon fraction, since the detector is much more sensitive to hydrogen than neon.

This blank analysis whilst showing that the helium extraction methods are adequate is still not completely satisfactory. The neon fraction must be reduced to less than 1×10^{-8} ccs. to avoid ambiguity in the neutron standard determinations. Thus although it is possible to exclude air contamination in the bulk of the neon fraction observed in the blank determination, this would not be possible where the helium fraction is of the order of 6×10^{-7} ccs.

It is regretted that time was not available to complete this section of the work.

CHAPTER V.

THE ESTIMATION OF HELIUM IN BERYLLIUM.

V. 1. Introduction.

The micro-analytical techniques for the measurement of helium discussed in the following pages are based on the results of many years of patient effort by Paneth and his collaborators, of whom special mention may be made of Glueckauf and Chackett who are largely responsible for the present form of the apparatus. Paneth recognised in the low detection limits of the inert gases a direct means of studying artificial transmutation of the elements, a field of study which at the beginning of his reseaches was largely the exclusive domain of physicists. Paneth has recently reviewed his work in the field of micro-analysis of the inert gases (55). The techniques have been applied to a large variety of problems of which mention may be made of the following: geological age determinations of rocks and minerals (103); age of meteorites (60, 102, 104); the analysis of atmospheric and stratospheric air (61, 105, 106); interaction of γ -rays with

beryllium (41); study of spallation reactions (107); interaction of neutrons with boron (108).

The first study of the helium produced in beryllium as the result of a nuclear reaction was made by Paneth and Glueckauf (41) in the course of which they were able to show that of the two postulated reactions,



reaction 2 was the one which occurred. Physical methods of study had been unable to decide, until this time, which of the two reactions occurred. The present work was undertaken as a further study of this reaction with a view to its use in neutron standardisation (100), and also to study the interaction of neutrons with beryllium.

An outline of the technique of helium measurement used will be given before the more detailed discussion. The sample of beryllium is dissolved in dilute sulphuric acid or potassium cupric chloride solution to release the helium from the metal. This process was considered to give the best promise of success, its great drawback being the large volumes of hydrogen released on dissolution of the metal. An attempt was made to remove the bulk of this hydrogen by diffusion through palladium, but the method was rejected being too slow

with the apparatus available. The hydrogen is therefore removed by controlled burning with helium-free oxygen. After passing through a further stage in which small traces of hydrogen are removed by circulation of the gas mixture over heated palladium, the helium is fractionally separated in a special apparatus. The helium is then measured by means of a Pirani gauge calibrated against a known volume of helium.

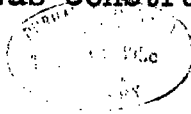
Soda glass is used throughout the construction of the apparatus to reduce effects from the diffusion of helium through glass. The only exceptions to this rule are the Pirani gauges and the vacuum jacket of the palladium furnace used to remove traces of hydrogen. Where heat is developed in the apparatus such as in the dissolving vessels, hydrogen combustion chamber, and palladium furnace, the particular section is immersed in a water bath, since diffusion of helium is much more rapid through heated glass, particularly in the presence of hydrogen. Care must be taken to ensure that all keys used in glass taps are also of soda glass, it being the practice of some manufacturers to construct the tap barrel of soda glass and the key of 'Pyrex'. The presence of one such tap in the apparatus can give rise to serious helium contamination. For a discussion of the many difficulties associated with the technique of helium micro-analysis the reader

is referred to the review of Paneth (55).

V. 2. The production of Helium-free Oxygen.

Owing to the low equivalent weight of beryllium a large volume of hydrogen is produced on acid-dissolution of the metal - approximately 2.5 litres /gram of beryllium. The use of a nearly saturated solution of potassium cupric chloride as solvent reduces the hydrogen production to about 1 litre/gram and this will require 500 ccs. of pure oxygen for its removal by the burning method. For the neutron standard determinations using 6 gram capsules of beryllium, 3 litres of oxygen would be required. The beryllium analyses should be checked by performing blank determinations before and after the measurement of the irradiated capsule to ensure correct working of the apparatus. These blank determinations would require the use of similar quantities of oxygen, and thus a total of 9 litres of helium-free oxygen are required.

A number of methods for the production of helium-free oxygen have been developed by earlier workers (41, 61), but apart from the work of Glueckauf on irradiated beryllium they have all been designed for comparatively small volumes. The possibilities of the electrolytic method used by Glueckauf (41) were considered, and indeed an apparatus was constructed for this



preparation, but the method was rejected, since the initial de-gassing of the solution involved transferring large volumes of water through the pumping system, and the later purification stages involving the adsorption of the oxygen on charcoal cooled in liquid nitrogen with subsequent pumping-off of the helium and neon contamination, reduced the method to that used later by Chackett and co-workers (102).

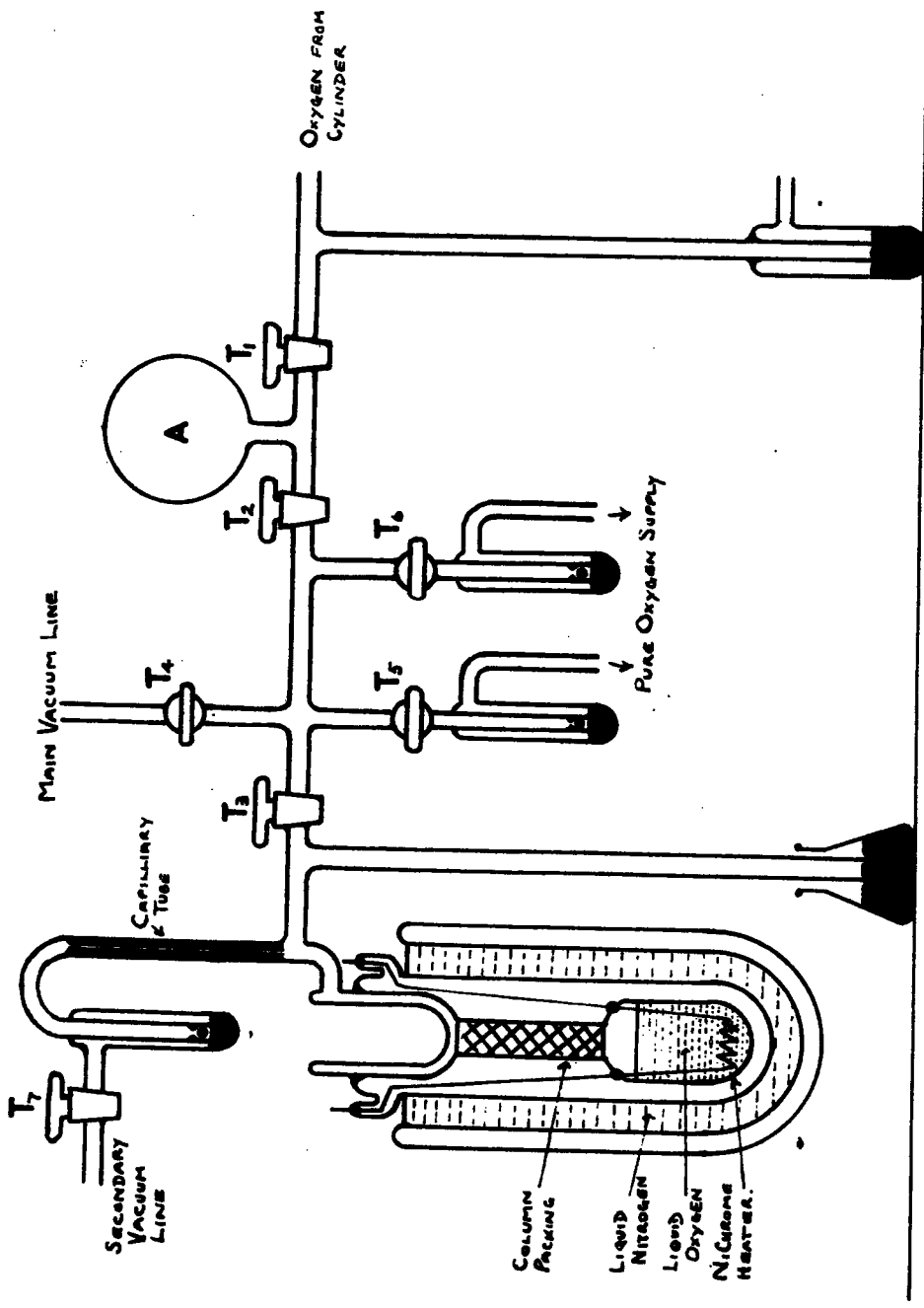
The method described by Chackett is suitable where the quantity of oxygen used is comparatively small (i.e. 50 to 100 ccs.), but when large volumes are required the method is somewhat laborious and requires a very large reservoir to offset the volume wasted when pumping on the liquid oxygen. Such large reservoirs are undesirable in this type of apparatus because of the long pumping-out period, and the difficulty experienced in detecting and isolating small leaks. The following method was therefore adopted.

The method consists in the fractional distillation of liquid oxygen and employs an apparatus similar to that used by Clusius and Riccobini (109) for the purification of low-boiling hydrocarbons. A similar unit was used by Lambert and Phillips (110) to purify oxygen for density determinations on the gas. During the course of this work two purification systems were used, and these are shown in figures 13 and 14.

The first system (Figure 13) consists of a vacuum jacketed boiler and column surmounted by a reflux-head and take-off system. Also shown in the figure are the lines for filling the still, and supplying the purified oxygen to that part of the apparatus in which it is required. Heat is supplied to the still electrically by means of an internal heater of 'Nichrome' resistance wire sealed into the boiler by means of platinum to glass seals. The wires are led out of the system by two further platinum seals in the vacuum jacket arranged so as to clear the surface of the liquid nitrogen in which the still is immersed. The column is packed with glass helices throughout its 20 cm. length, and is widened at its upper end to admit the finger trap reflux head. The annular space between the upper end of the still and the finger trap is reduced to as small a volume as possible, and the lead to the take-off system is made of capillary tube, both to limit the volume and serve as a flow impedance. Take-off is effected through a mercury non-return valve connected via tap T_7 to the secondary vacuum system the tap being used to adjust the take-off rate. In operation the still is immersed in liquid nitrogen to the level indicated, and the finger trap is filled with liquid nitrogen.

FIGURE 13.

Oxygen purification apparatus I.



The taps T_2 , T_3 , T_5 , T_6 , are opened and the system is evacuated via the secondary vacuum line through the take-off non-return valve and tap T_7 . The system is then rigorously evacuated through the main vacuum line via the tap T_4 , the earlier evacuation through the secondary line being performed only to avoid taking large volumes of gas through the diffusion pumps. Pumping is continued until a hard vacuum is produced, this state being indicated by a McLeod guage in the main vacuum line. The jacket of the distillation column is pumped at the same time through a connection not indicated in the diagram. Throughout this pumping period oxygen is bubbled slowly through the mercury reservoir to flush out any air contained in the tubing on the high pressure side of T_1 . When a hard vacuum has been attained pumping is discontinued on the system and vacuum jacket, and taps T_2 , T_4 , T_5 , and T_6 are closed.

The rate of oxygen flow is increased and tap T_1 is slowly opened to allow the bulb A to fill with oxygen, care being taken not to allow the flow of gas through the mercury reservoir to be interrupted, and then T_1 is closed. The still is cooled by surrounding it with liquid nitrogen, and the finger trap is filled. Taps T_2 and T_3 are then opened, the oxygen thus being

allowed to enter the still where it is condensed, and cools the still to liquid oxygen temperature. After allowing time for the still to cool, the tap T_1 is again opened, and oxygen from the stream allowed to enter the still. About 20 minutes was the usual time required to fill the boiler. When the oxygen used had been obtained by a commercial electrolytic process, the build-up of the non-condensable hydrogen impurity sometimes causes the condensation of oxygen to cease, and when this occurs it is necessary to remove the hydrogen through the take-off system, before the oxygen condensation can be completed. The tap T_1 is then closed, and after allowing the system to attain its equilibrium pressure of about 15 cms. of mercury, tap T_3 is closed. The gas remaining in this part of the line is then removed via T_4 .

The heater of the still is switched on, and the oxygen is refluxed for about 15 minutes, the tap T_7 being adjusted so that about 40 bubbles/minute of oxygen pass through the mercury non-return valve. Distillation is continued for about 8 hours, during which time the still requires little attention apart from topping-up the liquid nitrogen levels in the reflux-head and Dewar vessel. The volume of the liquid oxygen is then reduced to about one third by this process, and this purified oxygen is then stored in the

still. The Dewar vessel is usually sufficient to retain the oxygen overnight, but, should the pressure of oxygen rise above atmospheric, the manometer provides a safety-valve.

The system just described was used throughout the major part of this work, and was found to be satisfactory. It was eventually replaced by the system shown in figure 14 when leaks were found to have developed around the metal to glass seals, and in the second system the less desirable features of the first were removed. These undesirable features are:

1. The platinum to glass seals used to lead in the heater current are subject to large temperature changes, particularly those in the boiler.
2. The wire leads provided a good heat leak into the system during storage and were probably the main factor in lowering the efficiency of the still as a storage vessel.
3. The manometer, used as a safety-valve and a check on the distillation pressure, is a possible source of air leakage. This arises when the mercury is subjected to large fluctuations, such as occur during its operation as a safety-valve and when the oxygen becomes superheated. Experience with a similar system has led to

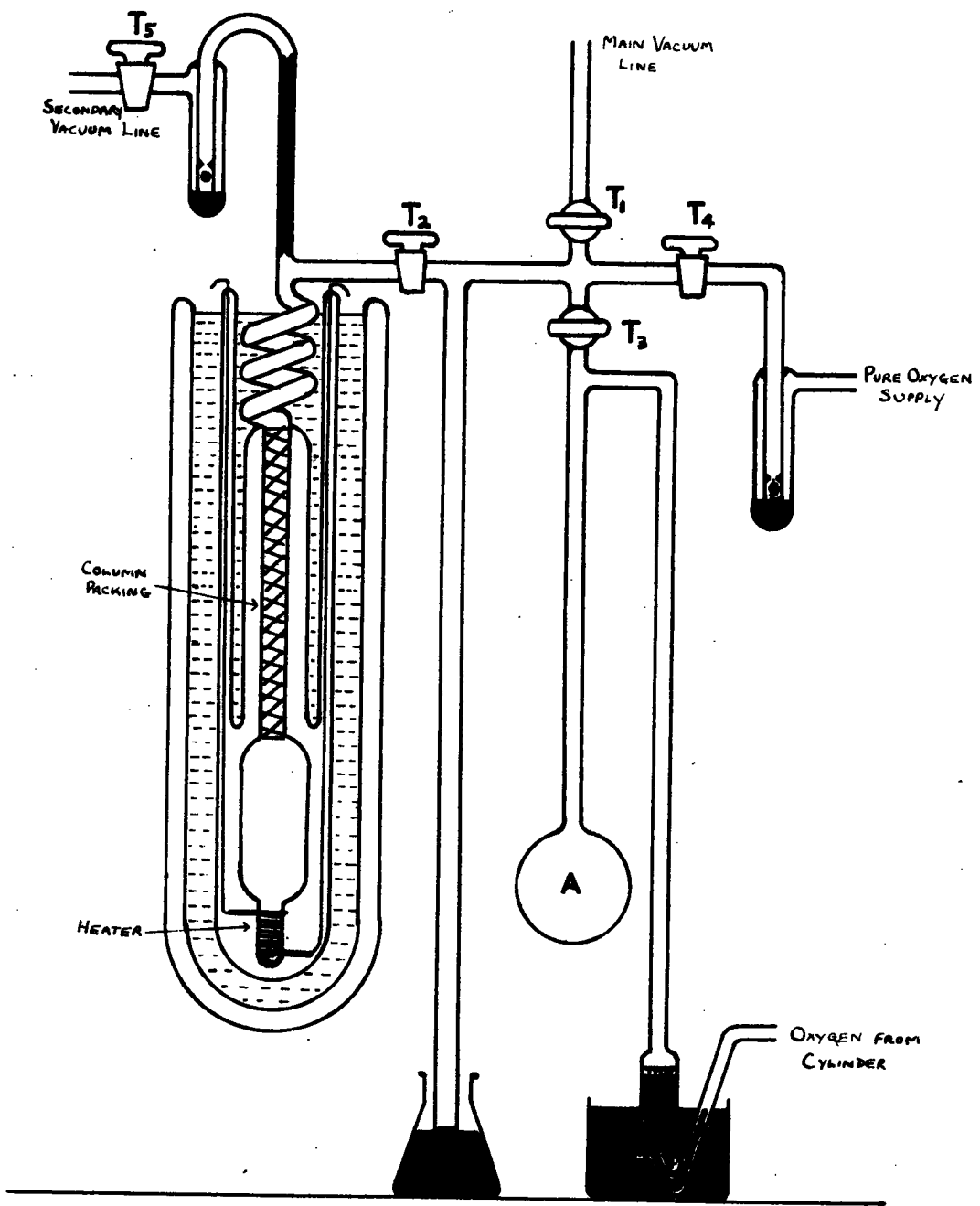
the suspicion that air is entrained in the mercury column under such circumstances.

4. The finger trap type of reflux head is wasteful of liquid nitrogen, and requires more constant attention than is desirable. This could be improved by having the whole of the finger trap immersed in liquid nitrogen, but owing to the difficulty experienced in making the internal and Dewar seals necessary, this was not adopted.

The system shown in figure 14 used an external heater of 'Nichrome' tape wound on a narrow glass tube in the base of the boiler and fixed with brass sleeves. The connections to the heating element were carried in two tubes projecting well above the liquid nitrogen level, a vacuum seal being made with platinum wire. In this model the column was packed with stainless steel gauze (Dixon packing). The reflux-head consists of a glass spiral which was completely immersed in liquid nitrogen so that evaporation of the coolant, apart from the normal losses of the Dewar vessel, occurred only through heat exchange with the oxygen. Since this still is not used as a storage vessel in the system, the manometer was dispensed with. The take-off system is the same as in the previous model.

FIGURE 14.

Oxygen purification apparatus II.



With the taps T_1 , T_2 , T_3 , T_4 , and T_5 opened the whole system was rigorously evacuated as before, and on the attainment of a hard vacuum the tap T_3 was closed. After first flushing out the lead line by bubbling the gas through the mercury, oxygen was passed into the small bulb A which was surrounded by liquid nitrogen. The oxygen was condensed and collected in A, which had a volume of about 60 ccs. the bulb being completely filled. With taps T_2 and T_4 closed, the bulb was opened to the pumps two or three times, for a few seconds, to remove any non-condensable gases.

The distillation unit was then immersed in liquid nitrogen to just below the internal seal, to allow the seal to cool slowly, and then the level was raised to completely cover the spiral. Tap T_1 , leading to the high vacuum line, was closed, together with the lead to the vacuum jacket (not shown in figure 14), before the immersion. T_2 and T_3 were then opened, and the liquid nitrogen surrounding the bulb A was removed to allow a small quantity of oxygen to condense in the still, tap T_3 then being closed, and the liquid nitrogen being replaced around the bulb A. Some 10 minutes was required for this small quantity of oxygen to cool the still, after which T_3 was again opened, the liquid nitrogen around A removed, and the oxygen

allowed to condense into the still. When all the oxygen had been transferred to the still, T_2 was closed and the bulb A was evacuated through T_1 , the bulb and connecting tubes being evacuated, when practicable, throughout the whole period when the still was in use.

The still heater was switched on and the oxygen refluxed, with the take-off operated as before, for about 8 hours at the end of which T_1 was closed, and T_2 opened. The bulb A was once more immersed in liquid nitrogen, that surrounding the still being removed, and the oxygen remaining in the still was boiled into A. When the transfer was completed the still heater was switched off, tap T_3 closed and the still once more evacuated via T_1 . The purified oxygen was stored in bulb A.

Pure oxygen is supplied to those parts of the apparatus in which it is required by means of mercury non-return valves. In figure 13 these are shown with the lead-in taps T_5 and T_6 , and that for the second system in figure 14 with the lead-in tap T_4 .

V. 3. Extraction procedures for Helium.

During the course of this work three different procedures were adopted for the extraction of helium from beryllium, the choice of method being determined largely by the size of the sample which varied from

about 50 milligrams to 6 grams. An outline of the three methods will be given.

Method 1.

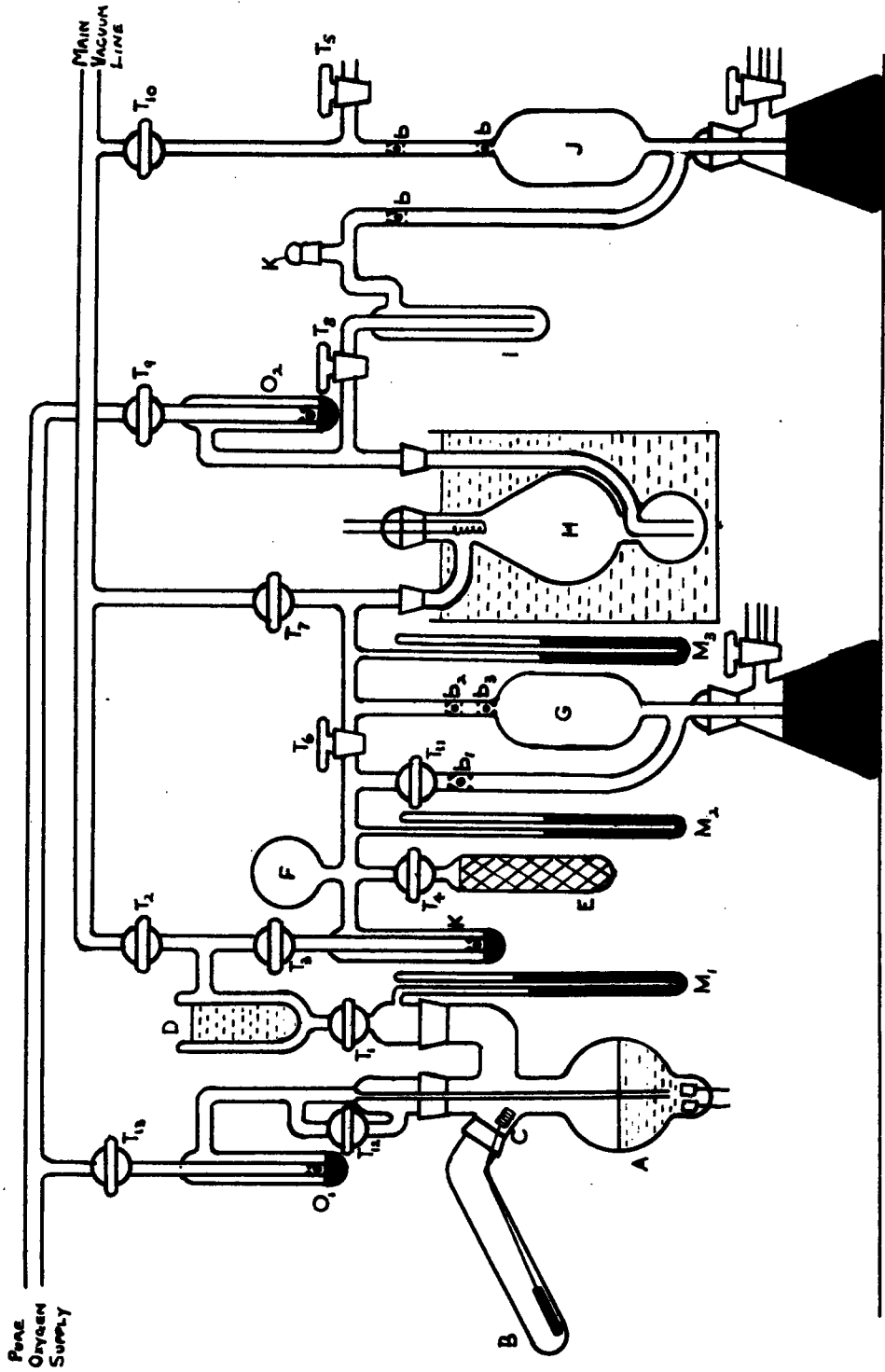
The first method, which was applied to samples of 500 milligrams to 1 gram, consisted in acid-dissolution of the metal, the evolved hydrogen together with the attendant helium being collected by adsorption on charcoal cooled in liquid nitrogen. The hydrogen was then removed by burning with helium-free oxygen, the remaining mixture of oxygen, helium, and traces of hydrogen being collected for further processing before the final analysis. The method is a modification of that previously used by Glueckauf (41), and the apparatus is shown in figure 15.

Sulphuric acid (20% v/v aqueous solution) nearly saturated with potassium persulphate was used to dissolve the beryllium. Solution in sulphuric acid alone was found to be too slow in practice, particularly in the case of machined samples, but the addition of persulphate considerably speeded up the process. 100 ccs. of this solution was contained in the flask A which had an overall capacity of about 350 ccs. The weighed sample of beryllium was contained in a small platinum cage C which was connected by means of a platinum wire to an iron slug B encased in a sealed sleeve of soda-glass. With the by-pass tap T_{12} open

FIGURE 15.

Apparatus for extraction of helium from beryllium.

(Method 1.)



the flask was evacuated through the high vacuum line via taps T_1 , and T_2 . The taps were then closed and the acid solution electrolysed by means of two platinum electrodes sealed into the flask, until a pressure of 1 cm. of mercury had been built up in the flask, this pressure being observed on the manometer M_1 . The electrolysis was stopped and the flask once more opened to the pumps. This process was repeated six times at the end of which the solution was completely free of dissolved helium and neon.

After the process of de-aeration, the sample of beryllium was lowered into the solvent by moving the iron slug B with an external magnet. Solution was allowed to proceed until a pressure of 60 cms. was observed on the manometer, when it was stopped by again moving the iron slug B. The Dewar type trap D was filled with liquid nitrogen, and the charcoal bulb E, which had been previously evacuated whilst baking at 200°C, was immersed in liquid nitrogen. The charcoal bulb E contained 35 grams of coconut charcoal. Taps T_3 and T_4 were opened. The tap T_1 was then opened to allow the hydrogen, together with its attendant helium, to flow, via the trap D and the non-return valve K, to the charcoal bulb E where it was condensed. This process was repeated until all the beryllium had been dissolved. There then remained in the flask a

residual pressure of hydrogen which was insufficient to pass the approximately 1 cm. level of mercury in the valve K. It was necessary to remove this and any helium remaining either in solution or in the gas phase.

The taps T_3 and T_4 were closed and the liquid nitrogen in the trap D removed, to allow the water condensed there to liquify and fall back into the flask through the tap T_1 , which was then closed. With the tap T_{12} closed pure oxygen was admitted to the flask via the tap T_{13} and the valve O_1 , and was bubbled through the solution to flush out dissolved helium until a pressure of about 3 cms. was observed on the manometer M_1 . The mercury in the Toepler pump G was raised to the ball-valves B_1 and B_2 , and the trap D once more filled with liquid nitrogen. The taps T_3 and T_6 were opened, and then T_1 was opened to allow the oxygen to flow into the vessel H. T_1 and T_6 were then closed, and the gas confined in the system between K, T_4 , T_{11} , and T_6 was transferred into the vessel H, using the Toepler pump G with T_{11} open, the gas in H being prevented from flowing back by the ball-ventil B_3 . This process was repeated three or four times with the exception that the tap T_6 remained closed, after which the greater part of the helium was contained in the charcoal bulb E the residue being in the vessel H together

with an excess of oxygen. Evidence for the correctness of this last statement is given by the fact that no helium was observed in the blank determinations following an actual measurement on irradiated beryllium, when these blank determinations were made without opening the flask from the previous measurement.

The tap T_9 was opened to allow pure oxygen from storage to enter the vessel H via the valve O_2 . It will be recalled from the earlier discussion on the purification of oxygen that this gas was stored as liquid at the temperature of liquid nitrogen. The pressure of oxygen in the line will not therefore exceed the vapour pressure of the liquid at the temperature of liquid nitrogen (approximately 15 cms. of mercury), and hence the pressure of oxygen in the vessel H can never exceed this value, and in fact is always slightly less owing to the presence of a 1 cm. level of mercury in the valve O_2 .

The vessel H is a specially designed chamber for the combustion of hydrogen-oxygen mixture with the minimum risk of explosion. The vessel is filled with oxygen to a pressure of 15 cms. as described above. Tap T_4 is opened and the liquid nitrogen surrounding the bulb E is lowered until a hydrogen pressure of 30 cms. is registered on the manometer M_2 . The tap T_6 is carefully opened to admit hydrogen to the vessel H

via the upper side-arm at the junction of which is a heated platinum spiral. The hydrogen is ignited and the resulting flame travels down the body of the vessel which is conical in shape. As the flame travels down the vessel a greater surface of contact is presented to the reaction mixture causing a corresponding increase in the reaction rate, resulting in a decrease in hydrogen pressure. This decrease in pressure retards the advance of the burning front causing the flame to withdraw to the narrower part of the vessel and the reaction rate decreases. The liquid nitrogen level around E is meanwhile further lowered to admit more hydrogen, the bulb F acting as a ballast to minimise the pressure changes occurring. Pure oxygen is continuously supplied to maintain a pressure of 15 cms. in H, the tap T_9 remaining open throughout the period of burning. However, even with the presence of the ballast vessel F, the hydrogen pressure would sometimes fall dangerously low with poor adjustment of liquid nitrogen level around E, the control being difficult to adjust, and in such case T_6 was closed until the hydrogen pressure built up again. This process was continued until the hydrogen pressure in E and F fell below 30 cms. with no nitrogen surrounding the bulb E. The taps T_6 and T_9 were then closed.

The mercury in the Toepler pump was then lowered,

the gases in the vessel H being prevented from escape by the ball-valve B_3 , and the tap T_{11} was carefully opened to allow hydrogen to enter G, being then closed. The Toepler pump was then raised and hydrogen bubbled past the ball-valve B_3 and was burnt in the chamber. This process was repeated until no residual pressure was observed on the manometer M_2 . Throughout this process the oxygen pressure was manually adjusted to maintain the pressure at just above the stoichimetric requirement. The final pressure in H was of the order of 3 cms. of which the greater part was contributed by the water vapour in the vessel. The vessel H now contained all the helium together with a residual pressure of oxygen, water vapour, and traces of unburnt hydrogen.

The trap I was then surrounded with liquid nitrogen, the tap T_8 opened, and the gases transferred by means of the Toepler pump J to the next section of the apparatus via the tap T_5 , this next section being the circulating system. This process was continued until no residual pressure was observed on the manometer M_3 , the water vapour in H having been condensed in the trap I. With the Toepler pump J raised, oxygen is admitted to the vessel H to a pressure of 1 cm. and the trap I is surrounded with warm water thus vapourising the water condensed there and freeing any dissolved helium. The trap was once more surrounded with liquid nitrogen,

and the gases in H transferred to the circulating system as before. This process was repeated three times to ensure that all the helium was transferred to the next section of the apparatus.

The method just described was found to be satisfactory for samples of beryllium yielding from 500 ccs. to 2 litres of hydrogen, but for smaller samples the method was unwieldy in practice. Indeed as experience of helium analysis was acquired the method was found to be unnecessarily complicated and was later abandoned even in cases where the hydrogen production was as much as 6 to 7 litres. With such large volumes the apparatus became more difficult to operate. In the apparatus described by Glueckauf (41) the dissolving vessel is exposed to the charcoal reservoir via a trap cooled in liquid nitrogen, no non-return system being included as at K in figure 3. Under such conditions it is not possible, in the writers opinion, to ensure a quantitative transfer of helium since there will be exposed to the charcoal the large volume of the flask. The non-return valve K was included to remove the possibility of non-quantitative transfer, but there are difficulties associated with this when large volumes of hydrogen are to be handled. With large volumes of hydrogen a large equilibrium pressure is built up on the charcoal, this in turn means that the flask can only be emptied

to that pressure, and hence the dissolving cannot be completed in one stage. This considerably lengthens the time required for an analysis. The difficulty could presumably be removed by increasing the quantity of charcoal in the bulb E, but with 90 grams of charcoal in the bulb little improvement was observed. Any further increase in the quantity of charcoal above this level increases the difficulty of de-gassing. There also arises the possibility of helium retention on charcoal observed by Wardle (111), a phenomenon which seems to depend on the source of the charcoal. The results obtained when only 30 grams of charcoal were used are in agreement with other measurements performed by a different method, and retention of helium is not suspected in this case. However, in making up the charcoal to 90 grams it was not possible to use the same material, and helium retention was suspected although the method was rejected before this observation could be confirmed.

A further difficulty observed in handling larger volumes of hydrogen was that after about three litres of hydrogen had been burnt the reaction became much slower, and the flame disappeared completely. During such times the glow of the platinum spiral was extinguished, and in some cases an hour or more was required before conditions necessary to continue the burning

were attained. This was assumed to arise from the accumulation of nitrogen or argon (from the oxygen) in the burning vessel - the trouble did not arise with oxygen obtained by a commercial electrolytic process.

Method 11.

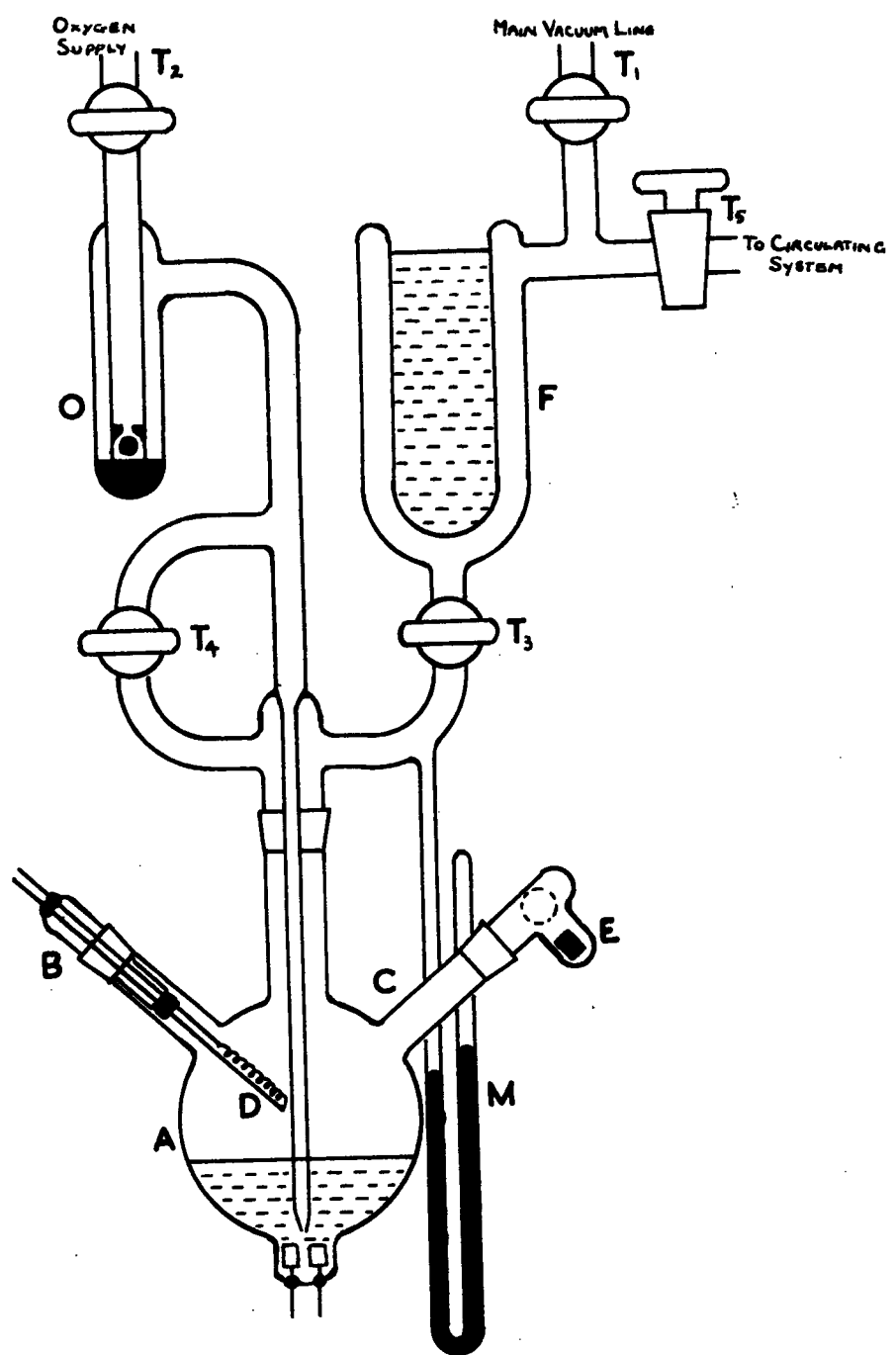
This method was applied to small samples of mass approximately 50 milligrams. The apparatus, shown in figure 16, consists of a four-necked 500 ccs. flask containing 100 ccs. of a 20% aqueous solution of sulphuric acid nearly saturated with potassium persulphate. One of the necks is not shown in the figure. The neck B carries a heating coil of platinum tape D sealed into a B-14 soda glass cone which fits into B. The neck C carries another cone joint E having three side-arms distributed as shown in figure 16, these small side-arms carrying samples of beryllium. The construction is the same for the fourth side-arm not shown in the figure. Two electrodes of platinum foil are sealed into the base of the flask.

The taps T_1 , T_2 , and T_3 are opened and the flask evacuated through the main vacuum line, after which the tap T_3 is closed. The solution is electrolysed, the current being adjusted to give a rapid stream of bubbles, until the pressure inside the flask is about 1 cm. of mercury on the manometer M. The electrolysis is then stopped, and the flask once more evacuated

FIGURE 16.

Beryllium dissolving vessel.

(Method II).



through T_3 . This is repeated six times at the end of which the solution is completely de-aerated. T_1 and T_3 are then closed. From a knowledge of the dimensions of the flask and the mass of beryllium to be dissolved, the pressure of oxygen required for complete combustion of the hydrogen evolved on acid-dissolution of the metal, can be calculated. This pressure of oxygen can then be admitted to the flask through the tap T_2 and the valve O. The flask is then immersed in the water-bath W to the level indicated in the figure, and the platinum heating spiral switched on, the current being adjusted so that a bright red glow is produced.

The sample-holder E is rotated to allow a sample of beryllium to fall into the solvent, and the hydrogen produced burns quietly, the flame, visible in a darkened room, being confined to the region around the glowing spiral. This continues until hydrogen is no longer evolved. The trap F is filled with liquid nitrogen, and the tap T_5 is opened. T_3 is then opened to allow the residual gas to be transferred to the circulating system, T_3 then being closed. T_4 is closed, and pure oxygen is bubbled through the solution via the valve O and tap T_2 , until a pressure of 1 cm. is observed in the flask by means of the manometer M. The oxygen supply is then cut off, and T_3 again opened to transfer the gas to the circulating system. Water is condensed

out by the trap F. This process is repeated six times to ensure quantitative transfer of the helium to the circulating system. The tap T_5 is then closed, and the heater D switched off.

The sample-holder E is constructed with several side-arms so that a number of samples can be analysed without opening the flask to the atmosphere. Samples of un-irradiated beryllium are included in practice to perform the blank analyses necessary to check the working of the apparatus. The use of this method enabled analyses to be performed rapidly. Although the method used only small samples, it can readily be applied to larger samples, as the following method, applied to samples of mass approximately six grams, will show,

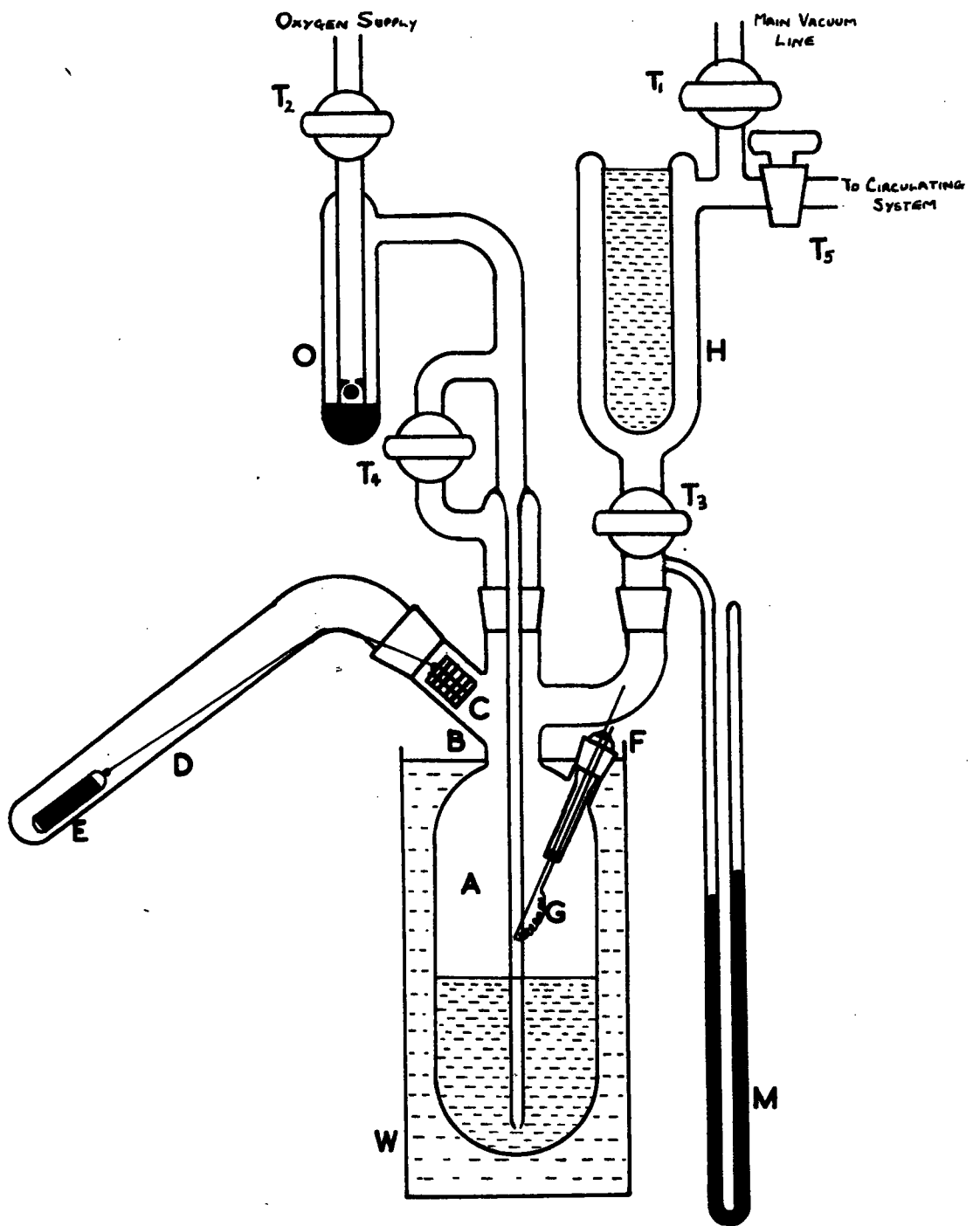
Method 111.

The apparatus is shown in figure 17, the main reaction vessel consisting of a cylindrical flask A of 2 litres overall capacity, and fitted with three side-arms in addition to the main neck. The side-arm B is fitted with a long arm D, and contains the beryllium sample in a platinum cage C which is attached to the iron slug E by means of a thin platinum wire. The arm F carries the platinum heating coil G as described in method 11, the coil being situated just above the surface of the solvent. A water-bath W

FIGURE 17.

Beryllium dissolving vessel.

(Method III).



surrounds the main body of the flask.

For approximately 6 grams of beryllium the solvent consists of 1 litre of a nearly saturated solution of potassium cupric chloride. This reagent reduces the hydrogen yield to about 1 litre/gram of beryllium, as compared to 2.5 litres/gram with sulphuric acid. It is desirable to limit the hydrogen production so as to allow a less stringent tolerance level of helium impurity in the purified oxygen required to burn the hydrogen. The method to be described could handle much larger quantities of hydrogen were it not for this limitation. The quantity of solvent used is in excess of that required for complete solution of the beryllium for the following reason. During the dissolution of the beryllium the metal becomes coated with a layer of deposited copper which retards the rate of solution, often to such an extent that solution of the beryllium ceases. This can be avoided by using a large excess of solvent.

The taps T_1 , T_3 , and T_4 are opened and the flask evacuated through the main vacuum line, T_3 then being closed. It is not possible to de-aerate the potassium cupric chloride solution by electrolysis since chlorine is evolved during this process, and this is an undesirable material to handle in a vacuum apparatus of this type. The solution was therefore de-aerated by flushing
ing

the solution several times with pure oxygen, in the following manner. The tap T_4 is closed, and pure oxygen is passed into the flask via T_2 and the valve O, until a pressure of about 3 cms. is recorded on the manometer M. This gas is then pumped away through the high vacuum line via the tap T_3 , the flask remaining open to the pumps for about 1 minute before T_3 is closed. It was found experimentally that this process should be repeated 15 times in order to ensure complete de-aeration, and in practice this was extended to 20 times in order to be quite sure that all helium and neon had been removed. On the final flushing the tap T_4 was opened before pumping out the oxygen, after which T_3 was closed.

The tap T_2 is opened, and the flask filled with oxygen to the limiting pressure of about 12 cms. determined by the vapour pressure of liquid oxygen in the reservoir. The heating coil is switched on, and the beryllium sample lowered into the solvent by moving the iron slug E. When the first of the hydrogen is burnt the flame extends to the walls of the flask A, but this rapidly diminishes and the flame is confined to the region of the platinum spiral, and its size can be controlled by regulating the depth of immersion of the sample. More oxygen is automatically added to make up for that used, the pressure in the flask

being regulated by the vapour pressure of the liquid oxygen in the reservoir. With experience the burning can be controlled without explosive conditions being attained. When only a little beryllium remains T_2 is closed to cut off the oxygen supply. At this juncture the manometer M is observed continuously in order to follow the progress of the reaction, the reading decreasing as oxygen is used up until a small residual pressure is attained. Oxygen is then added, by manual operation of the tap T_2 , in small quantities until the burning is complete. With practice it is possible to end up with a pressure of 2 to 3 cms. of which the greater part is contributed by the water vapour pressure of the solution. The heater G is then switched off.

The trap H is filled with liquid nitrogen, the tap T_1 closed and T_5 opened. T_3 is then opened to allow the gas to pass on to the circulating system, water being removed by the trap H. T_3 and T_4 are then closed and oxygen is passed into the flask to a pressure of about 1 cm. This gas is then transferred to the circulating system via T_5 . The solution is flushed in this manner a total of five times when all the helium has been transferred to the circulating system, this being checked by a subsequent flushing of the solution and examination of the flushing gas for helium.

The three procedures outlined for the extraction

of helium from beryllium all result in the helium being collected in the circulating system, the helium being in admixture with a large excess of oxygen and traces of hydrogen. It is important in the method used for the final analysis of the helium that all traces of hydrogen are removed, and this is performed in the circulating system which will now be described.

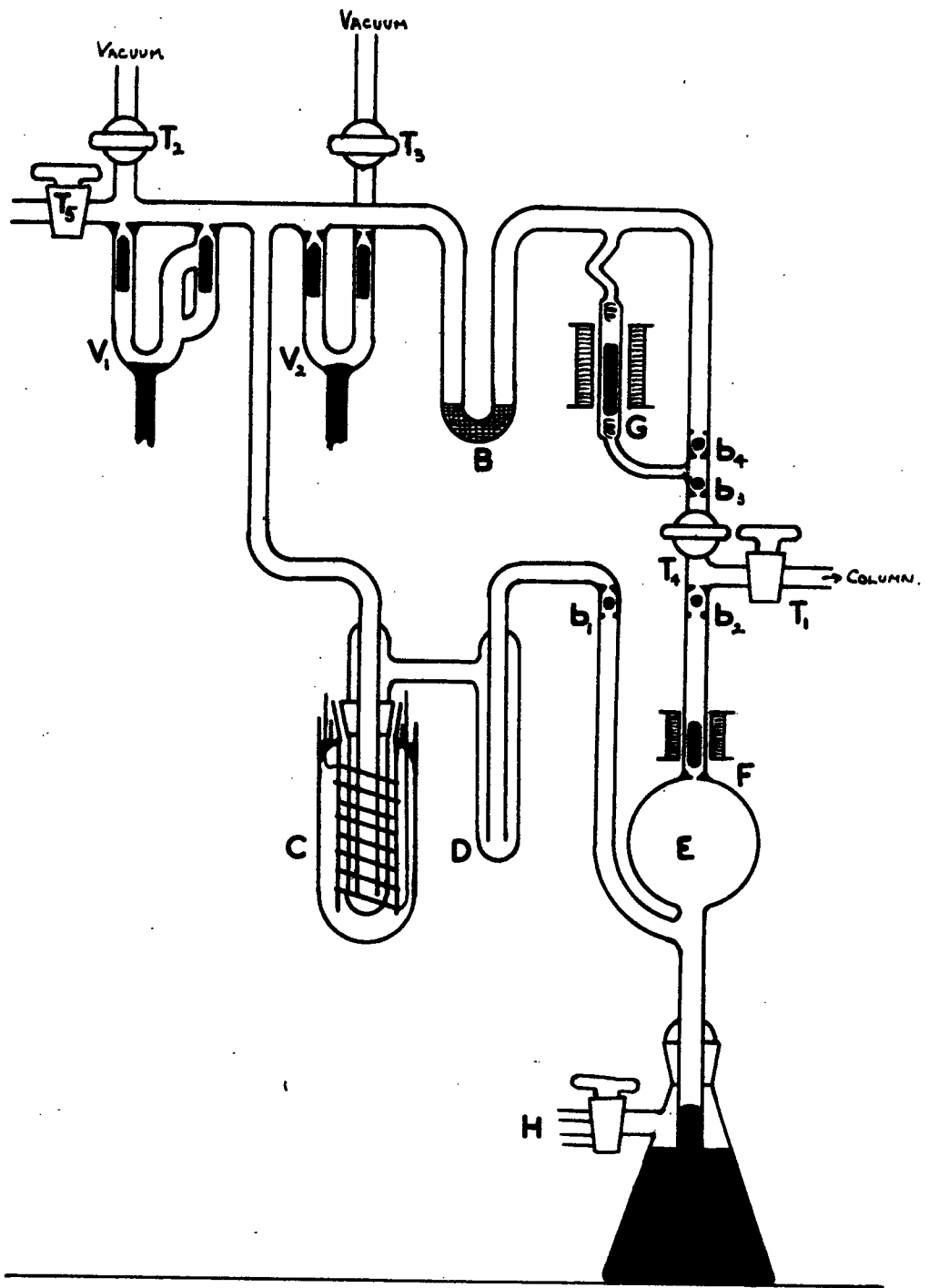
V. 4. The circulating system.

In this system the mixture of helium, excess of oxygen, and traces of unburnt hydrogen, is passed over heated palladium which catalyses the combustion of hydrogen and oxygen to water. The gases are circulated around the closed circuit by means of the pump G (figure 18), the intermittent action of the solenoid causing the close fitting iron slug, which is contained in a soda-glass envelope, to rise and fall, and this, together with the action of the two ball-valves B_3 and B_4 , allows gas to circulate in the system. The gas is thus caused to pass over heated palladium in the furnace C, the detailed design of which has been described by Paneth and his collaborators (108). The design of the present method of removing trace quantities of hydrogen is due to Chackett and collaborators (102).

The system is rigorously evacuated through the ventils V_1 and V_2 with the taps T_2 and T_3 open, the charcoal in the U-tube B being baked at 250°C during

FIGURE 18.

The circulating system.



this evacuation. When the system is evacuated the taps T_2 and T_3 are closed and the ventill V_2 raised. The ventill V_1 is raised only to such height as to close the U-tube at its lower end. The tap T_5 which is the same as T_5 in figures 15, 16, and 17, is opened and the charcoal bulb B is immersed in liquid nitrogen. As gas is transferred from the helium extraction systems via T_5 it forces its way past the mercury in the ventill V_1 , and is condensed on the charcoal in B. The several quantities of gas which are transferred from the helium extraction systems in order to ensure quantitative transfer of helium, serve to sweep out the intervening tubes. The ventill V_1 acts as a non-return valve. When all the gas has been transferred the ventill V_1 is closed. The helium, together with excess of oxygen and traces of hydrogen, is now confined in the circulating system.

Liquid nitrogen is placed around the trap D, and the bulb B is allowed to warm up to room temperature the gas pressure in the system rising as it is released from the charcoal. In the case of extraction methods I and II the final pressure attained is about 3 to 4 cms. but is greater in III being of the order of 15 cms. Tap T_4 is opened, and the solenoid around the ventill F is activated to raise the stopper. The palladium furnace is switched on, and the current adjusted so that the 'Nichrome' tape winding glows at a dull red heat.

The outer jacket of the furnace is immersed in water to cool the system. The gas is circulated by means of the pump G. For extraction methods I and II the circulation of the gas is continued for about thirty minutes, but in III this is lengthened to 2 hours. Water is condensed out in the trap D. When the hydrogen has been removed the palladium furnace, and the pump G are switched off. The system now contains helium with a large excess of oxygen.

Before the helium can be measured it must be separated from the excess of oxygen, and for this purpose the method adopted by Glueckauf (105) for the separation of the helium and neon in atmospheric air is used. The design of the present system is due to Chackett (102), and although somewhat more complicated than should be necessary for the separation of helium from oxygen it is used in this work in order to check that no air leaks have occurred during the previous operations. An air leak would be indicated by the pressure of neon in the gas mixture, and in practice this was always looked for after the measurement of the helium. Although the fractionating column has been described, a brief account is included here for the sake of completeness.

V. 5. The fractionating column.

The method developed by Glueckauf (105) for the quantitative separation of the helium and neon in air

depends upon the fractional adsorption of the gases on charcoal cooled in liquid nitrogen. A single adsorption unit consists of a quantity S of solid adsorbent in contact with a vessel of volume V . At equilibrium the distribution factor 'a', defined by

$$a = \frac{1}{1 + \alpha(S/V)} \quad (1)$$

gives the fraction of the initial material in the gas phase, and is a characteristic of the gas whose adsorption coefficient is α . When a mixture of gases is present in the adsorption unit, the equilibrium distribution of the gases will be dependent upon the distribution factors of the gases, which in turn depend upon the relative values of S and V . There is an implicit limitation to linear adsorption isotherms, and gas mixtures with no mutual interference. With the condition that the best separation of two gases may be considered achieved when a maximum proportion of one of the gases would have to be transferred to the other phase in order to produce equal ratios of the two gases in both phases, Glueckauf shows that for optimum separation the distribution factors are simply related as

$$\underline{a + b = 1} \quad (2)$$

When a series of adsorption units is used the gaseous phase is transported from one adsorption unit to

the next. The adsorbent of the first stage is then again connected with an evacuated space, and the adsorption equilibrium re-established with the gas initially adsorbed. This process is repeated, the gas from any one stage being combined with the adsorbent of the next. The gas from the final stage is collected in a storage vessel. Glueckauf has calculated the amounts of material in the various units 'm' and stages 'n' of the fractionation process, deriving the following general expressions :

$$A_n^m(g) = A_0 \frac{(n-1)!}{(m-1)!(n-m)!} a^m (1-a)^{(n-m)} \quad (3)$$

$$A_n^m(s) = A_0 \frac{(n-1)!}{(m-1)!(n-m)!} a^{(m-1)} (1-a)^{(n-m+1)} \quad (4)$$

where A_0 is the initial quantity of gas, $A_n^m(g)$ is the amount of gas in the gaseous phase, and $A_n^m(s)$ is the amount adsorbed in the m^{th} unit after n operations. For a system of 'm' units the amount of gas A , A_s , transferred to the storage vessel after 'n' fractionation processes is

$$A_s = A_m^m + A_{m+1}^m + A_{m+2}^m + \text{---} + A_n^m \quad (5)$$

the summation beginning with the m^{th} process since no gas is delivered to the storage vessel until this operation. The amount remaining, A_r , in the system is

$$A_r = A_{n+1}^m + A_{n+2}^M + \text{-----} + A_{\infty}^m \quad (6)$$

Similar expressions are valid for another gas B.

During the course of the fractionation of two substances A and B, the successive fractions delivered to the storage vessel F_x will be given by

$$F_x = A_x^m + B_x^m \quad (7)$$

the total amount of gas in the storage vessel ΣF_x is

$$\Sigma F_x = A_s(x) + B_s(x) \quad (8)$$

In the course of the process both the quantities A^m , B^m , go through maxima, this being illustrated in figure 22 which shows an experimental curve obtained for the fractionation of the helium and neon in a sample of air. Figure 22 is drawn as a continuous curve, but in reality, by the nature of the process, it is a step function .

It can be seen from equation 8 that the gas accumulating in the storage vessel is a mixture of the two components. Glueckauf considers the question of the number x of fractionations required to give an optimum degree of separation. If the fractionation is cut off too early the gas in the storage vessel will be of a high degree of purity, but as the fractionation continued an increasing amount of the component with the higher adsorption coefficient will be collected. A state

of separation is required in which A_s together with the contamination B_s represents as nearly as possible the initial quantity of the gas A. The fractionation number n is deduced approximately as

$$n = 2m - 1 + \frac{\log \frac{A_0}{B_0}}{\log \frac{1-b}{1-a}} \quad (9)$$

and it can be seen that if A and B are present in nearly equal quantities the number of fractionations is approximately twice the number of adsorption units, irrespective of the adsorption factors of the two gases. The ratio of two successive fractions of gas from the m^{th} adsorption unit is, from equation (3), given by

$$\frac{A_{n+1}^m}{A_n^m} = \frac{n}{n - m + 1} (1 - a) = z(1 - a) \quad (10)$$

where for the optimum number of fractionations given by (9) the value of z is 2. An expression is also deduced for the degree of purity of the separated products as a function of the adsorption factors, the number of adsorption units, and the fractionation number.

The expressions deduced above are applicable to an ideal fractionation system, in which all the adsorption units are identical. In practice this is difficult, if not impossible, to achieve, and the number of operations for optimum separation together with the purity of the separated product is best determined by experiment.

The design of apparatus used in the present work is due to Chackett (102), and comprises 15 adsorption units. The construction of the fractionating system is shown in figure 19, the adsorption units being indicated. Each unit consists of a charcoal bulb (C_n) connected to a vessel (A_n) which is in turn connected to a second vessel (B_n). The bulb C_n contains 1 gram of coconut charcoal as adsorbent. The mixture of gases to be analysed is condensed on the charcoal which is cooled to the temperature of liquid nitrogen, the set of bulbs, A_n , B_n , being filled with mercury to the level indicated by the horizontal dotted line 1. The sets of bulbs are supplied with mercury from two separate reservoirs not shown in figure 19. When the mercury in the bulbs A_n is lowered to the level indicated by the horizontal dotted line 2, there is exposed to the adsorbent C_n the volumes A_n , and the adsorption equilibrium is set up. The mercury is then raised, the action of the cut-off tubes preventing the gaseous phase from being returned to the adsorbent. As the mercury rises in the bulb A_n , that in the bulb B_n is lowered to the level 2 and the gas enters the volume space provided by the operation. The mercury in B_n is then raised, the action of the cut-off allowing the gas to be transferred to the adsorbent C_{n+1} . The set of bulbs B thus act as Toepler pumps. The end fractions from unit 15 are

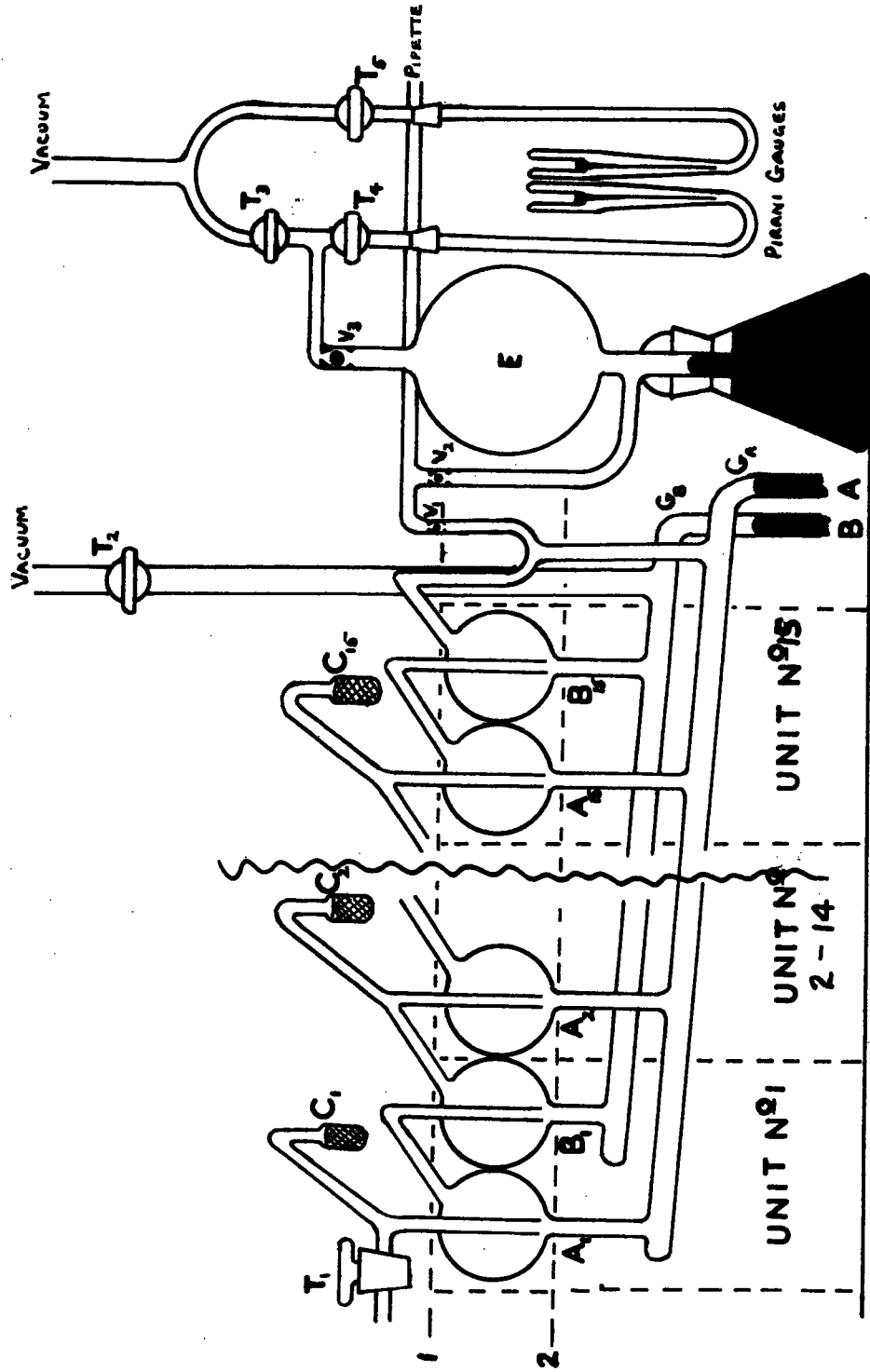
collected in the storage vessel E, after passing the U-tube D. At the end of a pre-determined set of operations, an operation being considered as the transfer of gas from one unit to the next, the fractionation is stopped, and the accumulated gas can then be measured. This is done by raising the mercury in the storage vessel E, thus compressing the gas into the space defined by the ball-valve V_3 , and the taps T_3 and T_4 , the gas being then measured by admitting it into the Pirani guage system via T_4 ,

The function of the fractionating system being outlined, the discussion of final stages of the determination of helium in beryllium can be completed.

The fractionating column is first rigorously evacuated through the tap T_2 (figure 19), and the charcoal in the bulbs C_n baked at 250°C for half an hour to remove adsorbed gases and activate the charcoal. When a hard vacuum has been attained, indicated by means of a McLeod guage, the mercury is raised in the column to the level indicated by the horizontal dotted line l. When the mercury is in this position it will be observed that only the charcoal bulb C_1 is exposed to the tap T_1 . The charcoal bulbs are then immersed in liquid nitrogen, and the mixture of oxygen and helium present in the circulating system may now be transferred to the fractionating column.

FIGURE 19.

The fractionating column.



For helium extraction methods I and II the whole of the gas in the circulating system is transferred to the first bulb C_1 , the amount of gas being comparatively small, and readily accommodated on the charcoal. The procedure is as follows. The mercury in the Toepler pump E (figure 18) is raised to the cut-off point with the tap T_4 closed. The solenoid F is switched on to raise the ventil, and the tap T_1 carefully opened to allow the gas contact with the charcoal C_1 of the fractionating column. This operation must be performed very carefully at this stage as a sudden flow of gas into the column may be sufficient to depress the mercury level in the cut-off tube to such an extent that gas passes into the bulb A_1 . Apart from upsetting the separation process, the violent movement of mercury may easily fracture the delicate structure of the column. The mercury in the Toepler pump E will begin to rise as gas is adsorbed on the charcoal and at this point the mercury in the pump may be slowly raised by opening the tap H slowly to the atmosphere. When the mercury reaches the ball-valve B_2 , the tap T_1 is closed and T_4 opened. The mercury is then lowered in E by opening H to the secondary vacuum line. This procedure is adopted to avoid violent bubbling of gas from the circulating system into E, which would be under vacuum if T_4 were not opened. The ball-valves B_3 and

B_4 should be held open with a magnet to allow free flow of gas through T_4 .

The tap T_4 is again closed and the Toepler pump raised as before, T_1 being carefully opened to admit gas to charcoal C_1 of the column, and then T_1 is again closed. The mercury in E is lowered with the solenoid F switched off so that a mercury seal is made at the vent, thus preventing gas from flowing back into the circulating system. The Toepler pump is then operated a further five times, T_1 being opened after each stroke to admit the gas to C_1 . This procedure serves to transfer the helium quantitatively to the charcoal C_1 . At the end of the final Toepler stroke, the mercury is raised to the ball-valve B_2 , and the tap T_1 is opened. T_1 remains open throughout the rest of the procedure.

When the extraction method III is used this procedure must be modified since the final volume remaining in the circulating system is too much to accommodate on the charcoal C_1 . Accordingly, after the removal of traces of hydrogen, the bulb B (figure 18) is again surrounded with liquid nitrogen to condense the oxygen. Tap T_4 is then closed, and the mercury in E raised to the ball-valve B_2 . The tap T_1 is opened to admit the gas to the first charcoal bulb, and may remain open. The mercury in E is lowered, and the vent V closes forming a gas-tight seal. After allowing about

30 seconds for the gas in the circulating system to come to equilibrium, the Toepler pump is again raised to B_2 . It was found experimentally, using an air sample analysis, that some 15 operations of the Toepler pump in this manner, served to quantitatively transfer the helium and neon to the column.

After allowing ten minutes for the heat of adsorption of the gas on the charcoal to be dissipated - the temperature of the adsorbent being an important parameter in the adsorption equilibrium - the column is operated by alternately lowering and raising the mercury in the sets of bulbs A and B. In this particular system the mercury levels are automatically altered by a system of electrically operated gas valves. At the end of 15 operations, the column is stopped and the mercury in the bulb E (figure 19) is raised to the ball-valve V_3 . The tap T_4 is then opened, and the deflection of the galvanometer in the electrical system of the Pirani gauges observed. No deflection should be observed. T_3 is then opened to the high vacuum line, and the galvanometer again observed. No deflection should be observed since no gas is delivered to the storage vessel during the first 15 operations of the column. The taps T_3 and T_4 are then closed and the mercury in the storage vessel E is lowered. Should a deflection be observed after 15 operations of the column the run must be

rejected, the column not having been completely freed of adsorbed gases during the pumping period. More will be said on this point later.

The column is then operated for a further 21 operations at the end of which the gas is transferred to the Pirani guage system as before. During these 21 operations the liquid nitrogen is successively removed from charcoal bulbs C_3 to C_{15} , in order to facilitate the removal of any neon present. C_1 and C_2 remain immersed to hold back oxygen. Reference to figure 22 will show that some 80 further operations would be required to quantitatively remove neon from the column with the charcoal at liquid nitrogen temperature. Since helium is quantitatively removed after 36 operations, C_3 could be allowed to warm up after operation 25, C_4 at operation 26 and so on. For practical convenience the charcoal bulbs are immersed in liquid nitrogen in batches of 4. Thus $C_{1,2,3,4}$, are together, as also $C_{5,6,7,8}$, $C_{9,10,11,12}$, and finally $C_{13,14,15}$. The charcoal is lowered from around the first set after operation 26, C_1 and C_2 being constructed so that they can be separately immersed, whilst C_3 and C_4 are allowed to warm up. $C_{5,6,7,8}$ are allowed to warm up after operation 30, and so on.

Earlier work on this apparatus has shown that neon is quantitatively transferred to the storage vessel after 61 operations of the column, i.e. 25 operations

after the removal of the helium, under the conditions given (61). The gas in the storage vessel is then transferred to the Pirani gauge system as before.

At the end of a complete determination, the mercury is lowered in the column, the system then being opened to the main vacuum line. The liquid nitrogen is removed from C_1 and the oxygen thus released is pumped away. The charcoal is then baked in preparation for the next run.

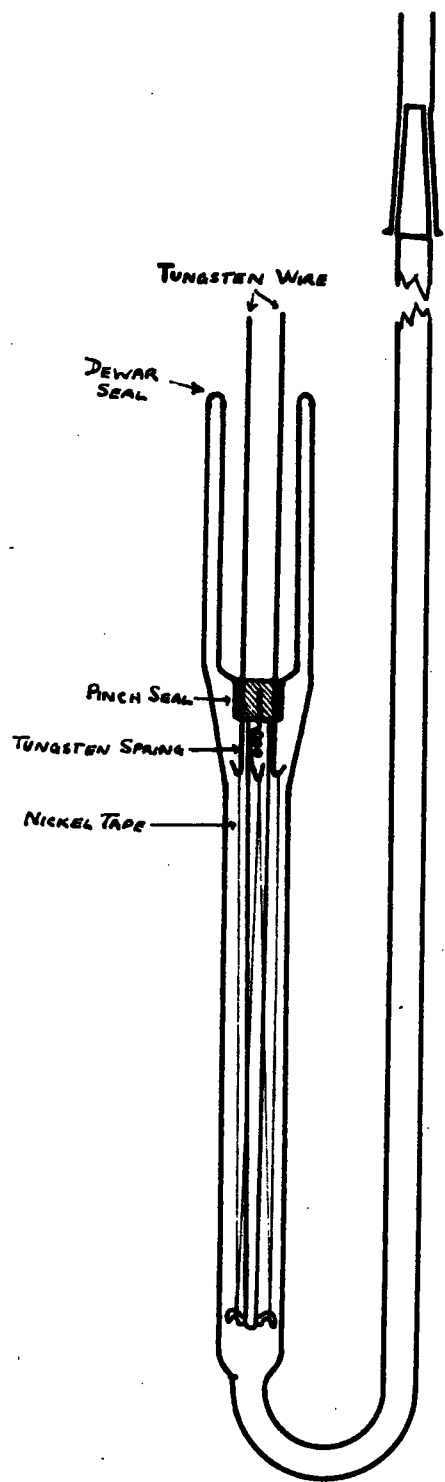
V. 6. The Pirani Gauges.

The Pirani type of pressure gauge has been used for the measurement of micro-quantities of helium by several workers, many different designs being used (55,102,112). One of the major difficulties with this type of gauge is the problem of 'drift', the term being used to describe the movement of the zero of the recording device, e.g., a galvanometer needle, with time. Little is known of the reason for this phenomenon, but during the course of this work it was suspected to be due to small thermo-e.m.f's produced by temperature differences in the bi-metal junctions present in the system. The present gauge was therefore designed to minimise these temperature differences, the elimination of the bi-metal junctions not being practical.

The design of the Pirani gauge is shown in figure 20. Two tungsten wires (0.1mm. diameter) are sealed through the glass envelope by means of a 'pinch' seal.

FIGURE 20.

The Pirani Gauge.



7

A piece of tungsten wire in the form of a short spring is also sealed into the pinch. The three wires are formed into hooks at their ends, as near the pinch as practicable. An 8 cm. glass rod sealed to the pinch runs axially down the glass envelope, being fashioned into two hooks at its free end. A length of nickel tape (30cms x 0.05mm x 0.003mm.) is stretched on the frame, provided by the 3 tungsten hooks and two glass hooks, in the form of a 'W', the nickel tape being soldered to the two outer tungsten hooks. Before soldering, the tape is tensioned by suspending 5 gram weights from its free ends. The tape is put under tension since it was found that this improves the stability of the gauge.

The glass envelope is made of 'Pyrex' glass in order to make the pinch seal to tungsten, the volume of the envelope being made as small as possible to increase the sensitivity of detection. A similar system was constructed completely in soda glass using platinum through seals, but this would not stand immersion in liquid nitrogen. Although 'Pyrex' is permeable to helium, no build-up of gas was observed in the Pirani system during operation, probably because the diffusion through the glass is very much slower at liquid nitrogen temperatures.

Two Pirani gauges are used in practice, one being

used for the measurement of the gas and the second provides a compensating arm in the Wheatstone bridge network used. The range of sensitivity enabled measurements to be made in the range from about 10^{-9} to 10^{-4} ccs. of helium.

The Piranis are mounted on the apparatus as indicated in figure 19, the pyrex to soda joint being indicated by a B10 cone and socket sealed with 'Apiezon W' wax. The whole of the system is immersed in liquid nitrogen to about 2 cms. below the waxed joints. The operation is as follows.

The Pirani's are opened to the high vacuum system via $T_{3,4,5}$, the charcoal in the U-bend being baked with a small flame at intervals. The charcoal is included to mop up gases released into the system via the tap grease. When a hard vacuum is attained the taps are closed, and a potential of 1 volt applied across the bridge. A potential difference of 1 volt is chosen to maintain the wire at approximately room temperature when the Pirani is immersed in liquid nitrogen, thus avoiding large changes in the mechanical condition of the wire. As soon as the potential is applied across the bridge, the Pirani system is immersed in liquid nitrogen to a level just below the Dewar seals. Five to ten minutes is allowed to cool the pinch seals slowly before complete immersion in liquid nitrogen. A period of two

hours is then required to bring the Pirani's to a steady state before measurement can be made.

With this system the drift was considerably reduced compared to that observed with another system (102). Measurements are made by observing the galvanometer spot and recording its position at half-minute intervals until steady conditions are assured. The admission of the gas to the Pirani gauge via T_4 cools the nickel wire thus changing its resistance and the out of balance current produced in the galvanometer is recorded. The gas is then pumped away via T_3 and the balance is restored. Readings of the position of the galvanometer spot are taken at half-minute intervals during the process, the deflection produced being determined graphically. The mean of the 'in' and 'out' deflections is taken as the true deflection.

The Pirani gauge is then calibrated by admitting a known amount of the same gas and recording the deflection produced, this known amount of gas being measured in a gas pipetting system, the design of which is due to Chackett (102). From the ratio of the deflections and the known amount of gas, the unknown amount is determined by simple proportion.

V. 7. The Pipetting System.

This system is designed to deliver an accurately known volume of gas to the Pirani gauge, the volumes

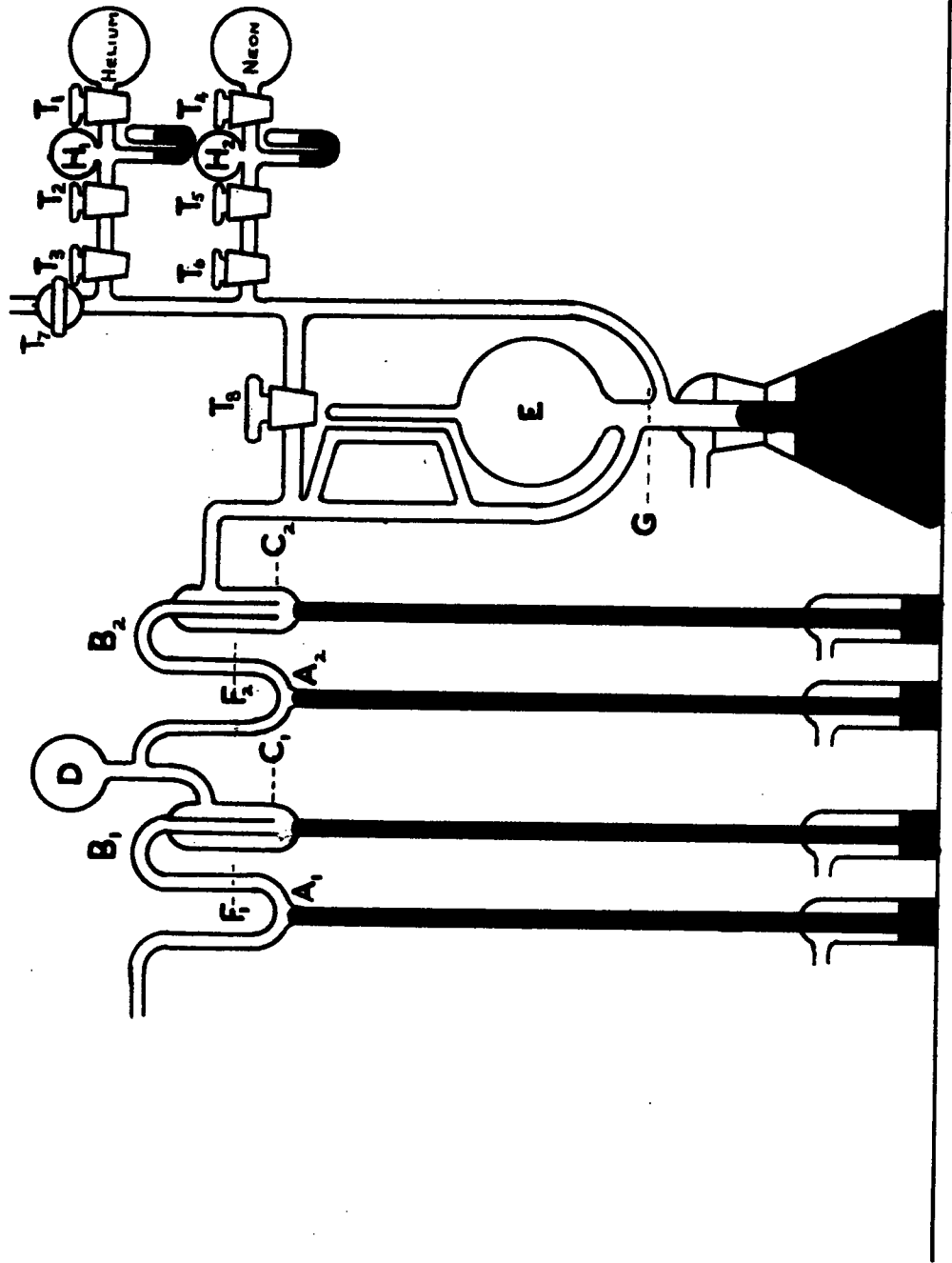
being in the range from 10^{-7} to 10^{-3} ccs. The design of the system is shown in figure 21.

The system is rigorously evacuated by opening it to the main vacuum line through T_7 , the pressure being observed in the McLeod gauge E. The mercury in the columns A_1 and A_2 is then raised to the etch marks F_1 and F_2 the tap T_7 being closed. T_1 is opened to admit a small pressure of helium to the bulb H_1 , T_1 being then closed. T_2 is opened to the bulb H_1 and then closed, thus confining a portion of the helium into the tube between T_2 and T_3 . The tap T_3 is then opened to admit this gas into the system. The mercury in the McLeod gauge E is raised, the level being brought to one of a number of etch marks, each marking accurately known volumes, on the closed limb of the gauge. Tap T_7 is then opened and the gas in the remainder of the system pumped away. The difference in the level of mercury in the two limbs of the gauge is then measured, and a correction applied for capillary depression. The temperature of the system is measured, and the quantity of gas in the system can then be determined.

Tap T_8 is closed, and the mercury lowered in the gauge to the etch mark G. The volume of the McLeod gauge and connecting tubes to the etch mark F_2 is accurately known. The mercury in C_2 is then raised to cut off a portion of the gas in the volume B_2

FIGURE 21.

The pipetting system.



which is accurately known. The level of the mercury is lowered in A_2 to a definite mark, and the gas confined in B_2 expanded into D, the volume of this system to the etch mark being known. Mercury in C_1 is then raised to cut off a known fraction of this gas in the pipette B_1 . Lowering the mercury in A_1 allows this gas to be expanded into the storage vessel E (figure 19), from which it can be transferred to the Pirani gauge. The mercury in A_1 is then returned to the level F_1 , and by lowering C_1 another quantity of gas can be measured, and again transferred to the Pirani gauge. This volume will be smaller but the correction factor can be determined from the known volume of the system. A second measurement is always made in practice to check on the working of the measuring system.

Small samples of neon can also be transferred to the Pirani gauge from the neon reservoir in the same manner.

V. 8. The Fractionation Calibration:-

In the earlier discussion of the fractionating column it was pointed out that the equations were derived for an ideal column in which all adsorption units were identical. This situation does not obtain in practice and the column characteristics were determined by experiment.

A small sample of air (approximately 1cc at N.T.P.)

is put onto the charcoal C_1 (figure 19), and the column operated in the manner described. After the first 15 operations have been completed, the succeeding operations are performed singly, the gas collecting in the storage vessel after each operation being transferred to the Pirani gauge and the deflection observed. In this way the experimental curve of figure 22 has been obtained, and this shows a well defined helium peak, followed by a flatter neon peak.

The adsorption factor of each gas can then be determined using equation 10, the resulting factors being a characteristic of the column. Using these adsorption factors it is then possible to calculate the shape of each individual curve of which figure 22 is compounded. The calculated curve is shown as a dotted line. The adsorption factors obtained are,

$$\underline{\text{Helium}} \quad a = 0.606$$

$$\underline{\text{Neon}} \quad b = 0.220$$

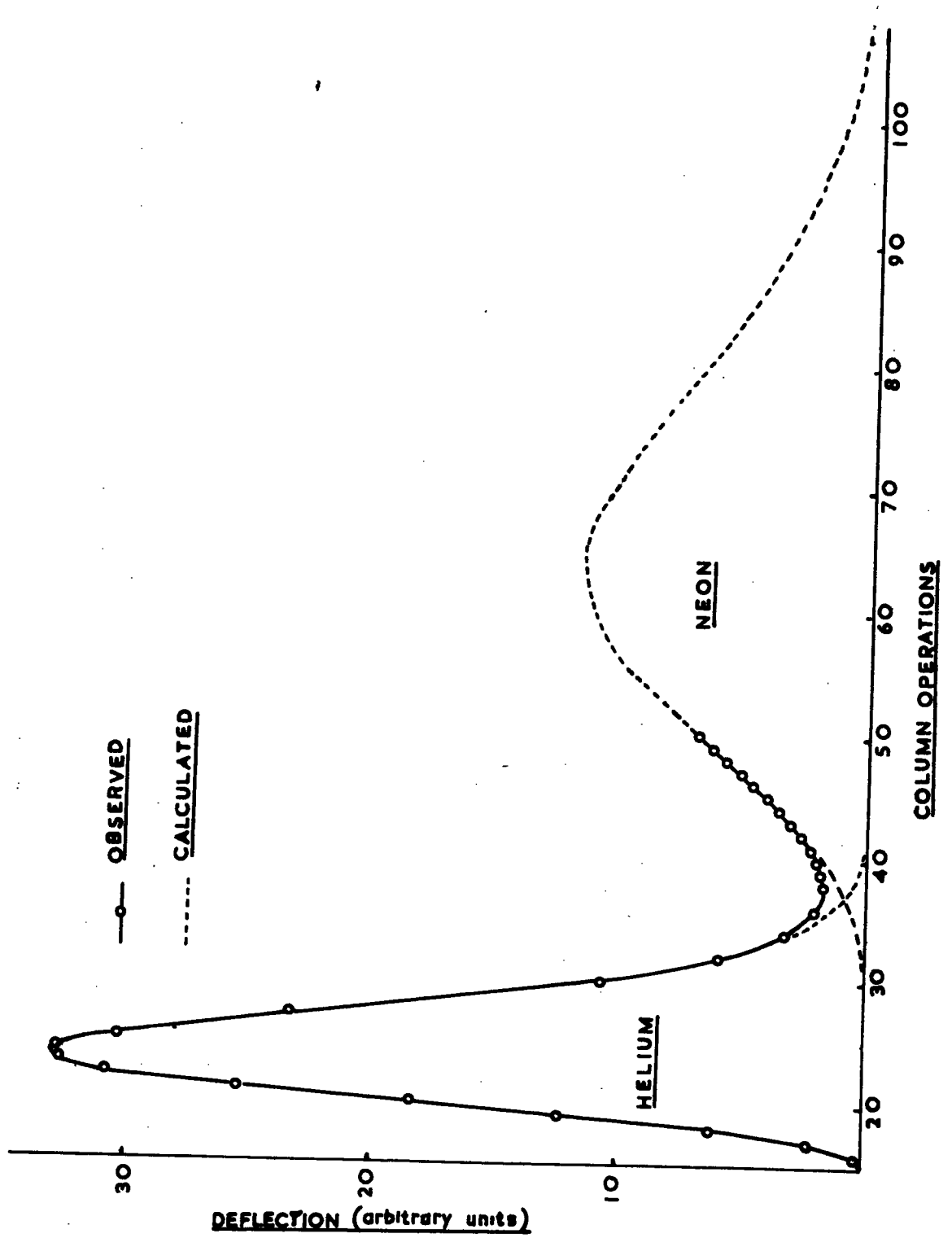
$$\text{i.e.} \quad a + b = 0.826$$

the result indicating that the optimum separation condition expressed in equation 2 is not fully realised.

Graphical integration of figure 22 reveals that for an air sample the error introduced by stopping the helium fractionation at operation 36 is less than 0.2%. When no neon is present the error introduced in stopping the helium fractionation at operation 36 is about 0.8%.

FIGURE 22.

Helium - Neon separation curve.



Thus a correction of 0.8% should be added to the helium observed from the dissolution of beryllium, a case in which no neon is observed.

Air sample analyses are conducted at regular intervals as a check on the correct working of the apparatus. The procedure and results of these analyses will now be discussed.

V. 9. Air Analyses.

An air pipette of the type shown in figure 23a is fitted to the apparatus at K (figure 15) by means of a B10 cone and socket joint. The taps T_2 and T_3 are opened to allow air to be admitted, the air being dried by the magnesium perchlorate packed in the tube. The temperature of the room and the atmospheric pressure are observed, and T_2 is closed. T_1 is then opened to the apparatus, and the sample of air is transferred to the circulating system using the Toepler pump J (figure 15), the vent V_1 (figure 18) being open. The Toepler pump E (figure 18) is then used to transfer the sample to charcoal C_1 of the column, and the analysis performed as described earlier.

The result of eleven air analyses performed at intervals during the course of this work are given. (see table XV.) The mean of these results together with their standard deviations is,

Helium = $5.279 \pm 0.006 \times 10^{-6}$ ccs/cc. of dry air.

Neon = $18.39 \pm 0.08 \times 10^{-6}$ ccs/cc. of dry air.

These results are in good agreement with those of

Reasbeck (61) obtained with the same apparatus, i.e.,

Helium = $5.285 \pm 0.010 \times 10^{-6}$ ccs/cc. of dry air.

Neon = $18.23 \pm 0.020 \times 10^{-6}$ ccs/cc. of dry air.

TABLE XV. AIR ANALYSES.

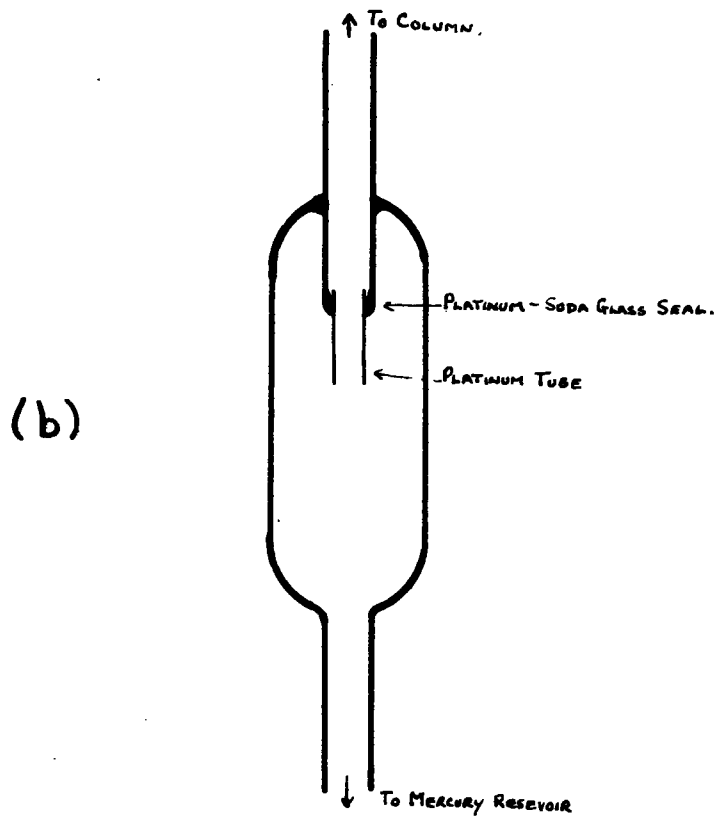
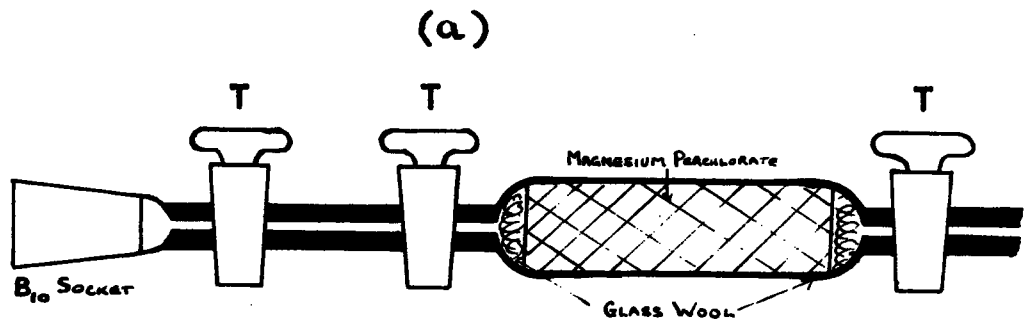
	Helium/cc. of air (ccs. $\times 10^6$)	Neon /cc. of air (ccs. $\times 10^6$)
1	5.272	18.42
2	5.281	18.38
3	5.293	18.45
4	5.278	18.28
5	5.282	18.36
6	5.269	18.52
7	5.288	18.30
8	5.276	18.26
9	5.274	18.37
10	5.278	18.41
11	5.285	18.29

The result for neon obtained in the present work is however somewhat higher than that obtained by Reasbeck. This cannot be due to systematic errors arising in the calibration of the air pipette since the result for helium is in close agreement, within the standard errors, with that of Reasbeck. However if the error is quoted as two standard deviations the results are in agreement. The air analysis results may be compared with those of

FIGURE 23.

(a) The air pipette.

(b) Air trap for fractionating column.



earlier workers given in Table XVI.

TABLE XVI.

	Helium/cc.of air (ccs. $\times 10^6$)	Neon/cc.of air (ccs. $\times 10^6$)
Ramsay (1905)	4.0	12.3
Claude (1909)	5	15
Watson (1910)	5.4	18.2
Glueckauf(1944)	5.24 \pm 0.03	-
Glueckauf(1945)	5.239 \pm 0.004	18.21 \pm 0.04

V. 10. Concluding Remarks.

In V. 5 it was pointed out that no deflection of the Pirani gauges should be observed for the first 15 operations of the column, but in practice a residual deflection was observed when the measuring system was used on its most sensitive range. An attempt was made to find the source of this residual deflection with a view to removing its cause; the apparatus used in helium extraction method I was in use at the time.

It was at first suspected that the residual deflection arose from mechanical vibration of the Pirani gauges on opening the admission tap, but this was checked by observing the galvanometer spot whilst opening and closing the tap. No discontinuity in the drift was observed. The whole apparatus, after pumping out in the normal manner prior to a helium determination, was operated without any gas in the system, the results of

this being shown in Table XVII, Nos. 1 and 2. The column alone was then operated after preliminary baking, the results are given Table XVII, Nos. 3 and 4. The average Pirani sensitivity on the measuring range used was 5×10^{-9} ccs. of helium/cm deflection.

TABLE XVII.

	Column Operations.		
	1 - 15	16 - 36	37 - 61
1	0.24cms.	0.57	-
2	0.15	0.50	0.60
3	0.29	0.44	0.70
4	0.13	0.42	0.52
Mean	0.20	0.48	0.61
Helium equivalent $\times 10^{-9}$ ccs.	1.0	2.5	3.0

It was observed that small bubbles of gas had collected on the column at the positions G_a and G_b (figure 19). These bubbles were only visible when the mercury in the column was lowered, and it was suspected that these were bubbles of air entrained with the mercury of the column reservoirs. It will be noted that if air is entrained in this way it has ready access to the storage vessel E by way of the U-branch D. This explanation of the residual

deflection is all the more credible in view of the rough proportionality between the observed deflection and the number of column operations shown in Table XVII. An attempt was therefore made to remove this effect by providing an air trap (figure 23b) in the lead from the mercury reservoir to the column. The air trap depends for its action on the observation that mercury 'wets' platinum so that an air tight seal should be provided by a platinum-mercury interface, so that any air entrained between mercury and glass should collect around the internal seal. After this was installed an improvement was noted in the residual deflection but after some weeks the value of the deflection became the same as before and the bubbles on the column re-appeared. It was therefore decided to operate the column using carbon dioxide at atmospheric pressure, the carbon dioxide being supplied from a cylinder of the liquid, it being considered that this should be substantially helium-free. This system brought some improvement, the fact that the residual deflection was not completely removed may be due to the possibility that some air was still entrained and that some time would be required before this could be completely replaced by carbon dioxide.

The residual deflection observed can be neglected for most of the measurements described in this work

being less than 1% of the total helium, but it does set a limit to the detection of helium.

CHAPTER VI.

THE ESTIMATION OF TRITIUM IN BERYLLIUM.

VI. 1. Introduction.

For reasons given elsewhere in this work a method was developed for the estimation of tritium produced in metallic beryllium on irradiation with neutrons. With the neutron fluxes available it was estimated that continuous irradiation of beryllium for one month would produce an estimated 4×10^{-9} ccs. of tritium/gram of beryllium. This quantity would be difficult to extract and measure by gas volumetric methods, but tritium is readily measured in such quantity by virtue of its β -radioactivity, the volume given above being approximately equivalent to 10^4 disintegration/minute. However, quantities of beryllium of the order of 1 gram were inconveniently large for the method developed, and in practice 100 milligrams samples were analysed, hence only 10^3 disintegration/minute were to be expected. It was therefore essential that the bulk of this material should be counted in order to ensure reasonable

statistical accuracy.

The method consists in attacking the beryllium in vacuo with bromine vapour to convert the beryllium to the bromide, the tritium released reacting with the bromine to form tritium bromide. A small amount of hydrogen bromide was present to act as carrier for the tritium bromide. The excess of bromine is then removed by admitting mercury vapour to the system thus leaving the hydrogen and tritium bromides. These gases were then passed over heated magnesium at 500°C to convert the halides to hydrogen and tritium, which were then transferred to a gas counter and the radioactivity of the mixture measured. The quantity of tritium in the beryllium can then be estimated.

In the extraction procedure described it is considered essential that the tritium should be in the same chemical form as the carrier, and it is useful to consider whether this will be so in this case. The tritium will be released from the beryllium in the atomic or molecular state, and it can be assumed that its properties as regards chemical reaction will not differ grossly from those of hydrogen. The equilibrium constant for the reaction



at 25°C is of the order of 10^9 , and from the known heat

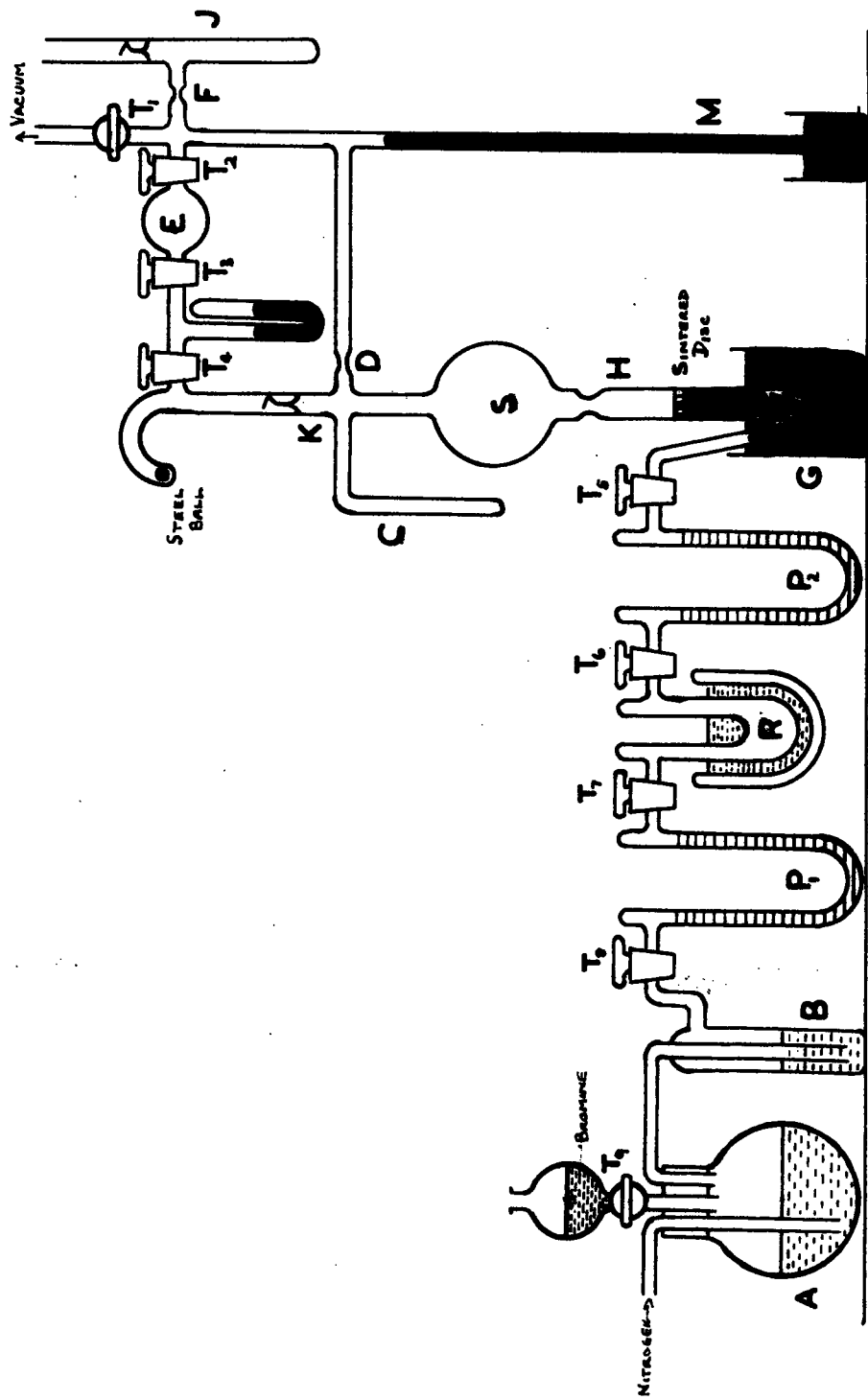
of reaction H at 25° , it can be computed, assuming H constant, that at $600^\circ C$ the value is 10^5 . Thus even at high temperatures the reaction favours the formation of hydrogen bromide in the presence of bromine vapour. During the course of the extraction the system favours conversion of tritium to tritium bromide. When the excess of bromine is finally removed by mercury there is the possibility that this will also attack the hydrogen and tritium bromides. Should this occur however the condition that the tritium should be in the same chemical form as the carrier will still be maintained.

VI. 2. Preparation of Pure Dry Hydrogen Bromide.

Hydrogen bromide was prepared by the bromination of tetrahydronaphthalene (tetralin), the apparatus being shown in figure 24. A stream of dry N_2 was passed through the tetralin in flask A with taps $T_{5,6,7}$, and T_8 open and allowed to bubble out through mercury in the beaker G, in order to displace air from the apparatus. The reservoir R was then cooled in liquid nitrogen, and bromine was allowed to drip into flask A from the separating funnel via tap T_9 . The hydrogen bromide produced was passed through the trap B which contained tetralin to remove any bromine carried over with the gas stream. After passing through the phosphorus pentoxide tube P_1 to remove water, the hydrogen bromide was condensed in the reservoir R. When sufficient

FIGURE 24.

Apparatus for the preparation of pure dry hydrogen bromide.



hydrogen bromide had been condensed the stream of nitrogen was cut off and taps $T_{7,8,9}$, were closed. The solid hydrogen bromide was then allowed to warm up to allow gaseous hydrogen bromide to bubble out of the mercury in G, this being observed by the white fumes produced on contact with air, to displace excess nitrogen. The hydrogen bromide was again frozen in R, T_5 being closed to prevent mercury sucking back from the reservoir G.

The reservoir S was then pumped out to a hard vacuum via the tap T_1 which was then closed. Hydrogen bromide in R was again allowed to warm up with T_5 opened and the delivery tube was placed under the sintered glass disc. The hydrogen bromide after further drying over phosphorus pentoxide was thus passed into the reservoir S. When about 30 cms. pressure of hydrogen bromide had collected in S the stream was again stopped by freezing R as before, and the gas in S was frozen down in the side arm C by immersion in liquid nitrogen. The system was then opened to the pumps via T_1 to remove any residual nitrogen. The tap T_1 was closed, the hydrogen bromide in C allowed to warm up and the collection of hydrogen bromide was continued until it began to bubble out of the manometer M, when it was stopped. The hydrogen bromide was again frozen down in the side arm C and the system once again pumped out via T_1 . The reservoir

S was then sealed by melting the glass at the constrictions D and H. The hydrogen bromide in C was again allowed to warm up. There was thus collected in C a quantity of pure dry hydrogen bromide.

T_{1,2,3,4}' are opened to the pumps until a hard vacuum is obtained the taps again being closed. The steel ball in the side arm is lifted with a magnet and allowed to fall on to the glass seal K which is broken on impact, thus admitting the hydrogen bromide to the space behind T₄. T₃ was then opened, and by slowly opening T₄ a small quantity of hydrogen bromide could be admitted to the bulb E whose volume was accurately known. The pressure was then measured in the system by means of manometer L, and then T₃ was closed. Room temperature was observed, and then T₂ was opened to admit the gas to the sample tube J which was immersed in liquid nitrogen. The hydrogen bromide was thus frozen down in the tube J, its vapour pressure being negligible at this temperature of liquid nitrogen, and the tube could be sealed off at the constriction F. A similar sample tube could then be sealed on to the apparatus, and the filling process repeated. In this way a large number of sample tubes containing accurately known quantities of hydrogen bromide could be prepared.

VI. 3. Purification of Bromine.

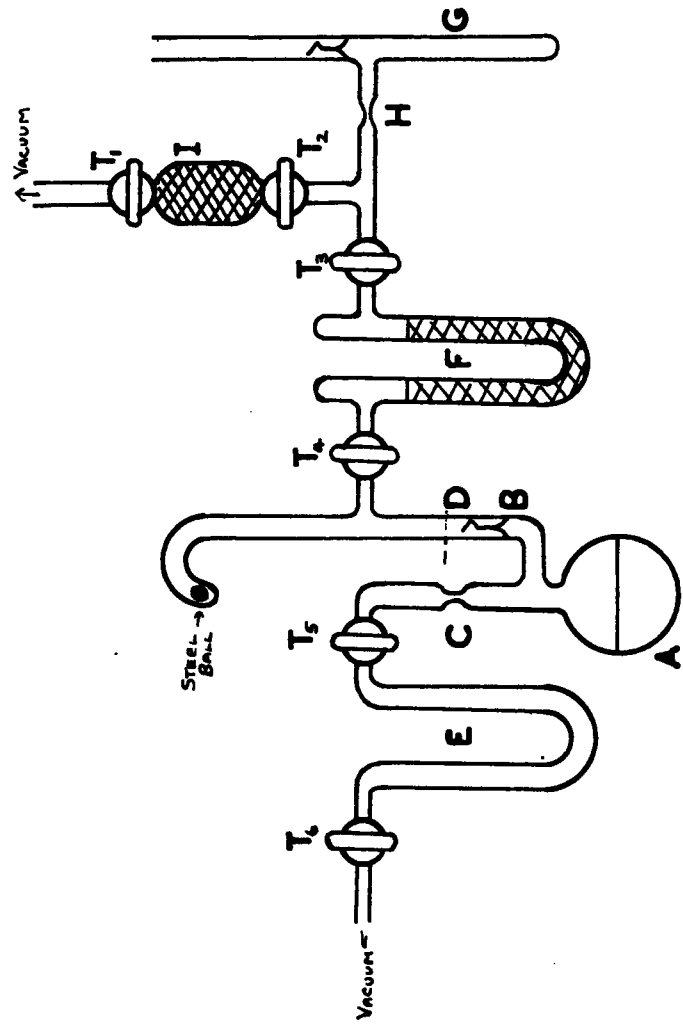
For the initial experiments with this method of

tritium estimation it was desirable that the bromine be freed from impurities. Commercial liquid bromine was used, the main impurities being water and hydrogen bromide. The bromine was therefore mixed with calcium oxide, to remove hydrogen bromide, and with magnesium perchlorate, to remove water, in the flask A (figure 25). The flask was frozen in liquid nitrogen and then opened to the vacuum system via T_5 and T_6 , the trap E being immersed in liquid nitrogen to trap out escaping vapour. $T_{5,6}$ were then closed and the bromine allowed to liquify. The system was then frozen again and the pumping operation repeated. This process was repeated four or five times in order to completely de-aerate the bromine, after which the bromine was again frozen, and the flask sealed off at the constriction C. After allowing the bromine to warm up the flask was shaken vigorously and allowed to stand for several hours, at the end of which the flask was sealed to the remainder of the apparatus at D.

$T_{1,2,3,4}$ were opened and the system rigorously evacuated through the high vacuum line. $T_{1,2}$ were then closed and the steel ball allowed to fall on to the glass seal B which was thus broken. The tube G was then frozen in liquid nitrogen and bromine after passing through the tube F, where it was further dried over magnesium perchlorate, was condensed in the tube G. When approximately

FIGURE 25.

Apparatus for the purification of bromine.



1 cc. of bromine was collected in G the tap T_3 was closed and the sample tube sealed off at the constriction H. A fresh sample tube could then be sealed on to the system and the process repeated. In this way 1 cc. samples of purified bromine were obtained for the subsequent analysis. The tube I was packed with potassium hydroxide pellets to prevent access of bromine vapour to the pumping system, but it did not prove a very efficient method, and bromine collected in the liquid nitrogen trap of the diffusion pumps.

The first four sample tubes obtained as above were analysed for impurity in the following manner. A sample tube was opened to an evacuated tube containing mercury vapour, and the bromine combined with the mercury quantitatively. This evacuated tube was then opened to a tube containing magnesium metal at 500°C , and, using a Toepler pump, any gases in the tube were transferred to a manometric system. Only in the first two of the bromine sample tubes was any gas removed from the system, and from this it was inferred that all other sample tubes were sufficiently free of impurity for use in the tritium extraction method. The first two sample tubes probably contained some residual hydrogen bromide not removed by the calcium oxide.

VI. 4. The Extraction of Tritium from Beryllium.

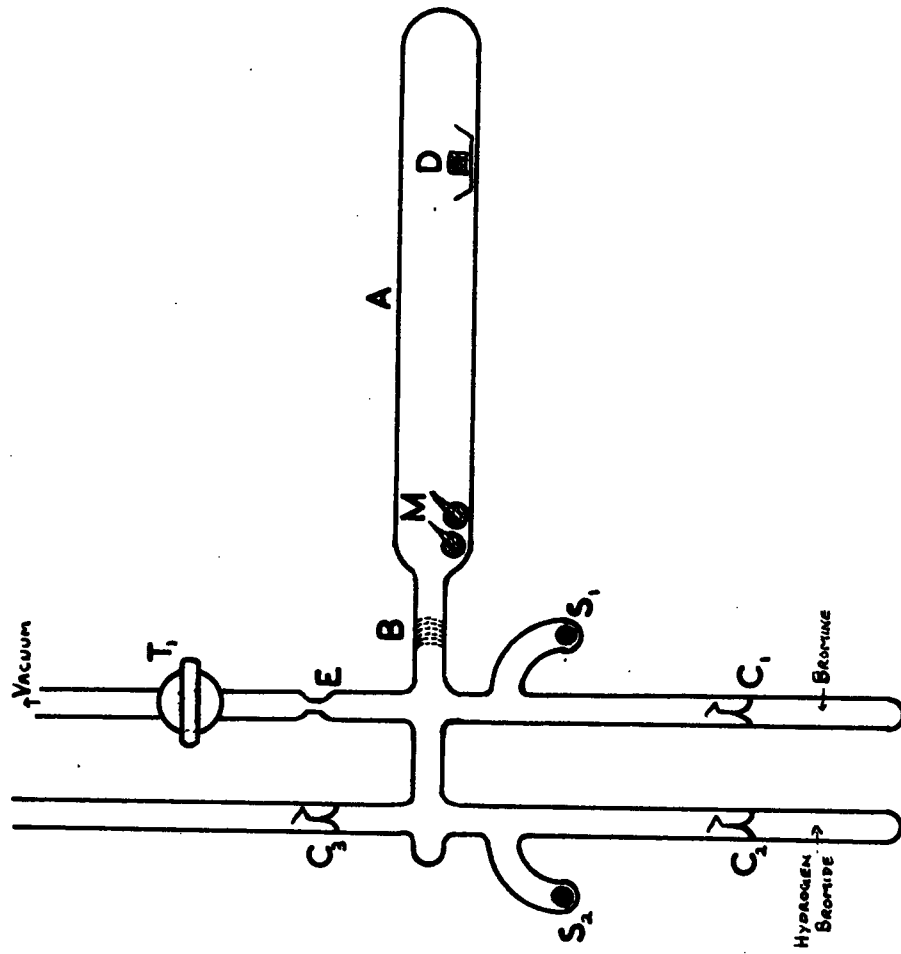
The apparatus, shown in figure 26, consists of a

silica tube A fixed to the 'Pyrex' vacuum line through a silica to 'Pyrex' seal B. Sealed on to the 'Pyrex' system are two sample tubes, one containing about 3×10^{-4} moles of hydrogen bromide, and the other 1 cc. of liquid bromine. The sample tubes can be opened to the system by breaking the glass seals C_1 and C_2 using the steel balls S_1 and S_2 . The beryllium sample is contained in a wrapping of platinum gauze for the single pieces, or in a platinum boat if in the form of turnings. The function of the platinum cover is to prevent attack on the silica by the beryllium when this is heated. An early experiment showed that beryllium readily attacks silica, presumably withdrawing oxygen, when heated. Two small sealed soda-glass bulbs M containing mercury, are also included in the tube at the position shown.

The reaction vessel is pumped out rigorously to a hard vacuum via tap T_1 , the tube being lightly heated with a gas flame to drive out water. When a suitable vacuum has been attained the sample tube is sealed off at the constriction E. The glass seals C_1 and C_2 are then broken, using the steel balls S_1 and S_2 which are afterwards withdrawn into their respective side tubes using an external magnet. Bromine and hydrogen bromide are thus admitted to the reaction vessel. The beryllium sample is then heated to redness and reaction occurs

FIGURE 26.

Reaction vessel for the extraction of tritium
from beryllium.



between the beryllium and bromine producing a voluminous white deposit on the cool walls of the vessel. The beryllium burns brightly in the bromine vapour, and would no doubt continue until all of it were used, but the deposition of beryllium bromide prevents ready access of the combustion materials to one another. The whole tube must be kept warm to prevent choking up with beryllium bromide. The last traces of beryllium are removed by strongly heating and causing the bromine vapour to pass over and over the heated metal. This flow can readily be achieved by first cooling one end and then the other in a bath of liquid nitrogen. When all the beryllium is used up the excess of bromine is then removed in the following way. The two mercury bulbs are heated until they break up, the hot mercury released into the reaction vessel immediately reacts with the bromine, a flame being observed to move along the tube. At the end of reaction with mercury no characteristic colour of bromine can be observed in the vessel.

In earlier experiments the final removal of excess bromine was performed by heating a strip of metallic copper in the system. This was quite effective as a scavenger, but was somewhat slow in practice, and had to be heated to quite a high temperature. The use of copper also impaired the life of the reaction vessel

since it left a coherent deposit on the walls which could not be removed. The use of mercury removes these difficulties.

The reaction vessels now contains tritium bromide together with hydrogen bromide carrier. This mixture must be converted to tritium and hydrogen for gas counting, since the presence of halogen and halogen acid in Geiger counters is undesirable.

VI. 5. Measurement of Tritium.

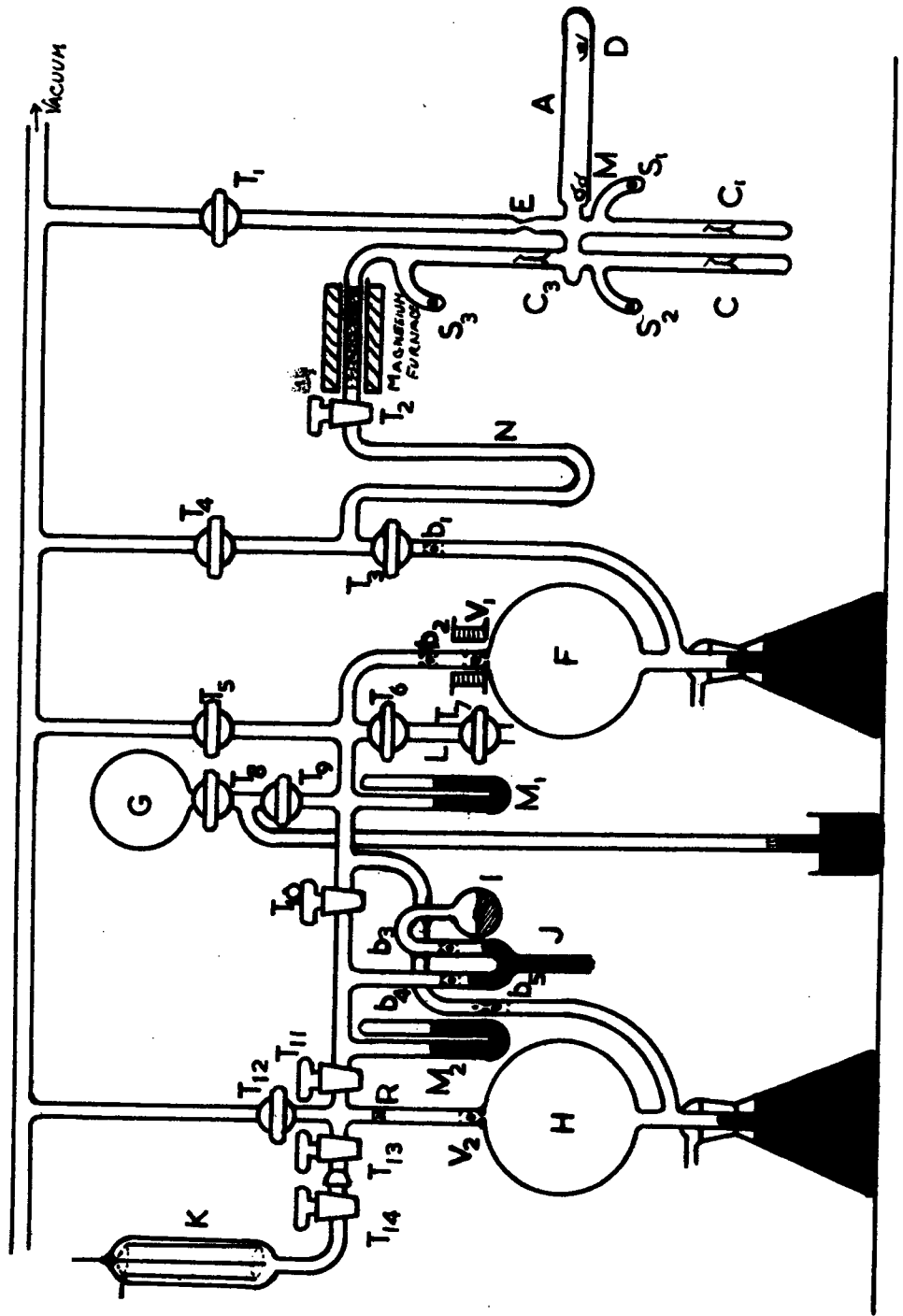
Figure 27 shows the complete apparatus for the extraction and measurement of tritium in beryllium. Reaction vessel A for the degradation of metallic beryllium and conversion of tritium to the bromide has been described. The remainder of the system is concerned with the conversion of the hydrogen and tritium bromides to elemental hydrogen and tritium, and the transfer of the gases to a Geiger counting system for measurement.

The whole apparatus is rigorously evacuated with all taps open, with the exception of T_7 which opens directly to the atmosphere. Tap T_9 is closed and hydrogen from a cylinder, after passing through coconut charcoal cooled in liquid nitrogen to remove impurities, is passed into the flask G via the mercury tight sintered glass disc P. When filled to atmospheric pressure tap T_8 is closed and the excess hydrogen in the connecting

FIGURE 27.

Apparatus for the estimation of tritium in

beryllium.



tube is pumped away. The hydrogen in G is required for counter filling.

It is required that the volume of certain sections of the apparatus be accurately known, and these volumes are determined by the method of gas expansion using the air pipette L. The volume of L has been accurately determined from the weight of mercury required to fill the space between T_6 and T_7 . The Toepler pumps F and H are raised to the ball-valves $B_{1,2}$, and B_5 , and the mercury tight sintered glass disc R. The taps $T_{5,6,9}$, and T_{10} are closed. Tap T_7 is opened to admit a sample of air into L, the atmospheric pressure being observed and T_7 is closed. T_6 is then opened to admit the sample of air to the volume space defined by T_7 , B_2 , T_5 , T_9 , T_{10} , and B_5 and the surface of the mercury of the manometer M_1 . The difference in level of the mercury in the manometer M_1 is observed using a cathetometer. After correction for the volume of L, the tap key T_6 , and the volume of displaced mercury in M_1 , the volume defined by T_6 , B_2 , T_5 , T_9 , T_{10} , and B_5 can be determined. Tap T_{10} is then opened to admit the air sample up to T_{11} . The pressure is again noted, and after correction for the second manometer M_2 , the increased volume can be determined. Continuing in this way, and making appropriate corrections for the volume of tap keys etc., the volume of each section of the apparatus

can be determined. The main volumes of interest are

- (1) that defined by B_2 , T_5 , T_6 , T_9 , T_{10} , and B_5 now referred to as V_a .
- (2) that defined by R , T_{11} , T_{12} , and the Geiger counter K , now referred to as V_b .
- (3) the cathode volume of the Geiger counter, this being determined by measurement of the diameter and length of the cathode and subsequent calculation of the volume of the cylinder. This volume will now be referred to as V_c .

The electric heater of the magnesium furnace is switched on, and the magnesium baked at 500°C for an hour, the system being opened to the pumps via taps T_2 and T_4 . The furnace consists of a brass tube covered in asbestos paper, around which is wound a layer of 'Nichrome' resistance tape. The whole is then covered with two or three layers of asbestos paper. 250v A.C. mains are used to supply the heater current which is controlled by means of a potentiometer. The temperature is measured by means of a calibrated thermocouple. This furnace surrounds a length of 'Pyrex' tube packed with magnesium turnings (Grignard reagent quality). After baking for one hour the tap T_4 was closed, and the U-tube N immersed in liquid nitrogen. Tap T_3 is opened

and the mercury in the Toepler pump F lowered. The taps T_6 , T_5 , T_9 , T_{10} should be closed and the mercury in the Toepler pump H raised to the ball B_5 and the sintered glass disc R.

The glass seal C_3 is then broken using the steel ball S_3 , the hydrogen and tritium bromides in A thus being allowed to pass over the heated magnesium. The Toepler pump is used to transfer the gases into the section V_a , the solenoid operated ventill V_1 preventing return of the collected gases. Some ten to fifteen operations of the pump F are required to quantitatively transfer the gas from A to V_a . The purpose of the trap N is to remove unconverted bromides from the tritium and hydrogen for recycling over the heated magnesium. This could be performed by closing T_3 , removing the liquid nitrogen around N, and cooling with liquid nitrogen some part of the reaction vessel A to bring the bromides back over the heated magnesium. The procedure above could then be repeated. In practice this was found to be unnecessary, the bromides being completely converted to hydrogen and tritium after one passage of the gases through the heated magnesium.

The quantity of hydrogen and tritium collected in the volume V_a can now be determined. The pressure in the system is measured using the manometer M_1 , and the

temperature observed. After correction of the volume V_a for the increase due to movement of the mercury in M_1 , the yield of hydrogen can be obtained, and is compared with the quantity of hydrogen bromide used in the sample tube. This provides a check on the correct working of the extraction system. The Geiger counter is then filled.

The bulb I contains absolute alcohol which was distilled into the bulb after a short treatment with Calcium metal to remove traces of water, present in the alcohol. The alcohol is confined by the mercury in the U-tube J; in order to indicate the ball-valves B_3 , and B_4 in the diagram the mercury is shown half way down the U-tube, but in actual practice it is pushed right up to the ball-valves, particularly during the calibration operation. The alcohol is frozen in liquid nitrogen after which the mercury in J is lowered below cut-off. The taps T_{11} , T_{13} , and T_{14} are opened, and the bulb I is warmed until a 2 cm pressure of alcohol is registered on the manometer M_2 . T_{11} is then closed, and I again frozen to condense the alcohol between T_{10} and T_{11} , the mercury in J being raised to the ball-valves B_3 and B_4 .

From the known volumes of V_a and V_b the pressure of hydrogen required in V_a to give an 8 cm. partial pressure of hydrogen in V_b is calculated, i.e.,

$$P_a = \frac{8V_b}{V_a}$$

With the system used P_a is greater than that recovered from the hydrogen bromide. The mercury in the Toepler pump H is then lowered slowly, and when the level of mercury is about 1.5cm above the ventill V_2 the steel ball is pulled down with an external magnet to close the ventill, thus preventing alcohol escaping from V_b . H is fully lowered and then raised again to R. This is repeated several times until the tritiated hydrogen in V_a is transferred to V_b . Tap T_8 is opened to admit hydrogen from the storage bulb G to the space behind T_9 , T_8 being then closed. With the Toepler pump H raised to R and B_5 , the tap T_9 is opened slowly to admit a pressure of hydrogen into V_a , this pressure, together with that of the tritiated hydrogen transferred to V_b , should be equal to P_a . The gas measured out is then transferred to V_b using the pump H as before.

It is desirable, before counting, to thoroughly mix the hydrogen and alcohol in the counter system. The alcohol is added as a quenching agent for the Geiger discharge. The gas mixture is then thoroughly mixed by expanding into the Toepler pump bulb (H) several times. Finally the mercury in the Toepler pump is raised to the sintered glass disc R, and the taps T_{13} and T_{14} are closed. The tritium activity may then

be observed.

The current practice in gas counting is to assume that all disintegrations occurring in the cathode volume are recorded. When this is assumed, the observed activity A_o , after correction for counter paralysis time and background, is converted to the total activity of the tritiated hydrogen by multiplying by the ratio V_b to V_c . The total tritium content/gram of beryllium is then given by,

$$N_t = \frac{A_o V_b}{\lambda_t V_c M}$$

Where N_t is the number of tritium atoms/gram of beryllium, M the mass of beryllium used, λ_t the disintegration constant of tritium ($1.058 \times 10^{-7} \text{ mins}^{-1}$), and A_o the observed activity corrected for paralysis time and background. The quantities V_b and V_c have already been defined.

BIBLIOGRAPHY.

1. Cranberg, L., R.B.Day, L.Rosen, R.F.Taschek, M.Walt: Progress in Nuclear Energy, I.1, 107, (1956).
2. Li, C.W., W.Whaling, W.A.Fowler, C.C.Lauristen: Phys. Rev., 83, 512, (1951).
3. King: Rev. Mod. Phys., 26, 327, (1954).
4. Gardner, W.L., N.Knable, B.J.Moyer: Phys. Rev., 83, 1054, (1951).
5. U.S.A.E.C. : Neutron cross-sections, B.N.L.325, (1955).
6. Grace, M.A., L.E.Beghian, G.Preston, H.Halban: Phys. Rev. 82, 969, (1951).
7. Day, R.B. : Phys. Rev., 102, 767, (1956).
8. Ajzenberg, F., T.Lauritsen: Rev. Mod. Phys., 27, 77, (1955).
9. Bartholomew, G.A., B.B.Kinsey: Canad. J. Phys., 31, 49, (1953).
10. Ross, M., J.S.Storey: Ann. Rep. Prog. Phys., 12, 29L, (1949).
11. Bjerge, T. : Nature, 137, 865, (1936).
12. Allen, K.W., W.E.Burcham, D.H.Wilkinson: Proc. Roy. Soc., A192, 114, (1947).
13. Stelson, P.H., E.C.Campbell: Phys. Rev., 106, 1252, (1957).
14. Battat, M.E., F.L.Ribe: Phys. Rev., 88, 159, (1952).
15. Rusinov, L.I. : Phys.Zeits.Sowjetunion., 10, 219, (1936).
16. Ollano, Z. : Nuovo Cimento, 15, 604, (1938).
17. Houtermans, F.G. : Nachr.Wiss.Gottingen, 1, 52, (1946).
18. Funfer, E., W.Bothe: Zeits.f.Physik., 122, 769, (1944).

19. Teucher, M. : Zeits.f.Physik., 126, 410, (1949).
20. Bernstein, quoted by Agnew (Ref. 22).
21. Martin, quoted by Agnew (Ref. 22).
22. Agnew, H.M. : U.S.A.E.C. Report No. LA-1371 (1952).
23. U.S.A.E.C. : Reactor Handbook-Physics, p.19, (McGraw-Hill).
24. Fowler, J.M., S.S.Hanna, G.E.Owen:
Bull. Am. Phys. Soc., 29, No.7, X5, (1954).
25. Livey, D.T., P.Murray. : J. Nucl. Energy, 2, 202, (1956).
26. Hinton, C. : Endeavour, 16, 65, (1957).
27. Hughes, D.J. : Pile Neutron Research,
p.27, (Addison-Wesley, 1953).
28. Hurwitz, H., R.Ehrlich. : Progress in Nuclear Energy,
Series I, Vol. I, p.343, (1956).
29. Sanders, J.E., D.J.Littler. : A.E.R.E. Report No.
N.R.D.C.35, (1954).
30. Krasin, A.K., B.G. Dubovsky: J. Nucl. Energy,
4, 520, (1957).
31. Barschall, H.H. : Rev. Mod. Phys., 24, 131, (1952).
32. Hanson, A.O., J.L. McKibben: Phys. Rev. 72, 673, (1947).
33. Bethe, H.A. : U.S.A.E.C. Report No. L.A.1428, (1952).
34. Taylor, H.L., O. Lonsjo, T.W. Bonner:
Phys. Rev. 100, 174, (1955).
35. Beyster, J.R., R.L. Henkel, R.A. Nobles:
Phys. Rev. 97, 563, (1955).
36. Shapiro, P., V.E. Scherrer, B.A. Allison, W.R. Faust:
Phys. Rev. 95, 751, (1954).
37. Fowler, J.M., G.E.Owen, S.S.Hanna : NYO-3864 (1957).
38. Fowler, J.L., J.M.Slye : Phys. Rev. 77, 787, (1950).

39. Paul, E.B., R.L. Clarke: Can. Journ. Phys., 31, 267, (1953).
40. Segre, E. : 'Experimental Nuclear Physics', p,350-3, (J.Wiley, and Sons. 1953).
41. Glueckauf, E., F.A.Paneth: Proc. Roy. Soc. A165, 230, (1938).
42. Atkinson, R.d'E., F.G.Houtermans : Zeits.f.Physik. 54, 664, (1929).
43. Lord Rayleigh : Nature, 123, 607, (1929).
44. Watson, W.W., A.E.Parker : Phys. Rev., 37, 167, (1931).
45. Olssen, E. : Zeits.f.Physik, 73, 732, (1931).
46. Neir, A.O. : Phys. Rev., 52, 936, (1937).
47. Bleakney, W., J.P.Blewett, R.Shaw, R.Smoluchowsky, Phys. Rev., 50, 545, (1936).
48. Cockroft, J.D., W.B.Lewis : Proc. Roy. Soc., A154, 257, (1936).
49. Dee, P.I., C.W.Gilbert : Proc. Roy. Soc., A154, 291, (1936).
50. Kirchner, F., H.Neuert : Naturwiss, 25, 48, (1937).
51. Bethe, H. : Rev. Mod. Phys., 9, 167, (1937).
52. Wheeler, J.A. : Phys. Rev., 59, 27, (1941).
53. Ajzenberg, F., T.Lauritsen: Rev. Mod. Phys., 24, 336, (1952).
54. Leachman, R.B. : Peaceful Uses of Atomic Energy, Vol. II, 198, (Geneva, 1955).
55. Paneth, F.A. : Endeavour, 12, 3, (1953).
56. Jenkins, E.N., A.A.Smales: Quart. Reviews, 10, 83, (1956).

57. Anderson, H.L., E.Fermi, L.Szilard : Phys. Rev., 56, 284, (1939).
58. Kahn, H. : Nucleonics, May 1950, p,27; June 1950, p,60.
59. Handbook of Chemistry and Physics - Chemical Rubber Publishing Co. (1954-5).
60. Paneth, F.A. : Occasional Notes . Roy. Astro. Soc., No. 5, 57, (1939).
61. Reasbeck, P. : Ph.D. Thesis, Durham 1953.
62. Barrer, R.M. : 'Diffusion in and through solids', (Cambridge).
63. Cottrell, A.H. : 'The Physics of Nuclear Reactors', Brit. Journ. of. App. Phys., Supp.No.5, S43, (1956).
64. Guth, E., C.J.Mullin : Phys. Rev., 76, 234, (1949).
65. Nathans, R., J.Halpern : Phys. Rev., 92, 940, (1953).
66. Harvey, J.A., J.E.Sanders : Prog.in Nucl.Energy, Series I, Vol.I., p,44, (1956).
67. Bethe, H. : Rev. Mod. Phys., 9, 167, (1937).
68. Battat, M.E., F.L.Ribe : Phys. Rev., 89, 80, (1953).
69. Suttar, A.R., I.L.Morgan, E.L.Hudspeth : Phys. Rev., 100, 960, (1955).
70. White, D.W., J.E.Burke : 'The Metal Beryllium', p,658, (American Society for Metals, 1955).
71. Schlogl, F. : Zeits.f.Naturforschung, 3A, 229, (1948).
72. Mamasakhlisov, V.I. : Zhur.Eksptl'.i.Teoret.Fiz., 25, 36, (1953).
73. Caldirola, P. : J.de.Phys.et.rad., 8, 155, (1947).
74. Fermi, E. : 'Nuclear Physics', (University of Chicago Press, 1955).

75. Dacy, J.E., R.W.Paine, C.Goodman : U.S.A.E.C.
Reactor Handbook-Physics, p3, (McGraw-Hill).
76. Van Patter, D.M., A.Sperduto, K.Huang, E.N.Strait,
W.W.Buechner : Phys. Rev., 81, 233, (1951).
77. Dissanaikie, G.A., J.O.Newton : Proc. Roy. Soc.,
A65, 675, (1952).
78. Gossett, C.R., G.C.Phillips, J.P.Schiffer, P.M.Windham,
Phys. Rev., 100, 203, (1955).
79. Blatt, J.M., V.F.Weisskopf : Theoretical Nuclear Physics,
Chapter VIII, (Wiley, 1952).
80. Gugelot, P.C. : Phys. Rev., 81, 51, (1951).
81. Cohen, B.L. : Phys. Rev., 81, 184, (1951).
82. Phillips, G.C. : Los Alamos Report A.E.C.U. - 404 (1949).
83. Cook, C.F., T.W.Bonner : Phys. Rev., 94, 651, (1954).
84. Beyster, J.R., M.Walt, E.W.Salmi : Phys. Rev.,
104, 1319, (1956).
85. Graves, E.R., R.W.Davis : Phys. Rev., 97, 1205, (1955).
86. Flerov, N.N., V.M.Talyzin : J.Nucl. Energy,
4, 529, (1957).
87. Rosen, L., L.Stewart : Phys. Rev., 107, 824, (1957).
88. Fowler, J.M., et.al. : See Reference 37.
89. Huber, P., R.Wagner : Helv.Phys. Acta., 30, 257, (1957).
90. Fowler, J.M., et. al., : See Reference 37.
91. Peisach, M. : Private Communication.
92. Fireman, E.L. : Phys. Rev., 91, 922, (1953).
93. Ribe, F.L. : Phys. Rev., 103, 741, (1956).
94. Perkin, J.L. : Phys. Rev., 81, 892, (1951).

95. Frye, G.M., J.H.Gammel : Phys. Rev., 103, 328, (1956).
96. Ribe, F.L., J.D.Seagrave : Phys. Rev., 94, 934, (1954).
97. 'Reactor Handbook - Physics', p,18, (McGraw-Hill, 1955).
98. Wattenberg, A. : Ann. Rev. Nucl. Sci., 3, 119, (1953).
99. 'Conference on Neutron Source Preparation' - Harwell, 1954, A.E.R.E. Report No. NP/R1577.
100. Martin, E.B.M., G.R.Martin : See Reference 99.
101. Reasbeck, P. : Private Communication.
102. Chackett, K.F., P.Reasbeck, E.J.Wilson : Geochim. et. Cosmochim. Acta., 3, 261, (1953).
103. Holmes, A., F.A.Paneth : Proc. Roy. Soc., A154, 385, (1936).
104. Paneth, F.A., H.Gehlen, P.L.Gunther : Zeits.f.Electrochem., 34, 645, (1928).
105. Glueckauf, E., F.A.Paneth : Proc. Roy. Soc., A185, 89, (1946).
106. Wiborg, B.S. : Ph.D. Thesis. Durham, 1954.
107. Martin, G.R., S.J.Thomson, G.Wardle, K.I.Mayne : Phil. Mag., 45, 410, (1954).
108. Paneth, F.A., E.Glueckauf, H.Loleit : Proc. Roy. Soc., A157, 412, (1936).
109. Clusius, K., L.Riccobini : Zeits. Phys. Chem., 38, 81, (1938).
110. Lambert, B., C.S.G.Phillips : Phil. Trans., 242A, 415, (1950).
111. Wardle, G. : Ph.D. Thesis, Durham, 1954.
112. Paneth, F.A., W.D.Urry : Zeits. Phys. Chem., A152, 110, (1931).

113. Barrett, L.G. : U.S.A.E.C. Document No.
KAPL-M-LGB-12, (December, 1956).
114. Richmond, R. : Harwell, private communication.